CONSORZIO RFX
Ricerca Formazione Innovazione

2012 Activity report

Index

1. INTRODUCTION AND KEY OBJECTIVES

The 2012 programme of Consorzio RFX, presented and evaluated at the 27th meeting of the RFX Scientific-Technical Committee on 2 November 2011, was scrutinized and discussed by the Board of Directors of Consorzio RFX in order to adapt the final programme to the available resources, so that the final approval of the programme, together with the associated relevant budget, was given by the Consorzio RFX Management Board on 20 April 2012.

The programme was confirmed to be focused upon the two main research lines, the realization of the NBI Facility and the exploitation of the RFX-mod experiment, and articulated in the following main objectives:

- to start the construction of the ITER Neutral Beam Test Facility;
- to realize the Ion Source and the Neutral Beam Injector for the Test Facility;
- to operate the RFX-mod device in RFP configuration at full plasma current;
- to contribute to the tokamak and stellarator physics with experiments in RFX-mod both in RFP and tokamak configuration and by continuing the collaboration with other laboratories;
- to realize of the quench protection system and the fast power supplies for JT-60 SA in the framework of the Broader Approach scheme;
- to participate in the realization of the magnetic sensors and the LIDAR diagnostic for ITER;
- to contribute to EU activities for DEMO.

The activity for the implementation of the NBI Facility was, for the first year, performed under the Agreement on the Neutral Beam Test Facility, signed between Consorzio RFX and F4E. The Workprogramme 2012, proposed by Consorzio RFX, was approved by the Programme Committee (in which ITER, the evolved Domestic Agencies and Consorzio RFX are represented) and the Liaison Committee between F4E and Consorzio (foreseen in the Agreement). As reported in Cap. 3, substantial advancement in designing of SPIDER and MITICA components has been obtained together with he start of the procurement of the majority of SPIDER components and the auxiliary systems (cooling, gas and vacuum).

The work on site for construction of buildings and basic infrastructures started in the beginning of September 2012, and the first hall for the installation of the SPIDER power supply should be ready at the end of 2013. The activities at RFX and in other laboratories aimed to prepare the local NBI Operational Team continued including a substantial progress in the procurement of the small ion source NIO1

A delay in the experimental RFX programme was a consequence of the cut in the investments due to the lower budget made available by the Bodies, compared to that estimated necessary for the execution of the activities foreseen in the Programme 2012 evaluated by the CTS.

Despite the reduction in budget which affected the diagnostic programme, however the RFX operation has led to new results relevant also for the international tokamak and stellarator program thanks to an intense experimental activity in RFX and effective international collaborations. RFX was operated at plasma current above 1.5 MA focusing on key issues: plasma-wall interaction, MHD stability active control, three-dimensional physics and turbulence-related transport. As a proof of the qualified activity performed at RFX, it is worth mentioning the General Atomics Torkil Jensen Award, awarded to RFX to lead a successful operation at q95<2 in DIIID.

Significant advancement was obtained in the realization of the Quench Protection Circuits for JT-60SA. The activity progressed in line with the schedule of the contractual activities with the successful completion of the prototype tests and the complete validation of the QPC design. This relevant result allows proceeding in time with the construction of the units to be installed in JT-60SA.

2. RFP AND TOKAMAK EXPERIMENTAL PHYSICS

2.1 Introduction

The 2012 RFX RFP and Tokamak Physics program has produced a variety of results advancing the understanding of the RFP as a fusion concept and directly contributing to the development of the international tokamak and stellarator program, including ITER, JT-60SA and JET. This effort has been based on an intense experimental activity in RFX, on a rich theory program and on international collaborations.

Important advancements have been obtained in the understanding of high current plasma up to the values of 1.7 MA with an emphasis on items such plasma-wall interaction, MHD stability active control, three-dimensional physics and turbulence-related transport, all fitting in the headlines of the European and international program. Experiments at higher currents have been postponed due a failure of a saddle coil. A significant portion of the experimental campaigns has been devoted to the issue of recycling control and efficient fuelling. Systematic studies of the effects of the various wall conditioning procedures, in particular intensive tests of wall lithization, have opened encouraging perspectives towards a situation of improved density control and improved overall performance. Also, equilibrium configurations characterized by the strong reduction of m=0 modes have been explored as a means to enhance the fuelling efficiency and obtain peaked instead of hollow density profiles, with interesting results.

As for the MHD control the recently upgraded hardware and software architecture have been fully tested and characterized in terms of speed, ameliorated latency of the feedback cycles and flexibility and then routinely used. Innovative and more efficient algorithms of the feedback control have also been tested producing altogether a significant progress that keeps RFX at the leading edge in the field.

New results on core and edge plasma transport and turbulence in helical states have been achieved with a deeper analysis of the role of micro-tearing modes in limiting the confinement of the internal transport barriers and with a very detailed characterization of the edge turbulence pattern and its relationship with macroscopic radial electric fields and flows in presence of MHD modes. The interpretation of those results has taken advantage of the improvement of tools for 3D equilibria reconstruction, part of which imported from the Stellarator community and also of temperature diagnostic developments allowing a better characterization of the dynamics of the helical regimes.

The understanding of the helical states has also improved thanks to experiments where a 3D magnetic boundary was produced by the feedback control system.

The recognition and the breadth of the RFX fusion science program is also evidenced by the success obtained in competitive projects that stemmed from it. Two examples among all: the positive outcome of the application to a private funding competition for the upgrade of the MHD control system, which was selected against many projects in the general physics and technology areas of the European Fusion Programme, and the General Atomics Torkil Jensen Award for innovative experimental proposals that was awarded to RFX. An experiment based on a pioneering experiment done in RFX-mod operated as a tokamak, was then carried out on DIII-D, where a configuration with q95 <2 was successfully maintained for almost 0.5 s in a L mode discharge, thus expanding the operational space of large scale tokamaks. Besides the already mentioned experiments on DIII-D, themes of common interest to the wide fusion community have been addressed on JET, TCV, ASDEX Upgrade, Compass and the TJII stellarator.

The following paragraphs describe in some detail the RFX experimental activity, addressing in particular the experiments carried out to reduce recycling, characterize and exploit the upgraded MHD feedback control system, characterize the Quasi Single Helicity, unveil the details of the 3D nature of the radial electric field and flows at the plasma edge and exploit the collaboration efforts on international devices. One section (2.3) summarizes the activity on the conceptual design of RFX modifications. Times are in fact mature to condense the experience gained in eight years of intense experimental and theoretical works and project RFX-mod towards new scenarios for a substantial improvement of the RFP performance and of the contribution to the Fusion international research. An overview of the large involvement of the RFX group in the international fusion science program is also given in sec. 2.4, where the main collaborations with international Tokamak devices are summarized.

The main operation schedule resulting for the 2012 experimental campaigns of RFX-mod is shown in fig. 2.A. It includes 17 weeks of shutdown for machine and diagnostic maintenance, while experiments have been distributed in 35 weeks of operation.

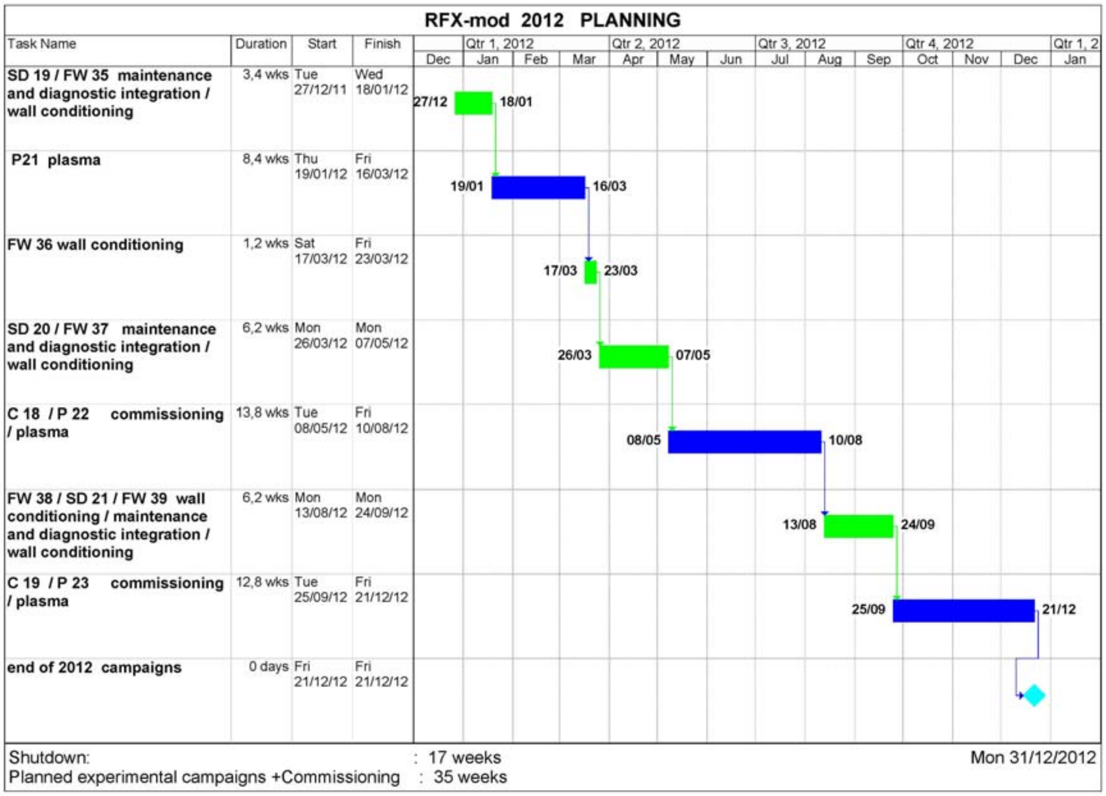

Fig. 2.A: RFX-mod program schedule for 2012

2.2 Exploration, understanding and improvement of RFX performance at plasma current above 1.5 MA

2.2.1 Scenario development

As mentioned above, in 2012 the high current operation was conditioned by the failure of a second saddle coil. After the event, on a statistical basis the region of the two coils has become an obvious attractor for the locking of the modes (fig. 2.1), with enhanced PWI that at the highest current induces localized heating and uncontrolled release of hydrogen. Consequently, the scenario development of the RFP plasmas has been pursued at Ip = 1.5-1.7 MA. A large fraction of high current discharges were performed in He to improve density control. This allowed decoupling the density from other parameters.

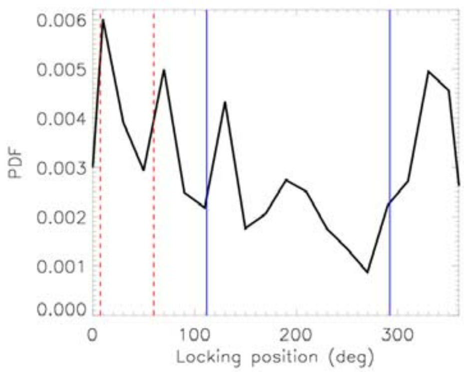

Fig. 2.1: statistics of the toroidal position of mode locking after the failure of a second saddle coil: red vertical lines indicate the positions of missing coils, blue lines correspond to the gaps

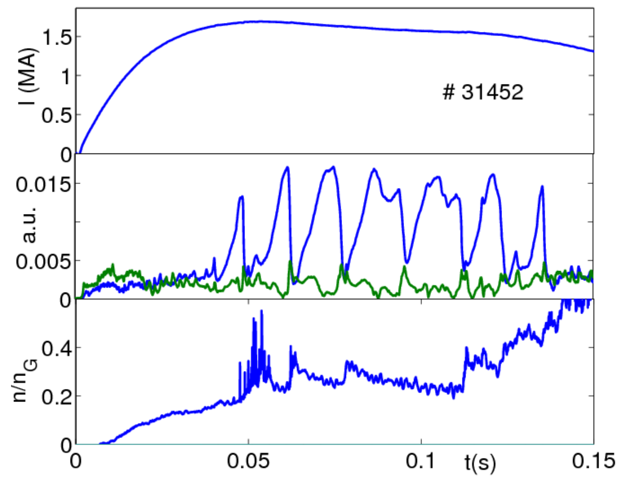

Fig. 2.2: Top: plasma current, middle: dominant (blue and secondary 8green9 mode amplitude; bottom: Greenwald fraction in a plasma discharge with Li conditioned wall, showing QSH phases at n/nag >0.4)

The operational range where Quasi Single Helicity states develop was extended to higher densities: QSHs were obtained up to n/nG~0.4 in well-conditioned discharges; an example is shown in fig. 2.2, which refers to a discharge with Li wall conditioning.

For different reasons, related to the necessity of a formal licensing procedure, tokamak operations were not performed in 2012, but will very likely be resumed in 2013.

2.2.2 Plasma-wall interaction and density control

During 2012 a substantial part of the RFX-mod experimental time was dedicated to the subject of density and plasma wall interaction control, in particular with the aim to test the effect on plasma of the carbon wall lithization. This experiment had an impact on the shutdown periods, since Lithium forms undesired compounds not easily removable from tiles when exposed to air.

Two different lithization techniques, already preliminarily tested in the past years, were explored. The first by the evaporation of a total of about 14 grams of Lithium in different sessions by means of the Liquid Lithium Limiter (LLL) device on loan from ENEA-Frascati. The second technique consisted in injecting several Lithium pellets for a total of less than 0.5 grams on Helium plasma discharges by means of a new multi-pellet launcher, developed by PPPL Laboratory, Princeton, US.

The LLL was extensively used as evaporator during a 5 weeks long campaign. The availability of only one evaporator yielded a Lithium coverage over one half of the machine only, as indicated by the Secondary Ions Mass Spectroscopy analysis of carbon samples exposed during evaporation at 0, 60 and 120 degrees in the toroidal direction from the LLL position. In each experimental session, before Lithium evaporation, the RFX-mod wall was conditioned by long He glow discharge cleaning (GDC) and He discharges, in order to deposit Li on clean carbon surfaces not containing Hydrogen from previous plasma discharges. The total amount of evaporated Lithium was 14 g, about 1-2 g per day.

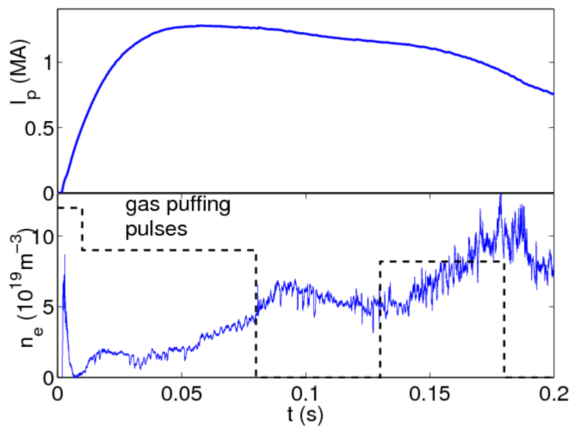

Fig. 2.3: time evolution of plasma current (top) and electron density (bottom) during a discharge after Li deposition. Puffing from inlet valves is superimposed to the density

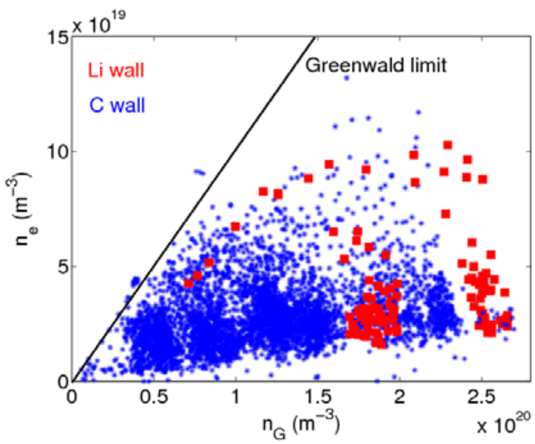

Fig. 2.4: points obtained with Li conditioned wall (red) in the Greenwald plot (data refer to plasma with well sustained current and well controlled density)

A better control of the plasma density with a lower recycling was observed as a macroscopic effect: fig. 2.3 shows that the time evolution of the electron density in a plasma discharge following Li deposition is well correlated to the gas puffing pulses. In particular, density decreases after the gas pulse (with a delay due to the effective gas entrance into the plasma after the inlet valve pulses), which is a clear sign that recycling R<1. The operational advantage of a better density control allowed increasing the plasma density at high plasma current up to $ne/n_G \approx 0.5$, expanding the region of the Greenwald plot filled by RFX-mod (fig. 2.4). In addition it was observed that when the wall is Li conditioned a higher feeding rate is necessary to sustain the plasma density. This behavior is associated to a reduction of the recycling, in particular at high density, as shown by the behavior of H influxes in fig. 2.5. Nevertheless, different trends were observed at two toroidal locations, one (left plot) close to the evaporator and the second one 90° apart (right plot). In the first case the H influx was significantly lower with a Li conditioned wall, especially at high density (3-fold decrease). On the contrary, the same effect was not seen far from the evaporator, where lithization has little or no influence on H influx: this on the one hand demonstrates that lithization is effective in reducing recycling, while on the other hand shows that with one evaporator the uniformity of the coating is an issue.

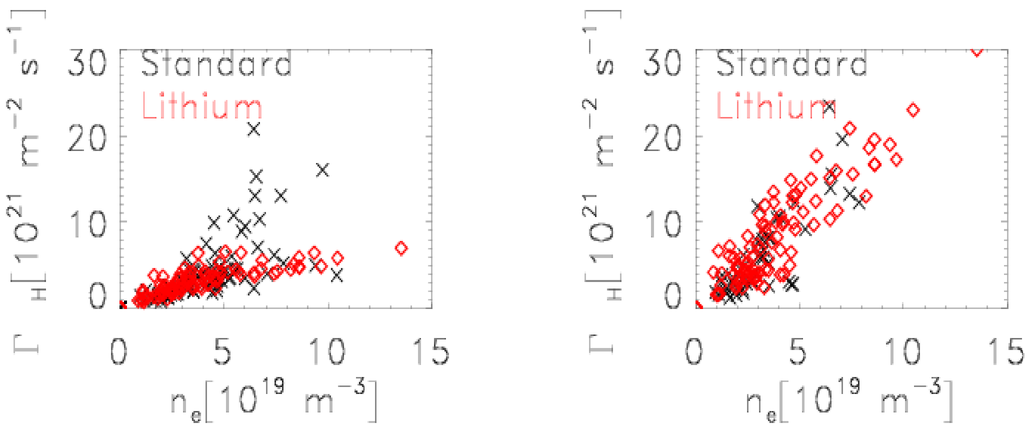

Fig. 2.5: hydrogen influxes close to the evaporation toroidal location (left) and at about 90° (right)

Though reduced, the recycling with lithium coated wall, evaluated by experimental data, remained close to 1, ranging between 0.95 and 0.99 and never exceeding 1, as it easily occurs in standard discharges (fig.2.6). As to the impurity behavior, Li conditioning reduces significantly oxygen and carbon influxes. The effect on oxygen is similar to that of boronisation with a reduction of a factor 2 with respect to the carbon wall, while the reduction of carbon influx is more pronounced. The effect on density and density profiles at the edge was found to be similar to what observed in past experiments with single Li pellet injection, with lower edge density and more peaked profile. Data from Thomson scattering show, in some cases, an effect on the edge temperature, somewhat higher: an example, comparing two similar shots, with and without Li conditioning, is given in fig.2.7. The effect on the core density profile, if any, was modest.

Following the positive experience made in the past years with the single Lithium pellet injector, that showed a good toroidal distribution of Lithium deposition and a measurable effect on plasma, a multi pellet launcher based on a dropper and a rotating impeller has been developed at Princeton and applied this year to RFX-mod (figures 2.8, 2.9, 2.10). With respect to the evaporator solution, the pellet technique has the potential advantage of allowing the deposition of a uniform and fresh Li layer in each discharge. A 4 weeks campaign allowed to test the device and to highlight the improvement that it will be necessary to design in order to have an effective lithization of the RFX first wall. During

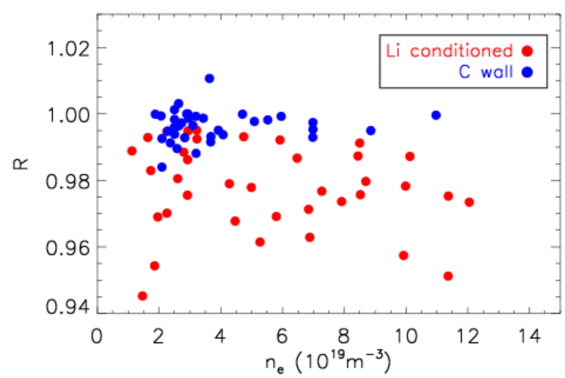

Fig. 2.6: recycling calculated in discharges with (red) and without (blue) lithium coated wall.

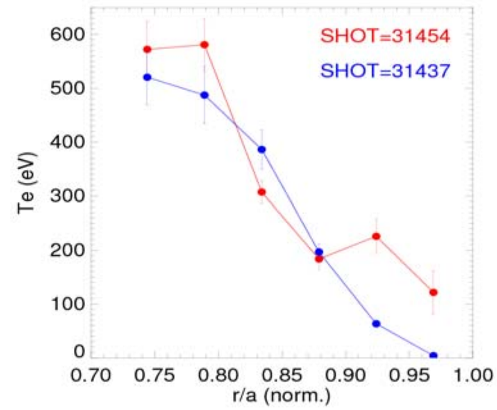

Fig. 2.7: edge electron temperature with lithization (red) and without (blue)

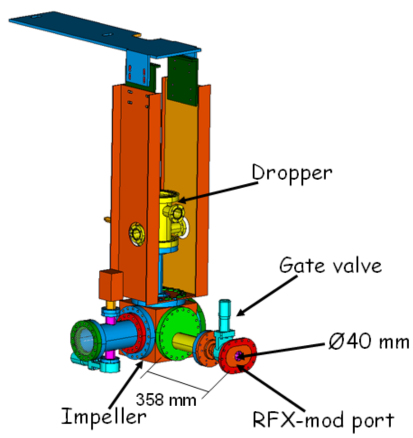

Fig. 2.8: drawing of the Lithium multi pellet injector

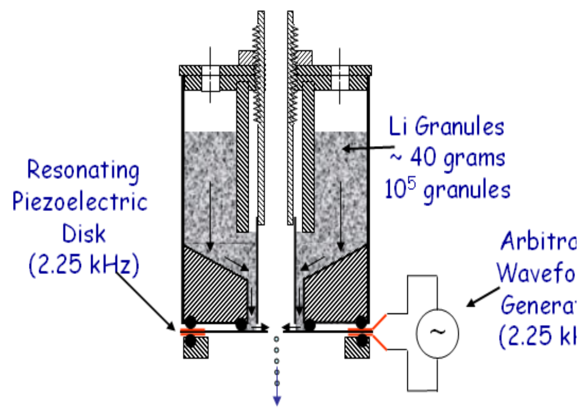

Fig. 2.9: drawing of the Li granule dropper apparatus

the experimentation, the injection of several pellets of diameter 0.76-1.05 mm, corresponding to 0.12-0.32 mg of Lithium per pellet respectively, with launch frequency up to 200Hz, during a single discharge was obtained. As an example, fig. 2.11 shows the injection of multiple Li pellets in He plasma. The masses of the pellets used with the multiple injector were very small in comparison to those of the single pellets injected in previous experiments (about 1/20), hence the repetition rate must be high in order to supply a significant amount of Lithium in the discharge: the 200 Hz would in principle be enough, but 2012 experiments showed that not all of the launched pellet entered the vessel, about half of being lost at the interface between impeller and vessel. Although during the experiments there was some indication from spectroscopic measurements of presence of Lithium all around the machine a deeper penetration of the pellets would enhance the toroidal uniformity of Li deposition. Actually, it was found that pellets did not penetrate much inside the plasma and the pellet ablation at the very edge of the plasma exposes to the risk of a prompt redeposition of Lithium.

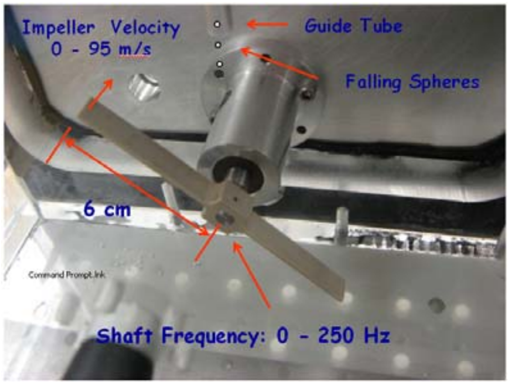

Fig. 2.10: the rotating impeller of the Li pellet launcher

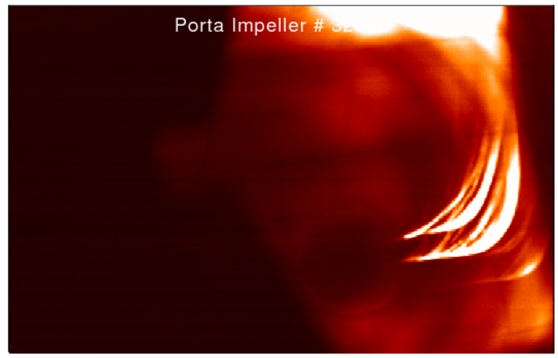

Fig. 2. 11: TV image of several Li pellets injected into a He discharge

The combined effect of bad coupling between injector and RFX, small masses and short penetration of the injected pellets made their effect almost negligible on the discharges. A design review of the injector has started and the modifications are planned in 2013. The main upgrade will be a new interface with RFX that will assure a higher flux of pellets into the vessel. At the same time, the modification should allow increasing the speed of the rotating wheel (at present limited to about half of its maximum value in order to maximize the pellet feeding efficiency), thus providing deeper penetration into the plasma.

The massive operation with Lithium injection in 2012 caused an additional issue when the machine was opened for maintenance, in order to prevent the formation of lithium carbide Li_2CO_3, which is difficult to remove due to the lack of direct access to the first wall. Several hours-long boronizations with cold and then hot wall before venting the vessel, minimization of the opening time and Argon flushing during opening have been adopted. These precautions were successful in preventing the formation of Li_2CO_3, as confirmed by visual inspection of the wall and by the fact that normal plasma operation were restored in typical times

In 2012 the characterization of GDC plasmas used to remove H from the wall has been done. He GDCs are efficient in extracting H_2 particles through physical sputtering. The cold weakly ionized plasmas have been characterized in different operative conditions by dedicated experiments with a set of diagnostics. More specifically, in addition to the traditional set of measurements of the GDC plant (equipped with gauges for anode voltage and current and in-vessel pressure measurement, and with a Residual Gas Analyzer-RGA), the voltage/current characteristic curves collected by a toroidal array of 72 equally spaced electrostatic probes have been analyzed, and the emission spectrum during GDC has been measured along 5 lines of sight (with different toroidal location and impact parameters). Finally, post-mortem analysis of graphite samples inserted at different toroidal locations has been performed to study the effect of GDC on the tiles. It has been found that in RFX-mod there is negligible effect of the Radio-Frequency assistance on the GDC effectiveness, in all the analyzed operative conditions. Moreover, as expected, a critical parameter is the anode current, rather than the discharge pressure: in fact H_2 extraction is more efficient when the anode current is increased. A toroidal non-uniformity in the ion flux to the wall is seen by both the electrostatic probe array and the spectroscopic diagnostics, with the flux having a Gaussian shape around the electrodes ≈30 toroidal degrees wide.

2.2.3 Transport studies

One of the most relevant topics related to transport analysis is the evaluation of the heat diffusivity profile χ_e in the region where the electron temperature profile exhibits a transport barrier during the SHAx states. The χ_e profile was evaluated during several SHAx by solving the energy transport equation in helical geometry method, using the helical equilibrium calculated by VMEC [GobbinEPS12] and the experimental T_e profiles (see fig 2.12). At the barrier the thermal confinement improves significantly, χ_e decreases to 5-10 m^2/s well below ~40-100 m^2/s typical of the outer regions [GobbinEPS12]. Furthermore, the ASTRA transport code, coupled to the RFX-mod helical equilibrium calculated by the perturbative code SHEq [Martines11], was applied to calculate the time evolution of the heat diffusivity profile by solving the heat transport equations. The time evolution of χ_e predicted by ASTRA and averaged in the barrier region agrees with the previously described evaluations and shows a progressive improvement of thermal confinement in the barrier region during the raising phase of the dominant mode. χ_e was evaluated on several SHAx plasmas, finding a weak increasing/decreasing trend with the secondary/dominant mode amplitude (see fig 2.13): at amplitudes of the normalized secondary modes greater than 0.8%, no cases of χ_e

below10 m^2/s were observed, meaning that a relevant fraction of heat transport is provided by magnetic stochasticity. Anyway the lowest values are greater than the corresponding neoclassical estimate of $\chi_{e,neo}<1$ m^2/s, indicating that other mechanisms are still deteriorating the confinement.

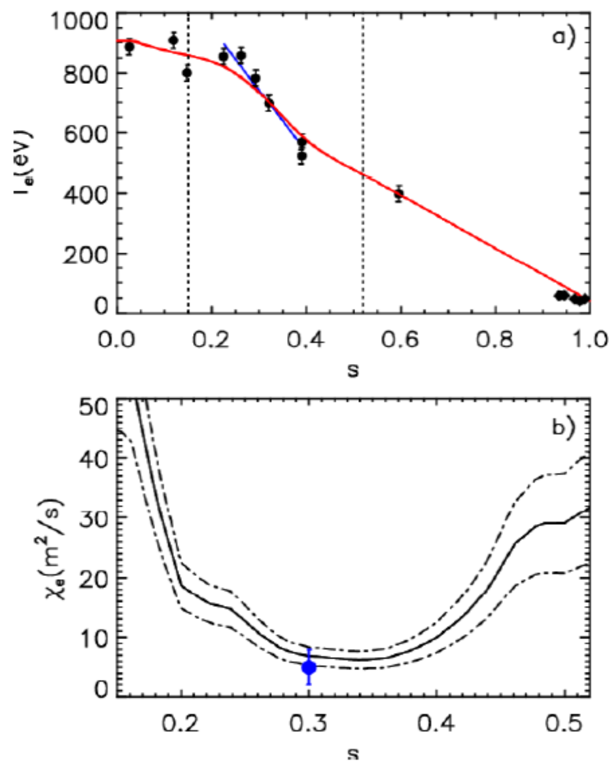

Fig 2.12: Example of T_e profile during QSH. Dots: data from DSX3 (circle) and edge (squares) diagnostics; the red line is a spline, the blue straight line is a linear fit in the barrier region. (b) Corresponding x_e profile in the barrier region obtained by using the spline (black solid line with errors given by the dashed ones) and the linear fit (blue dot).

In particular, linear gyrokinetic calculations by means of the GS2 code show that Micro Tearing (MT) modes are prone to become unstable during SHAx states [Predebon10]. Recent experimental observations confirm the presence of MT in RFX-mod plasmas in good correlation with the existence of the transport barrier. In particular, by means of highly resolved three-axial magnetic probes located at the plasma edge, quasi-coherent modes with extremely high toroidal and poloidal mode numbers (m/n ≈ 15/200) have been identified and characterized. Such wavenumbers imply a resonant condition *q(r) = m/n,* which is satisfied in the region where the maximum ∇T_e gradient forms. The experimental spectrum is found to be in good agreement with the linear predictions for MT modes, as shown in fig. 2.14, in particular when less sheared non-axysimmetric (and more realistic) q-profiles are considered in the calculations. The interpretation of the observed small-scale electromagnetic instabilities in terms of MT modes is reinforced by the agreement between the measured phase velocity and the theoretically predicted electron drift one, and by the dependence of the mode amplitude on the a/L_{Te}, where L_{Te} is the logarithmic gradient of the electron temperature, and on the normalized plasma pressure β.

MT instabilities make electron heat transport increase through the emergence of magnetic island chains and consequent field line stochastization; the related magnetic field perturbation *b* (perpendicular to the equilibrium magnetic field *B*) can be estimated through the quasi-linear expression $b/B \sim \rho_e/L_{Te}$. This estimate has proved to be quite accurate when compared to nonlinear gyrokinetic simulations in tokamak plasmas.

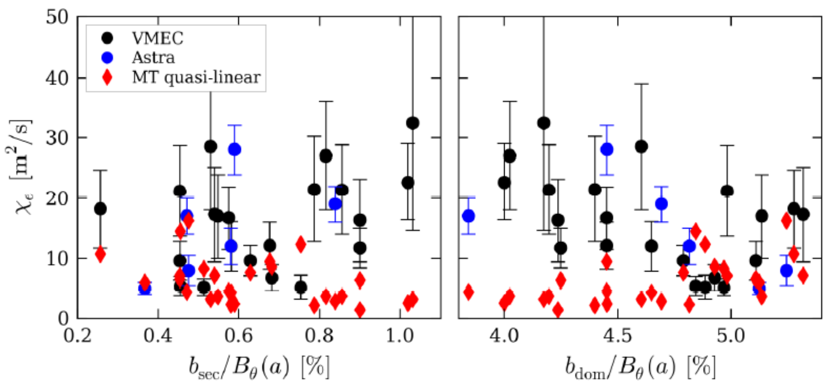

Fig 2.13: Values of χ_e estimated by using VMEC(black) and ASTRA (blue) for several SHAx cycles versus secondary mode (left) and dominant mode (right) normalized to the field at the edge B(a). Evaluated electron heat diffusivity due to the Micro Tearing modes χ_{MT} versus secondary mode and dominant mode is shown in red.

The heat diffusivity due to MT turbulence can be deduced by using the collisionless Rechester-Rosenbluth estimate $\chi_{MT} \sim (b/B) v_{th,e} L_c$, with $v_{th,e}$ electron thermal speed, and L_c longitudinal field correlation length, which for the RFP is roughly $L_c \sim 2\pi a$ [Predebon10]. Assuming a well developed MT turbulence, this evaluation of the conductivity has been applied to the SHAx barriers analyzed with VMEC/ASTRA: an increasing trend of χ_{MT} with the strength of the dominant mode and decreasing with the secondary modes is found (see fig 2.13). It turns out that $\chi_{MT} < \chi$ over most of the range, and $\chi_{MT} \sim \chi$ for $b_{dom}/B_\theta(a) > 5\%$, where b_{dom} is the amplitude of the dominant mode. The contribution of MT turbulence for low values of the dominant mode is in fact expected to be minor, these cases being typically characterized by not very high T_e gradients and thus rather weak excitation of MT instabilities. On the other hand, high values of b_{dom} lead to the best performances in terms of transport barriers, which correspond to a favorable condition for the onset of MT turbulence. In these cases MT modes provide about the whole amount of electron heat transport calculated with VMEC/ASTRA and are therefore good candidates as the mechanism that drives transport at the barrier.

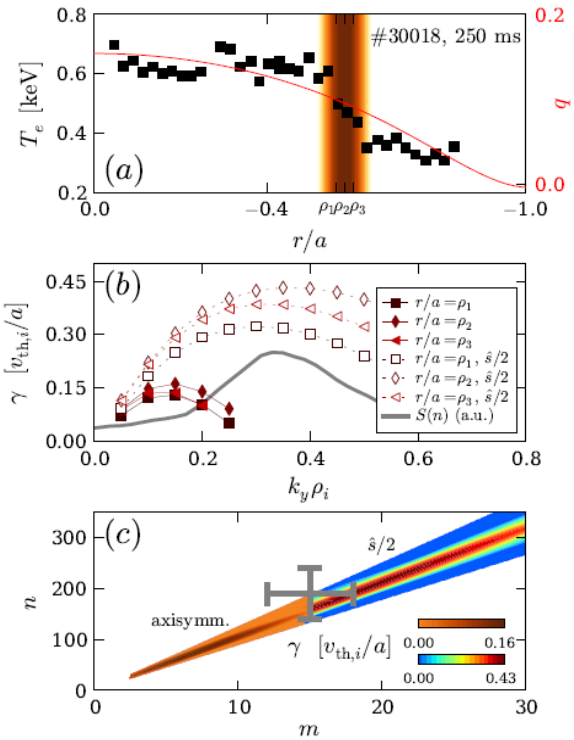

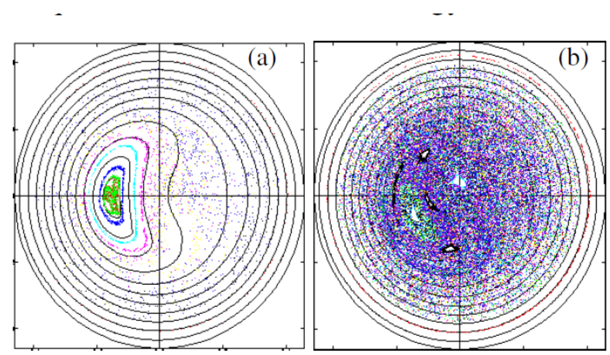

Fig. 2.14: For the shaded area of frame (a) the growth rates of the most unstable modes (all with micro tearing parity) as a function of the wave number $k_y\rho_i$ are in (b), solid symbols; open symbols represent the same dataset with q profile artificially flattened, s = s_{exp}/2, being s the magnetic shear; the gray line is the experimental spectrum S(n); in (c) the spectra are exploded on the (m, n) plane, with the experimental estimate of the measured wavenumbers at the edge (gray error bars).

Fig.2.15: Poincarè plot #24599, t=0.098 s. a) With m=0,1 modes; b) with m=0,1,2 modes.

The appearance of the thermal barrier in the QSH states is directly linked to the reduction of magnetic stochasticity in the plasma core thanks to the low level of the m=1 secondary modes. To show the effect on the magnetic surfaces of the m=0,1 secondary modes, the Poincarè plot has been drawn, by the field line tracing code FLiT. The residual magnetic chaos in the external region (fig 2.15) can still provide the anomalous transport observed in such region, while in the plasma center the m=0,1 modes provide good nested magnetic surfaces. To explain the anomalous transport and the flat T_e profile observed inside the transport barrier (see fig 2.12) a model for self-consistently generated vortical drift motion due electrostatic turbulence has been proposed [Sattin11] and more recently the effect of magnetic chaos produced from m=2 modes has also been evaluated. It is worth to be noted that errors affecting the evaluation of the m=2 tearing mode eigenfunctions from external measurements are typically twice those affecting the m=1, with one order of magnitude amplification of the edge measurement error. Only after the recent correction of Bt-Bp edge probes crosstalk an acceptable uncertainty in the evaluation of m=2 eigenfunctions has been reached. The inclusion of m=2 modes destroys nearly completely the core magnetic surfaces (fig 2.15b) while magnetic stochasticity in the region outside the transport barrier experiences only a slight increase. The evaluation of χ_e, according to the Rechester-Rosenbluth (RR) relation, $\chi_e = D_M v_{th}$, yields values close to those from the energy balance except at the position of the transport barrier, which vanishes with the inclusion of the m=2 modes (fig 2.16). Such discrepancy could be ascribed to the errors in the evaluation of m=2 modes and/or on the evaluation of magnetic diffusivity D_M. An increase of the number of magnetic sensors, included in the upgrades proposed for RFX, would allow the control of the m=2 modes.

Particle transport

The experimental electron density profiles, measured with a CO2 multi-chords interferometer, have been very recently reproduced with the ASTRA code by varying as input to the code in a minimization procedure the particle diffusion coefficients D in the centre, at the edge, and the pinch velocity V. The diffusion coefficient is assumed to be $D(\rho)=D_0(1-\rho^a)^b+D_a\rho^{15}$, and the velocity is given by $V(\rho)=V_{ExB}+V_{out}[\rho_1,\rho_2]$, where V_{ExB} is the inward pinch velocity and the term $V_{out}[\rho_1,\rho_2]$ is not zero only in the region $[\rho_1,\rho_2]$ of the internal temperature gradient. D and V are varied until the difference between the measured and simulated density profile is minimized. The analysis has been done in stationary conditions for a database of 10 SHAx states, with I_p=1.6-1.8 MA, at different average densities. Inside the thermal barrier, the average value of the particle diffusion coefficient results smaller by a factor about 2-3 with respect to the MH regimes, the pinch velocity is outward, of the order of 10 m/s, lower than the velocity required by a transport in a stochastic field. The outward velocity does not show a dependence on the normalized temperature gradient, confirming that particle transport in RFX-mod in QSH regimes is no more ascribable to stochastization of the confining magnetic field.

Transient phenomena allow to better quantify the diffusion and convection terms in the electron transport equation and ASTRA code has been recently used to simulate the density time evolution after pellet injection in SHAx regime (#30052, see fig 2.17). The experimental density profiles have been satisfactorily reproduced by assuming an outward velocity localized at r/a~0.9 during the MH phase (green curve in fig 2.17c) and at the position of the internal temperature gradients in the SHAx phase (pink curve, fig 17c). The outward velocity in the SHAx phase is lower than what expected for particle transport in a stochastic field, in analogy with the results of the simulations of the stationary cases. In the central region, the average value of the particle diffusion coefficient during the SHAx phase results smaller by a factor about 5 than in MH. It is worth to be noted that the spatial resolution of the 13 channels interferometer limits spatial resolution of the evaluated D and V, preventing the precise evaluation of the transport reduction in the barrier region. This could be the reason why the D reduction results smaller than the χ_e reduction at the transport barrier and occurs in a wider region.

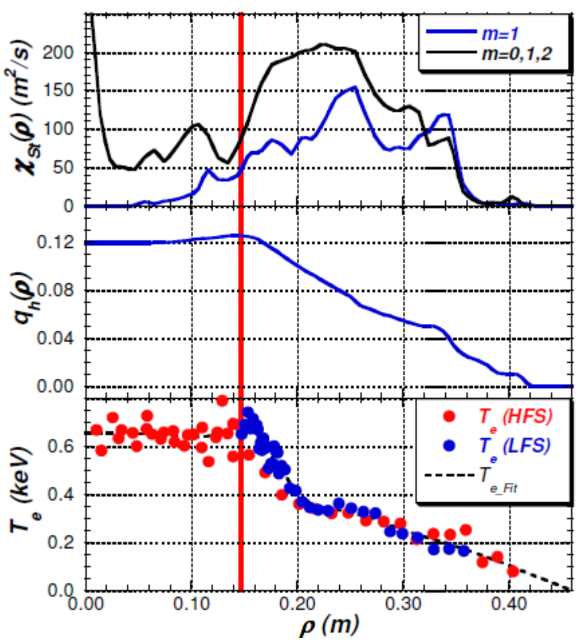

Fig. 2.16: #24599, t=0.098 s, from top to bottom: Magnetic thermal diffusion computed with and without m=2 modes, computed safety factor and experimental Te profile

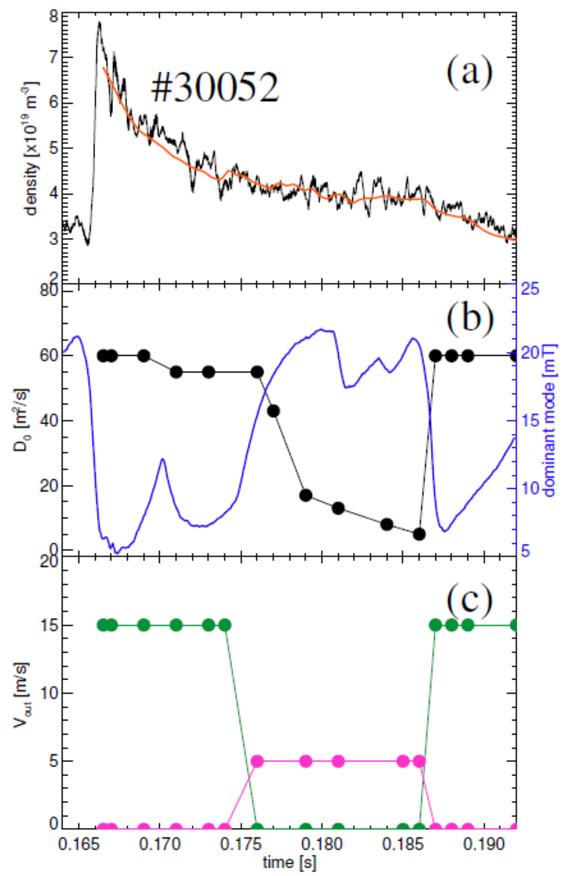

Fig 2.17: (a) Central line-integrated density as measured by the CO2 interferometer and simulated with ASTRA (red). (b) Time evolutions of central D_0, and of the dominant MHD mode amplitude (c) Time evolutions of V_{out}: green in MH phase(r/a=0.9), pink in SHAx phase (at the ITB location).

2.2.4.1 Edge turbulence and transport in the helical boundary of RFX-mod

The helical shaped plasmas obtained in high current RFP regimes reveals physical properties of the edge transport with profound analogies with other configurations. Although the residual helical ripple at the edge is very little [Gobbin11] it is sufficient to modulate all the kinetic properties of the plasma edge [Vianello12]. The experimental observations described so far have shown a strong correlation with the measured plasma displacement $\mathbf{D_r^{1,7}}$ of the pressure, the Plasma Wall Interaction (PWI) and the floating potential [Scarin11]. In order to better compare measurements performed at different poloidal and toroidal angles in relation to the inherently 3D magnetic topology, we introduce the definition of the helical angle *u,* which is equal to:

$$\upsilon = m\,\tilde{\theta}\,n\,\phi\,\varphi_{m,n}$$

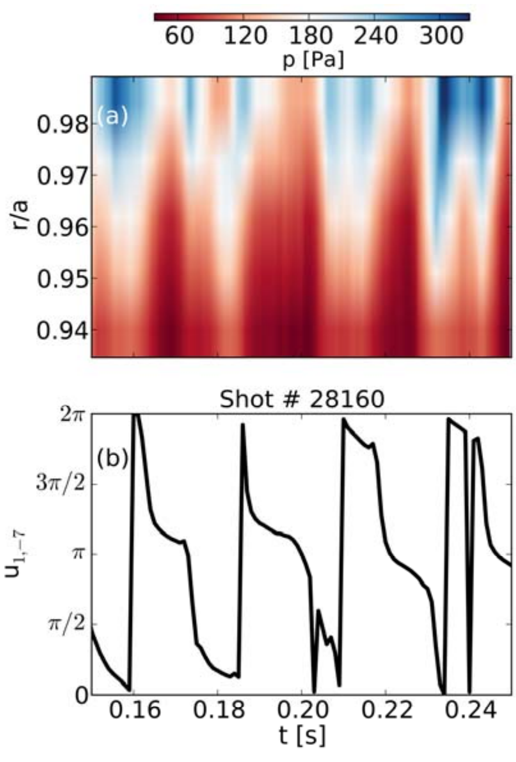

Fig 2.18 (a) Pressure profile as a function of normalized Larmor radius and time (b) Helical angle at the toroidal and poloidal position of the THB

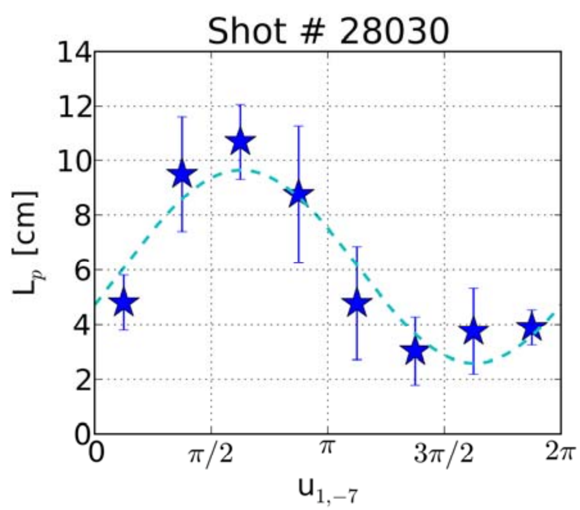

Fig 2.19 Pressure characteristic scale length as a function of the helical angle

The modulation of edge quantities so far compared with the plasma shift exhibits a clearer helical pattern whenever the same quantities are considered as a function of the helical angle *u.* As an example the pressure profile as a function of normalized minor radius and time is shown and compared to the corresponding helical angle in Fig 2.18. The profile oscillates in time, as reported also in [Agostini12], with higher values of pressure corresponding approximately to $u \approx 0$. A comprehensive picture can be drawn considering the evolution as a function of u of the pressure characteristic scale length $L_p = (\nabla p/p)^{-1}$ shown in Fig. 2.19.

The sinusoidal shape reveals the helical modulation of the entire pressure profile at the edge. Similar observation can be drawn for Plasma Wall Interaction as both particle influxes as estimated from H_α, impurity brightness and total radiation exhibit similar sinusoidal shape [Vianello12b]. These observations are consistent with recent experiments on DIII-D where the use of rotating RMP perturbation causes a consistent modulation of the signals from Beam Emission Spectroscopy and Reflectometer [Moyer12]. Also plasma velocity exhibits a helical modulation. Actually flow at the edge of an RFP is predominantly in the toroidal direction, i.e. perpendicular to the local field. The use of correlation techniques on the arrays of pins pertaining to the ISIS diagnostic allows the determination of the toroidal map of the perpendicular flow [Vianello12, Vianello12b]. Owing to the small diamagnetic contribution [Spizzo12] the observed helical velocity perturbation is translated into a perturbation of the radial electric field, shown as a function of the helical angle u in Fig 2.20. The estimate obtained from the ISIS diagnostic shown in panel (a) in blue symbols is compared with the estimate from the velocity fluctuations of the GPI diagnostic. Both measurements show the sinusoidal pattern of the electric field, thus showing that the helical ripple is sufficient to modulate the entire electric field radial profile in a region of few cm from the wall. An effort is in progress to simulate this behaviour in terms of different ion-electron diffusion rate caused by the modulation of the parallel connection length to the wall induced by the helical topology. The previous estimate of the electric field allows the reconstruction of a map of the electric field fluctuations at the wall as a function of toroidal and poloidal angle as shown in Fig. 2.20b.

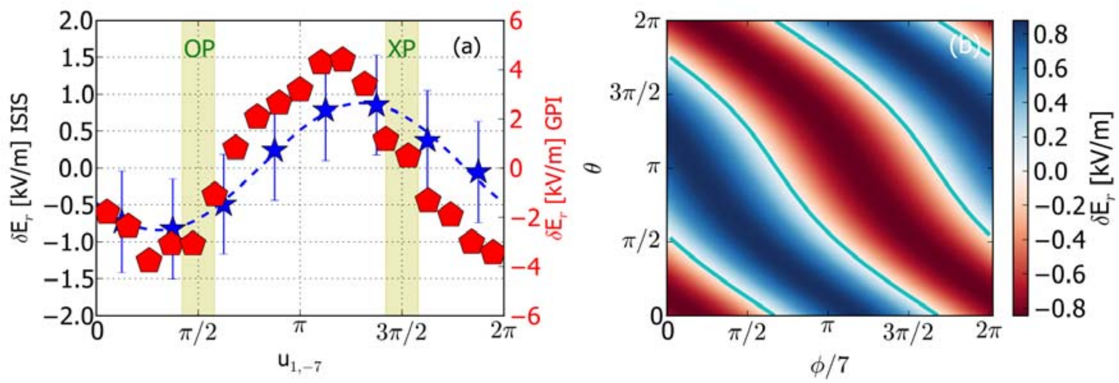

Fig 2.20 (a) Radial electric field fluctuations estimated from velocity fluctuations from the ISIS diagnostic (blue) and from the GPI (red) (b) Reconstructed poloidal and toroidal electric field fluctuations 1/7 period of the torus

The modulation of the flow and of the profiles has a natural consequence also on the modulation of small scale turbulence [Agostini12]. Radial and toroidal correlation lengths have been estimated from the GPI diagnostic: as shown in Fig. 2.21 they feature a sinusoidal behaviour as a function of the helical angle. These quantities may be interpreted as an estimate of the characteristic scale lengths of the blobs, thus suggesting that blobs internal structures is sensible to the modulation of the electric field. In a similar way the power spectral density of the fluctuations of both potential and density exhibit a helical modulation [Agostini12,Spolaore12] thus supporting the idea that the large scale magnetic perturbation influencing flow and profiles at the edge is acting also on small scale electromagnetic turbulence.

Indeed, changes in the pressure profiles have been shown to modify the entire spectral properties of the high frequency fluctuations. From the measurements of the k-spectrum of the fluctuations obtained through the GPI diagnostic it has been shown [Agostini12] that the toroidal dimension of the edge blobs is proportional to the spatial injection scale of the energy in the system λ* (see figure 2.22), and that this scale also represents the largest coherent structures (blobs). Moreover, the magnetic topology modulates the local distribution of the blobs, modifies the edge flow and hence the edge electric field with a stretching effect on the coherent structures at higher densities. According to these observations, not only has the plasma core of RFX-mod a helical shape, but also the boundary plasma, where all the edge properties are influenced by the magnetic deformation.

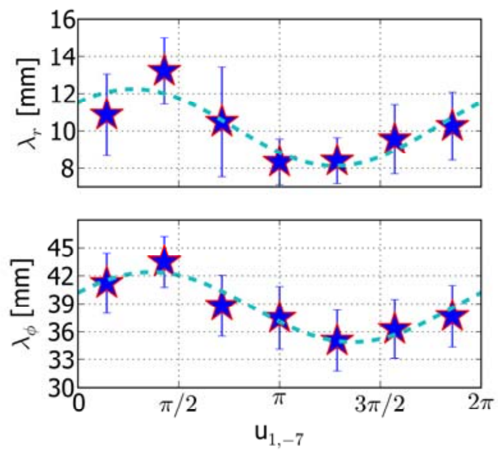

Fig 2.21 Radial (top) and toroidal (bottom) correlation length as a function of the helical angle

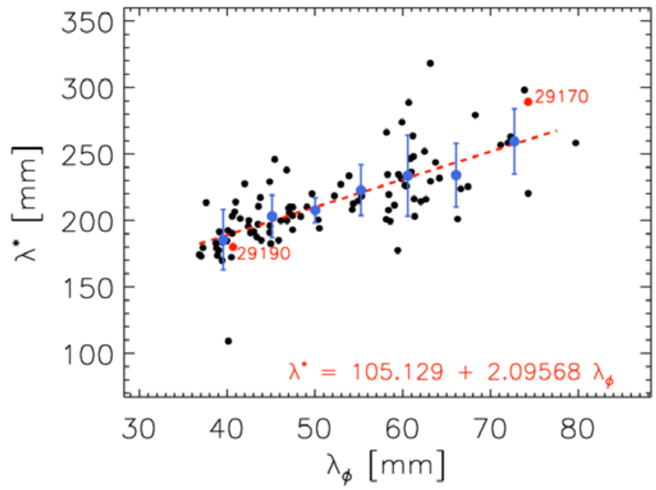

Fig. 2.22 Spatial injection scale of the energy λ* versus toroidal correlation length of edge fluctuations λ_ϕ. Each black point represents one plasma discharge, averaged during the current flat-top; the blue points are the averages with their rms value, and the line is the linear fit.

2.2.4.2 Long range correlation and magnetic topology

A very preliminary analysis has been devoted to the study of the macro-scale transport features in the RFX-mod edge. In particular, the presence of long-range (d_{corr}~1 m) correlations in a set of reproducible low plasma current discharges has been highlighted by the insertion at different radii (up to 5 cm) of two insertable probes (the so called U-probe and Gundestrup probe) 30° degrees toroidally separated and equipped with

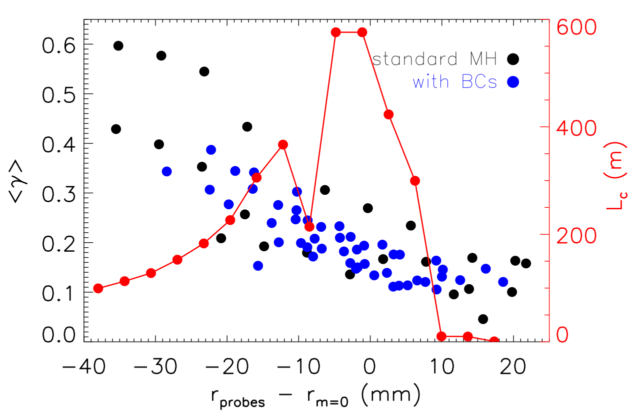

Fig. 2.23 Radial profile (plotted as a function of the relative radial position of the probes r_{probes} with respect to the q=0 surface $r_{m=0}$) of the average correlation <γ> (blue and black) between the electrostatic pins of the U-probe and the Gundestrup probe. The radial of the connection lengths L_c are also shown (red).

several electrostatic pins collecting floating potential. Fig. 2.23 shows the radial profile of the cross-correlation <γ> averaged over the flat-top phase of each pulse. A significant correlation (γ > 0.3) has been found only for probe insertions r_{probes}>35 mm. More in details, the correlation profile seems to be linked to the underlying magnetic topology and in particular to the presence at the edge of a chain of m=0 islands featuring good conserved flux surfaces (the associated connection lengths L_c are also shown in fig. 2.24) and poloidal geometry (due to the presence of a q=0 surface). This could explain why at the radial position of the islands, $r_{m=0}$, no correlation can be observed. The more internal regions, exhibiting a more toroidal magnetic pitch angle and finite L_c, could allow the formation of macro-structures with a significant toroidal extension and responsible for the observed correlation. A more accurate analysis is still in progress.

2.2.5 Advancing feedback control of MHD stability in fusion devices

Several advances have been obtained during the last year on the field of MHD feedback control with active coils in terms of new experiments and analysis of past experiments, modeling work, and development of new real-time control software and hardware, as recently reported in [Manduchi12]. It is worth saying that a deep integration of experiment and modeling characterizes most of the RFX-mod activities in this field. In particular, RFX-mod is providing useful data to benchmark codes that are used to model and design new control schemes for large tokamaks and ITER.

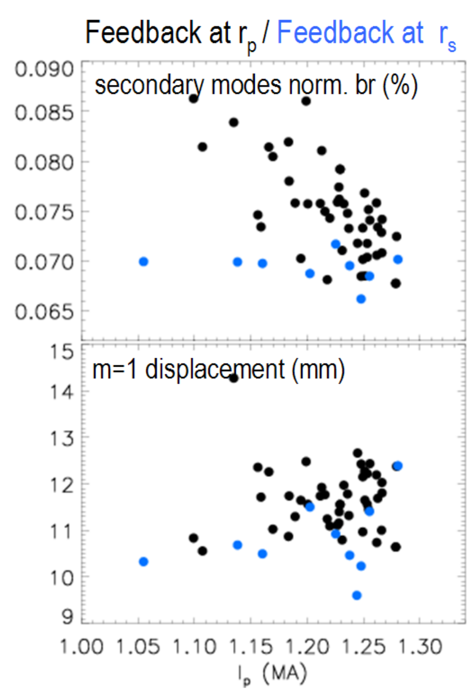

Fig.2.24: Secondary mode amplitude and maximum displacement associated with the m=1 modes for two similar sets of discharges with mode control at plasma (black) and sensor radius (blue).

Modeling of the tearing mode dynamics with the RFXlocking code, which combines a model of the tearing mode dynamics and a detailed description of magnetic feedback, has recently suggested a modification of the present algorithm used for tearing mode control, namely the so-called Clean Mode Control (CMC). The present CMC algorithm uses the radial field harmonic computed at the plasma radius, which requires the additional acquisition and real-time processing of 192 toroidal field measurements. RFX locking simulations suggested that comparable feedback performance can be obtained using radial field measurements at the sensor radius, avoiding the extrapolation step. Experiments confirmed this prediction and actually showed that a slightly better performance can be obtained in this way. This is shown in Fig. 2.24, which reports the secondary mode amplitude as a function of plasma current for similar discharges with feedback at plasma radius and at sensor radius. The new approach permits to spare a significant number of real-time acquisition channels and to simplify the real-time calculations.

Feedback control of tearing modes is particularly important in determining the interaction of the plasma with the wall. In particular, the properties of the Scrape Off Layer (SOL) in SHAx states are determined by the chain of m=0, n=7 magnetic islands [Martines10] that cause the typical helical pattern in the plasma-wall interaction and density accumulation. The application of m=1/n=7 3D boundary conditions through the magnetic feedback stimulates the occurrence of helical states in the plasma core, whereas new experiments done during this year have shown that the additional application of m=0/n=7 helical boundary conditions strongly affects the edge region, enlarging the m=0 island chain and the SOL volume, and inducing the formation of a dense and cold edge. These results summarized in Fig. 2.25 constitute a step towards an optimized helical RFP with controlled plasma-wall interaction.

Significant progress has been made in the field of resistive wall mode (RWM) control both in RFP and tokamak plasmas. The CarMa model, which includes a description of the plasma linear stability and a realistic description of the RFX-mod 3D wall and of its magnetic feedback system, has been validated against new experimental data. Recently an enriched version of the dynamic model has been developed, featuring the plasma response of RWMs with abs(n)=1, 2, 3, 4, 5, 6 [Marchiori12]. This is important to analyze the effect of a reduced set of coils, since it allows the simultaneous study of modes which could be amplified by the low n order sidebands produced by the coils through Resonant Field Amplification.

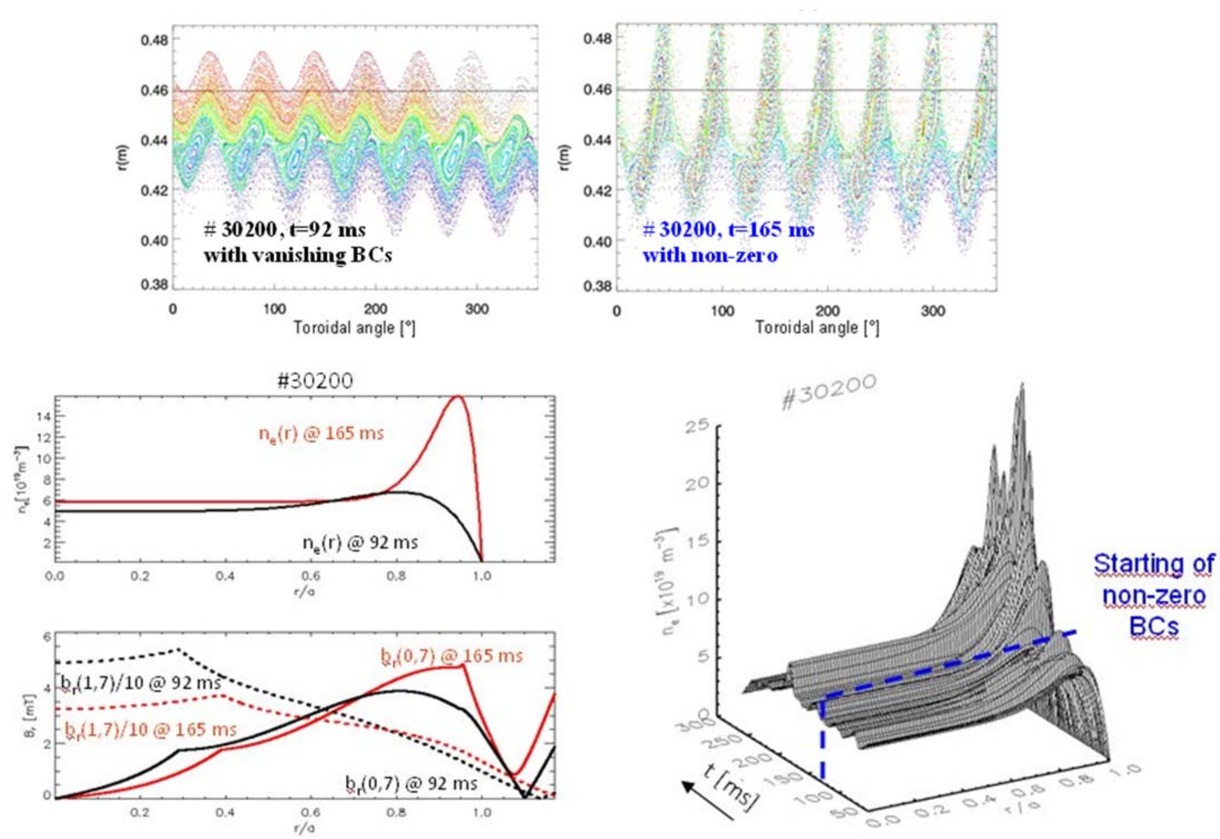

Fig.2.25: (UP) Poincarè plots at two different time instants: with and without the application of 3D boundary condition on the m=1/n=7 and m=0/n=7 modes. (BOTTOM) Density profile reconstruction (top) and m=1/n=7 and m=0/n=7 mode eigenfunction profile reconstruction (bottom) at two different time instants: with (red) and without (black) the application of 3D boundary condition on the m=1/n=7 and m=0/n=7 modes.

To investigate the reliability range of the model, dedicated experiments were also run destabilizing marginally stable modes by means of negative proportional gains in the control loop. Fig. 2.26 reports some results obtained with such approach applied to the m=1, n=3 RWM, showing the good agreement with the experiment. This new multi-modal version of the CarMa model, carefully validated as described above, has been then applied to interpret RWM control experiments in the RFP with a reduced set of active coils [Marchiori12].

The data obtained in the past in tokamak configuration with a reduced set of coils are being analyzed and a first series of results has been recently published [Baruzzo12].

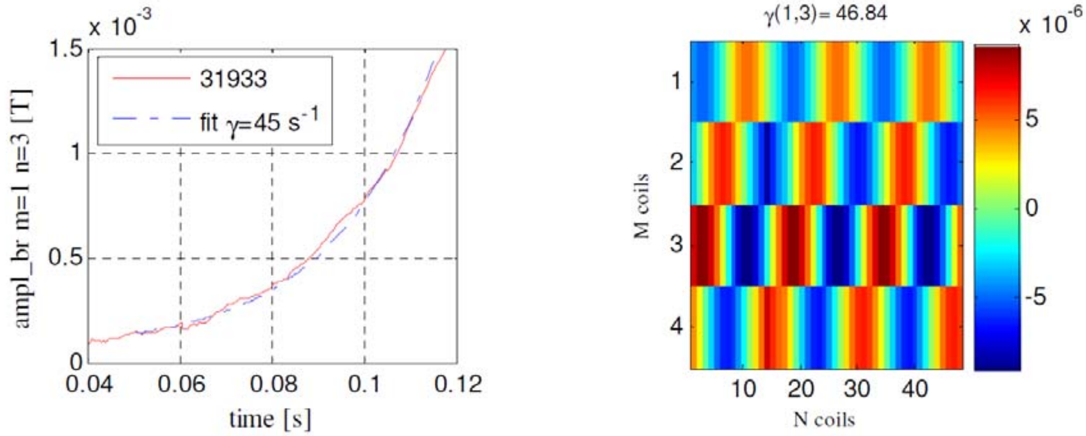

Fig.2.26: Destabilization experiments: in the left plot time evolution of (1, 3) harmonic component and exponential fit; in the right plot output associated to the most unstable mode exhibiting a clear (1, 3) pattern.

The explored configurations of reduced coils are 48 × 1, 24 × 1, 12 × 1, 6 × 1 and also 6 × 2, using six mid-plane coils and six upper coils located at the same toroidal angles as the mid-plane ones, to mimic as much as possible the situation typical of large D-shaped tokamaks. RWM control was successful with all sets of coils, using only proportional gain. An example of the effectiveness of different coil configurations is summarized in Fig. 2.27. These results give information not only on the minimal coil set able to stabilize a RWM, but also on the physics of this instability, in particular as far as mode rigidity is concerned.

An innovative algorithm to identify the linear response of the coupled system composed of the plasma, the 3D wall, and the feedback coils acting on the plasma have been recently developed by KTH. This new approach was initially developed in experiments at the Extrap-T2R device and applied during the last year also to the RFX-mod experiment, thanks to collaboration with the KTH group. The approach consists in injecting in the feedback loop a dithering disturbance, both with and without plasma. This disturbance is able to probe the response of the overall system over a wide range of spatial and temporal scales. The first results obtained in these experiments are being analyzed and will be the subject of a future publication [Olofsson12].

A significant upgrade of the RFX-mod real-time control system is underway and regards both MHD and axi-symmetric controls [Manduchi12]. The real-time control system of RFX-mod, in operation since 2005, was designed to fulfill the requirements of controlling

RWMs with the Virtual Shell algorithm. Mitigation of Tearing Modes with the Clean Mode Control was found to require more complex algorithms and three times more control signals than originally designed. The increased requirements limited the cycle frequency to 2.5 kHz and the increased number of signals and real-time computations introduced an overall latency of 1.5ms. In order to enhance the computing power and reduce the system latency, a major upgrade of the system has been designed, based on a new architecture, taking advantage of the rapid evolution of computer technology in the last years

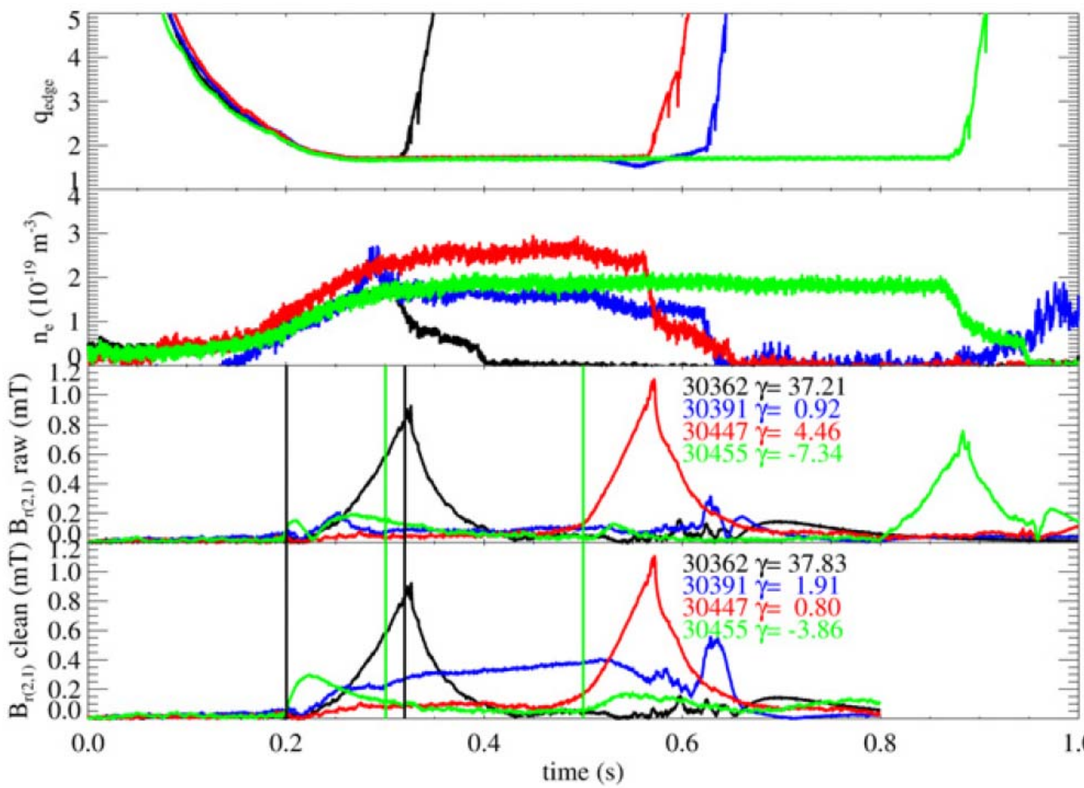

Fig.2.27: Time evolution of discharge parameters in different coil configurations: in the first panel the magnetic safety factor at the plasma edge is shown, in the second the electron density, in the third the m = 2 n = 1 radial magnetic field component and in the fourth the clean m = 2 n = 1 radial magnetic field are shown. Pulse 30362 (black) is a standard discharge without active MHD control, in pulse 30391 (blue) the m = 2 n = 1 radial magnetic field harmonic is controlled with the 48 × 1 outboard configuration from 0.02 s to the pulse end, in pulse 30477 (red) the (2, 1) component is controlled with the 12 × 1 configuration from 0.2 s to 0.5 s and in pulse 30455 (green) the (2, 1) component is controlled with the 6 × 1 with a first control window from 0.2 s to 0.5 s, no control for 20 ms and afterwards a second control window up to 0.8 s. The vertical lines are the intervals in which the mode growth rate has been calculated for the no control case (black) and for the controlled cases (green).

The central component of the new architecture is a Linux-based multi-core server, where individual cores replace the VME computers. The new architecture will merge into one server both the axi-symmetric controllers – horizontal equilibrium, toroidal field, and plasma current – and the MHD controller, allowing the latter to implement algorithms taking into account axi-symmetric quantities. The system is pervised by MARTe, a software framework for real-time applications written in C++, developed at JET, and currently used for the JET vertical stabilization and in other fusion dvices [Neto10]. Porting of the control algorithms under the MARTe environment and comparison with the old control system performance are ongoing activities.

2.2.6 RFP physics in a three-dimensional configuration

The analysis of the helical states has required an evolution both in terms of interpretative tools and experiments to be done in order to gain a better understanding and characterization of 3D effects.

The first step is the possibility to obtain an equilibrium reconstruction as much as possible determined through experimental data. Different approaches have been adopted on this topic: a non-perturbative approach with V3fIT/VMEC or the solution of the Helical Grad-Shafranov equation, and a perturbative approach with the SHEq code.

The use of the V3FIT code [Hanson09] coupled to the VMEC code [Hirshman83] as equilibrium solver can be now routinely used for equilibrium reconstruction in RFX-mod [Terranova10, Terranova11]. Significant improvements have been added to the reconstruction procedure in order to include as many diagnostics as possible to remove a possible degeneracy in the solution. As in the past the starting q profile is selected from a set of profiles determined according to the value of plasma current.

The electron temperature from the Thomson scattering and the electron density from the interferometer measurements can now be used with different T_e and n_e profile parametrization (polynomial, two-power, splines) and this allows a self-consistent inclusion of these kinetic measurements into the force balance equation thorough pressure. As no information is available on ions the same profiles have been assumed for ions and electrons and the ion pressure has been imposed to be a fraction of the electron one.

As it can be seen in figure 2.28 a reconstruction obtained using only magnetic data is unable to provide a correct fit to T_e measurements (dashed line). A better fit is obtained by including the pressure self-consistently.

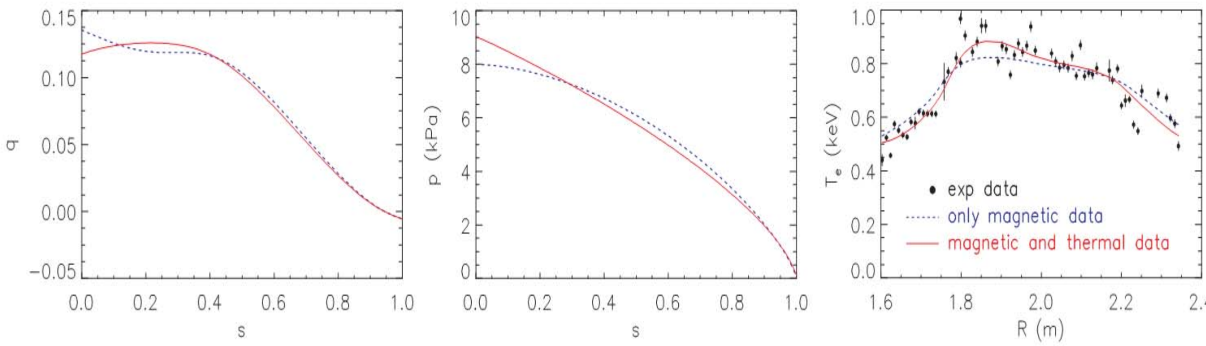

Fig. 2.28: q, pressure and T_e profiles for equilibria obtained using only magnetic signals and using also thermal signals.

The effect of pressure proved to be a significant improvement in many reconstructions, but it is not always a necessary constraint as in some cases the pressure effect is negligible due to low β values.

A significant improvement in the reconstruction was also obtained by constraining the q value at the edge. This was a requirement due to the limitation of the fixed-boundary approach where an indication on the axisymmetric part of the toroidal field at the edge is not possible by means of modelled diagnostics. To this end we designed in V3FIT a new synthetic diagnostic that computes the total current flowing in the toroidal winding system. As shown in [Terranova12] this proved to be a very effective solution.

The new equilibria are suitable for stability analysis with more realistic profiles (both for the magnetic field and pressure) and this will be part of next year's work.

As far as 3D effects are considered in the tokamak case, first attempts were made to obtain non axi-symmetric equilibria for the discharges observed on RFX-mod with a significant (m=2, n=1) mode in a way similar to what described in [Cooper11].

On the side of non-perturbative approaches, an iterative solution of Grad-Shafranov's equation in cylindrical geometry and helical symmetry has been developed in order to study the QSH-like phases of the RFX-mod experiment (see section 4.6 this Report). Even though a few numerical and mathematical tricks had to be applied in the procedure (i.e.: back-averaging technique, linear combination with Newcomb's eigenfunction), convergence has been reached and the final solution does satisfy the experimentally observed values of the radial and toroidal components of the perturbed magnetic field. A preliminary benchmark has been carried out by running VMEC under correspondent assumptions, showing promising agreement.

On the other side, considering a perturbative approach to helical equilibria, the code for the reconstruction of MHD mode eigenfunction in the plasma volume based on a Newcomb-like equation has been updated, so as to use a generic μ profile (instead of profiles resulting from the $\alpha-\Theta_0$ model). As a consequence, the SHEq code can now run with any parallel current density profile. Additional constraints derived from experimental data will allow determining the most likely shape of such profile.

Other codes devoted to the study of different physical phenomena such as gyrokinetic effects and Alfvènic modes have made use of VMEC equilibria.

As an example, as reported in sect. 4.3, work has started on GENE/GIST [Xanthopoulos09] codes coupled to VMEC equilibria to describe helical states.

In RFX-mod plasmas, perturbations with toroidal mode numbers *n* typically below 4 and frequency range between 100 kHz and 1.5 MHz have recently been identified as Alfvén eigenmodes by means of highly sensitive in-vessel magnetic probes. The nature of the modes has been identified by the linear relation between the frequency of the mode and the Alfvén plasma velocity.

In particular, two mode families have been recognized on the b_p spectra. One is composed of two eigenmodes at frequency above 400 kHz, which are present in almost all RFP plasmas, independently on the plasma conditions themselves. Such family has been recently interpreted as the sign of Global Alfvén eigenmodes (GAE), see [Spagnolo11]. The second one, appearing as three distinct eigenmodes in the frequency range from 100 to 400 kHz, occurs, instead, during the SHAx state phases of the discharge only.

An example of the power spectra of the poloidal field b_p signal deduced in a high plasma current condition is shown in fig. 2.29. One of the spectra (the green one), referring to a MH state, exhibits just the two GAE high frequency peaks. The other two spectra (black and red), evaluated during two distinct SHAx states are characterized by the occurrence of the three lower frequency peaks. The frequencies associated to the two time instants are different, accordingly with the variation of the Alfvén velocity in the two cases.

In order to propose an interpretation for such modes, with the aim of characterizing the role of the three dimensional equilibria on their occurrence, collaboration has been started with the Oak Ridge National Laboratory (Dr. D. Spong). The scope of such collaboration is to use the STELLGAP code, which can study Alfvèn continuum and gaps, along with their stability, in a wide variety of magnetic configurations. The idea is to study the undamped Alfvén eigenmodes, which could be easily destabilised by resonant energy transfer from energetic particles, using realistic RFX-mod equilibria, evaluated by means of the V3FIT code, constrained by the electron density and temperature profiles. The result of a test of the applicability of the code STELLGAP during a SHAx state is shown in fig. 2.30.

Power balance and heat transport analysis in RFX-mod plasmas featuring 3D helical magnetic topology have been performed thanks to the high time resolved T_e profiles obtained by a new double filter soft-X-ray (SXR) diagnostics recently installed (DSX3).

Electron temperature profiles are implemented in the heat transport equation, together with density measurements and resistivity, in order to determine the perpendicular electron thermal diffusivity χ_e. This procedure has required the reconstruction of the magnetic equilibria to estimate the safety factor profiles, the current density spatial distribution and the metric tensor in a suitable set of flux coordinates for helical geometry.

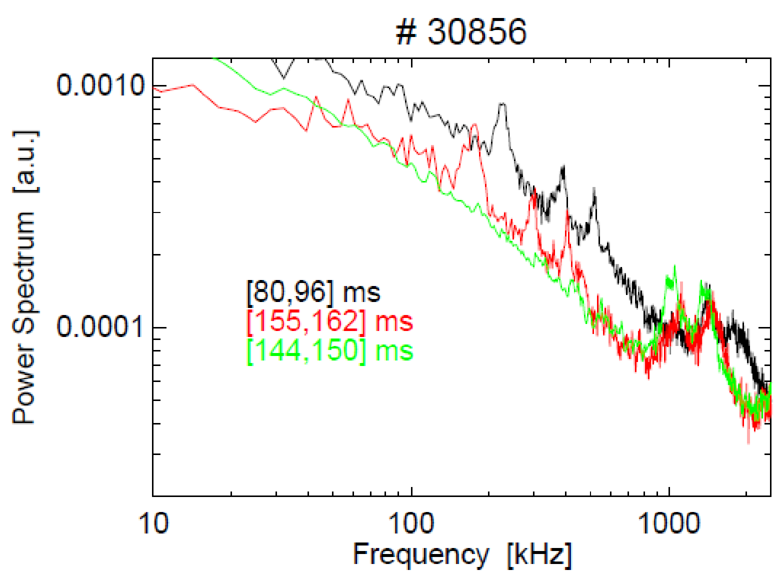

Fig. 2.29: Power spectrum of a b_p signal evaluated during three different time instants of a high plasma current discharge: black and red lines refer to SHAx states, the green one to an axisymmetric multiple helicity state.

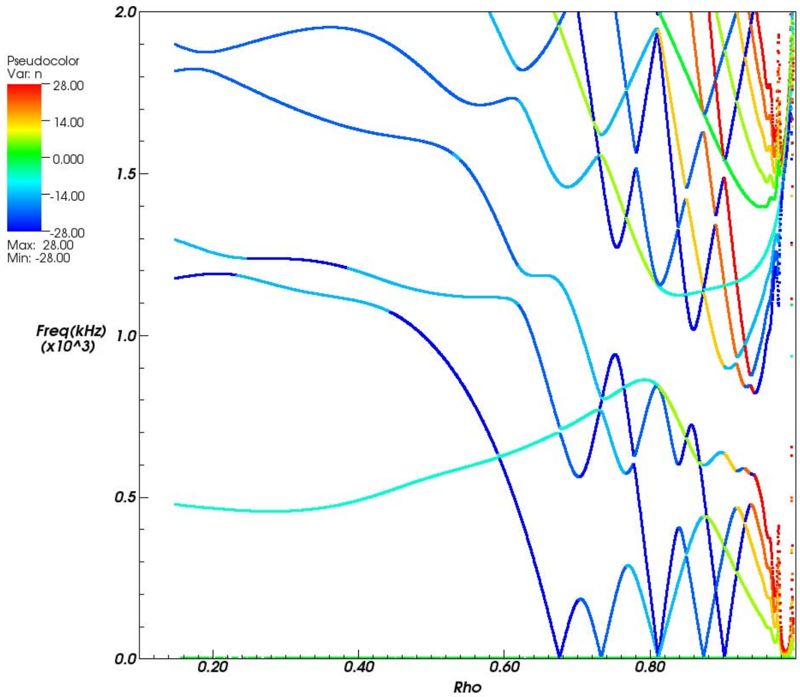

Fig. 2.30 Example of: Alfvén continua during a RFX-mod SHAx state as computed by the STELLGAP code. Different colours refer to the various toroidal mode numbers n.

The transport analysis has been performed both by a direct integration of the heat diffusion equation (with VMEC equilibrium) and using the transport code ASTRA [Pereversev02] (with equilibrium by SHEq) both in a stationary (i.e. for power balance studies) and in a dynamic operational mode. It has been shown that the time derivative of energy generally has a small effect on the χ_e determination, less than 5-10% thus negligible with respect to other source of errors.

As written above, some experimental campaigns were also dedicated to improving performances of helical states from different physical points of view such as increasing plasma density or extending the helical state duration.

Improved confinement SHAx regimes featuring a hotter plasma core and internal transport barriers are, presently, obtained only at medium-low densities. Higher n_e/n_G discharges are instead, more difficult to be sustained and feature quite a reproducible phenomenology characterized by localized plasma-wall interactions (PWI), an input power increase and edge density accumulation (with the typical hollow profiles) [Puiatti09]. This behavior could ultimately be related to the edge magnetic topology. In fact, when the machine operates in ultra-low q regime (F > 0.5, and thus without the presence of the m=0 islands at the edge), density profiles appear flat or peaked and the neutral particle penetration length increases by a factor ~100 [Auriemma07].

In this experimental campaign a way to exploit the aforementioned mechanism in order to obtain a more effective plasma core fueling has been tested. The idea consisted in puffing fueling gas during a phase of around 10-20 ms in which F is brought to positive values. According to the simulation, this experimental condition should allow an increased core penetration of the puffed particle. In fig. 2.31 the evolution of the density profiles for two discharges corresponding to two different gas puffing methods are shown: the traditional puffing during a negative F phase produces the typical hollow profile (red curves), while, when the gas puffing is applied on a F≥0 window, profiles become first peaked (dashed blue curve), allowing a better penetration of the puffed gas, and finally flat (blue continuous curve). This final condition opens the possibility to stimulate higher n_e/n_G SHAx states.

In 2011, an experimental activity has been proposed inspired by the markedly different features of chaos development in numerical cases characterized by resonant or non-resonant QSH states, in favor of the latter [Section 2.2.3, this Report]. The idea was to build up a non-resonant helical RFP equilibrium, i.e., a helical RFP state with non-resonant dominant mode in RFX-mod. The results of these experiments are reported in section 4.

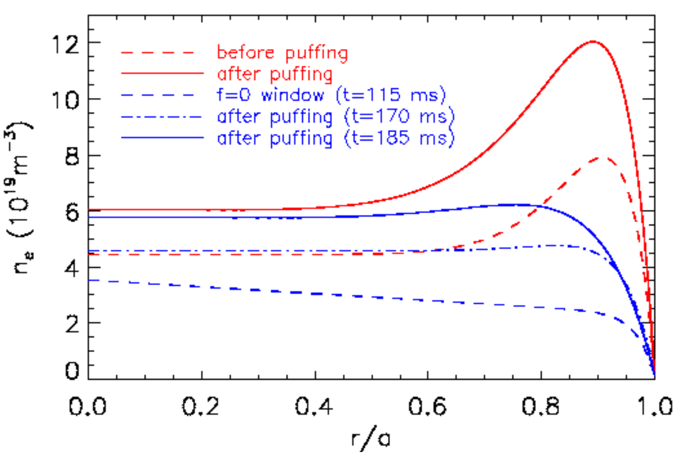

Fig.2.31: Evolution of the density profiles for two discharges with the same gas puffing program. The application of a F≥0 windows (blue curves) allows to obtain a similar central density value with a flat profile.

2.3 Goals and directions for potential upgrades of the RFX experimental facility

Based on the results obtained in RFX-mod since 2005 and on the positive perspective to provide important results both for the RFP and for the broader fusion community, an activity concerning the design of potential upgrades of the device has been carried out in 2012, as foreseen in the activity program. The aim is to explore completely new scenarios allowing substantial improvements of the RFP performance and crucial contributions to Tokamak and Stellarator physics issues.

As a result of four working group activities, as outlined in 2012 program, three combined main machine modifications have been identified as the most transitional ones, strictly related one to each other:

1) change the first wall, presently consisting of carbon tiles, with a metallic one
2) provide a conductive shell closer to the plasma
3) modify one access port to allow the tangential injection of a neutral beam

2.3.1 Change of the first wall

As discussed in sec. 2.2.2 a main issue for RFX-mod operation is the high hydrogen retention capability of the graphite tiles covering the vacuum vessel, which makes very difficult the recycling and density control. Especially in the high current scenarios, when the power load on the wall is higher and locally reaches several MW/m^2, hydrogen trapped into the graphite can be released in uncontrolled way, producing hollow density profiles with consequent cooling of the plasma edge. The change of carbon with a material characterized by lower H retention on the plasma pulse timescale would allow a substantial improvement of the density control. Indeed, positive results have been obtained in 2012 by the deposition of a Li layer on the graphite (sec. 2.2.2), but with some caveats: the deposition of a uniform Li layer is quite difficult and the lithization procedure is complex and time consuming, requiring long wall cleaning sessions before deposition.

Tungsten and molybdenum have been considered as potential new first wall materials for RFX-mod, and finally Tungsten has been selected for several reasons. First, the W melting temperature is higher (3700 ^{0}C for W, to be compared to 2900 ^{0}C for Mo) and comparable to the carbon one (3800 ^{0}C), allowing the sustainment of the highest power loads that in particular circumstances (e.g. stationary mode wall locking) can increase up to tens of MW/m^2. Moreover, due to the higher W mass, the reflection energy of the incident neutral atoms is higher (70% for W, 60% for Mo and 40% for C). This is important because a decreased recycling will imply the requirement of a more efficient core fuelling system, to be obtained mainly by an improved cryogenic pellet injection. However, a higher energy of reflected atoms will be also favorable, as such atoms will penetrate more deeply the plasma edge before ionization. It has to be mentioned, as an additional reason to prefer W, that present (JET, AUG) and future (ITER, FAST) large Tokamaks are using W as divertor and first wall material [Brezinsek 12], and therefore a W wall in RFX, combined with the advanced remote handling system of the tiles and the great capability of the spectroscopic diagnostic system will allow to effectively contribute to the main European program on the material and plasma wall interaction studies.

As for JET and AUG, the new tiles will be made by carbon covered with W, to avoid excessive weight (not sustainable by the RFX mechanical structure) and cost.

The investigation of potential supplier of the new tiles has been carried out, and first prototypes are being procured.

2.3.2 Change of the magnetic front-end to provide a conductive shell closer to the plasma

The aim of such modification is to decrease the magnetic field deformation related to the tearing modes. As shown in fig. 2.32, simulations by the RFXLOCKING code have shown that increasing plasma shell proximity reduces the deformation of the last flux surface. Such effect is clearly associated to a milder interaction with the wall, and is therefore complementary and synergetic with the previous modification concerning the change of the first wall. In addition, according to [Guo 01], a conductive shell closer to the plasma will decrease the error field threshold for tearing mode unlocking. The combination of these effects will allow completely new operational scenarios for the experimental study of MHD stability and plasma-wall interaction in the RFP.

Several possibilities have been analyzed, including the insertion of a shell between the vacuum vessel and the tiles (both maintaining the tiles in the present position and moving them inwards with a reduction of the plasma radius) and the possibility to remove the vacuum vessel using the external mechanical structure for vacuum seal (see fig. 2.33). The most promising solution is the latter, sketched in fig. 2.34. In this configuration, besides a closer shell-plasma proximity, the plasma radius will increase, with consequent decrease of loop voltage and confinement improvement. Moreover, such solution is considered as more reliable and flexible if compared with the insertion of a shell between vacuum vessel and first wall. The modified mechanical structure will sustain inside a new conductive shell (or the present one, to be evaluated), the new first wall (carbon covered with W) and the magnetic sensors.

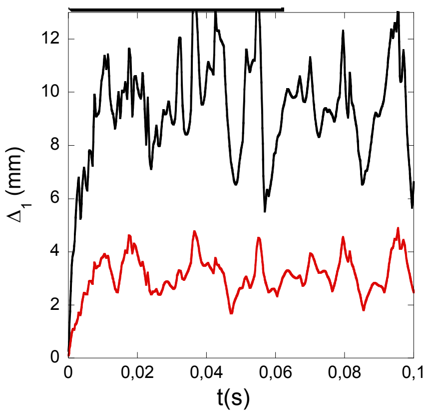

Fig. 2.32: example of the effect of an internal shell (red) compared to the present one (black) on the deformation of the last flux surface

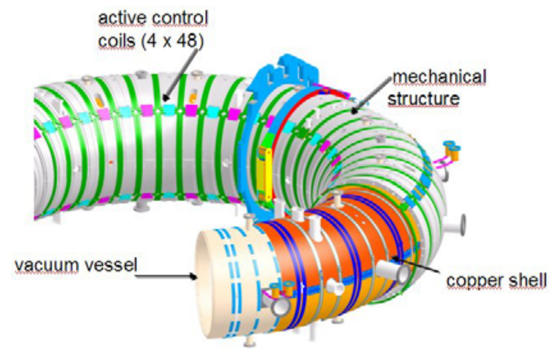

Fig. 2.33: present RFX-mod magnetic layout

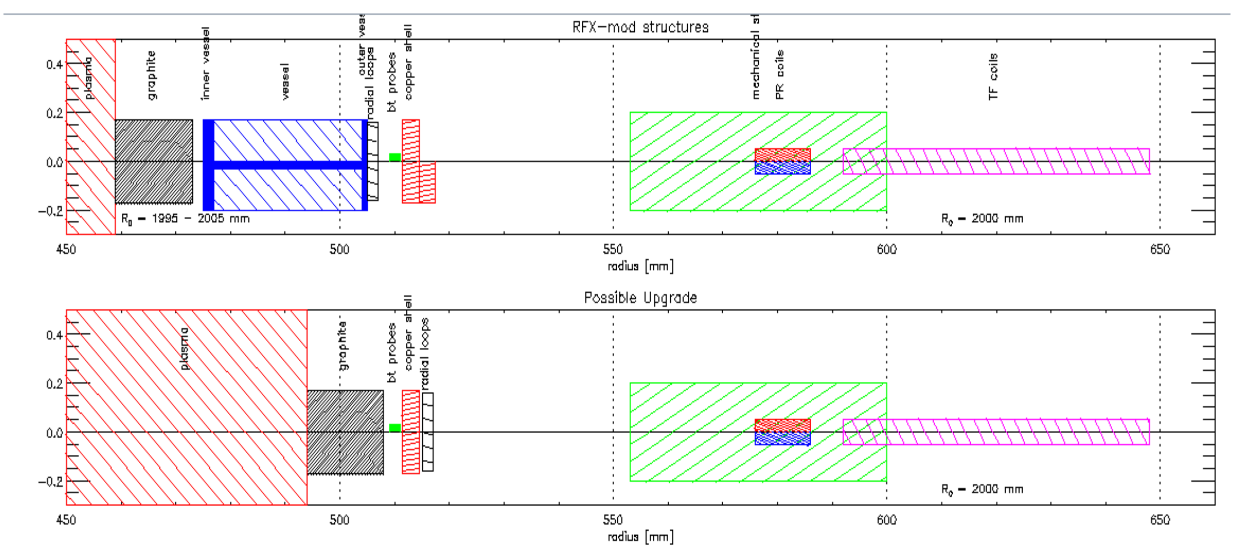

Fig. 2.34: sketch of RFX-mod magnetic front-end as it is at present (top) and with the removal of the vacuum vessel. Note that only the last centimeters of the plasma radius are shown.

While the sealing of the new access ports does not present relevant technological issues, more challenging is the vacuum sealing corresponding to the present poloidal and equatorial gaps, whose insulation must be compatible with the vacuum. The study of technical solutions is in progress, and dedicated experiments are planned for the first part of 2013. More specifically, the external equatorial gap, more critical due to many diagnostic and pumping accesses, will be welded, while for the internal one, interrupted only by dump, an eventual insulation is technologically simpler.

To evaluate the best position of the shell inside the mechanical structure, parametric studies are in progress to optimize the effect on the magnetic measurements and on the sidebands in the new geometry. In fact the high frequency magnetic measurements and the equilibrium measurements are to be placed inside the conductive shell, while the electrostatic measurements can be included in the new tiles. On the other hand, the coils for the feedback control system can be placed between the shell and the mechanical structure, but their position with respect to the actuators must be optimized to minimize the sideband pollution. An increase of the number of sensors will allow a better diagnostic of the field penetration in the passive structure.

An additional issue under consideration is related to the possibility of wall treatments presently based on baking to degas the wall especially after an air exposition: the mechanical structure cannot be heated, and alternative solutions are studied, including innovative techniques such as the use of flash lamps inserted by manipulators, combined with Pulse Discharge Cleaning sessions.

2.3.3 Tangential injection of a neutral beam

In combination with the previous modifications, taking advantage of the new arrangement of the mechanical structure, the modification of an access port to allow the tangential injection of the neutral beam on loan from AIST and already at Consorzio RFX is proposed [Dal Bello 11].

During 2012 several simulations have been performed to evaluate the potentialities of the application to RFX of the beam.

Calculations on the beam absorption have indicated that, both with H and D as filling gas, the beam is fully absorbed inside the plasma, both in the RFP and Tokamak operational density ranges.

In collaboration with the MST group, the TRANSP code has been used to simulate the density of fast particles produced in RFX-mod RFP plasmas: a detectable population of fast ions is produced, characterized by a confinement time longer than thermal particles, and accumulating in the plasma centre. Similar simulations for the Tokamak case are in progress.

In Tokamak configuration, the application of the beam will allow the exploitation of the advanced RFX-mod feedback control system: on the one hand, to study the relationship between external magnetic perturbations and flow in presence of a tangential momentum injection. In addition, the 1 MW power of the beam is higher than the ohmic power applied in RFX when operated as a Tokamak; the beam will therefore favor the access to the H-mode, where the control system can be used for ELM control studies.

2.4 Experiments in international Tokamak devices

2.4.1 Edge Physics on ASDEX-Upgrade

The already established collaboration between RFX and Euratom-IPP Garching for the studies of edge electromagnetic turbulence in ASDEX-Upgrade has continued also during 2012. It is worth remembering that RFX-mod, in collaboration with Euratom-ÖAW and Euratom-Risø/DTU associations, has installed on ASDEX a probe, which combines electrostatic and magnetic measurements, which has already given significant contribution in the studies of ELM filaments [Vianello11]. In November 2012 a new experimental campaign has been performed to which a researcher from RFX-mod has actively participated. The experimental campaign explored the physics of electromagnetic turbulence associated to ELMs during ELM mitigation discharges obtained through the application of Magnetic Perturbation.

ASDEX Upgrade is presently being enhanced with a set of in-vessel saddle coils. Four coils above (dubbed Bu coils) and four coils below the midplane (Bl coils) at the low field side are currently operational and it has been clearly shown that magnetic perturbations are effective in completely mitigating the ELMs [Suttrop11], although the effectiveness depends on the density values. On this purpose a density scan experiment within a single discharge with magnetic perturbation has been planned in order to investigate the effects on the electromagnetic turbulence associated to the ELMs in the different regimes. An example of the discharges obtained is shown in Fig. 2.35, showing the typical time traces of plasma current, plasma density, current as measured at the divertor plates and the current applied to the coil. The vertical colour lines indicate the time when the fast reciprocating probe has been inserted, studying a non-mitigated phase (cyan line), a period during non effective magnetic perturbation (orange line) and a region of ELM mitigation (green lines). In Fig. 2.36 the radial and poloidal components of the magnetic field are compared respectively during the time interval marked in cyan (panel (a)) and in green (panel (b)). Clearly the fluctuations result remarkably different in the two cases: the typical feature of filaments highlighted in the cyan box in Fig 2.36 (a) is not present in panel (b) where indeed radial component of the magnetic field result less bursty exhibiting a much more regular behavior. Further investigations are now in progress.

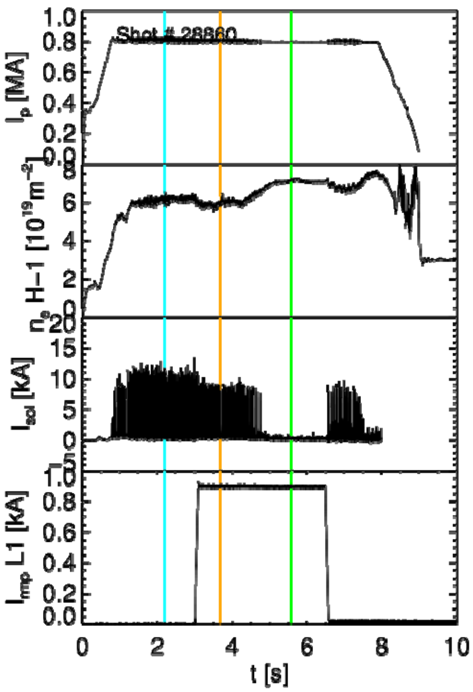

Fig. 2.35 Typical time traces of discharges in ASDEX-Upgrade. From top to bottom, Plasma current, electron density, current at the divertor plates and current in the coil for RMP. The vertical lines indicate the strokes for the fast movement of the reciprocating manipulator

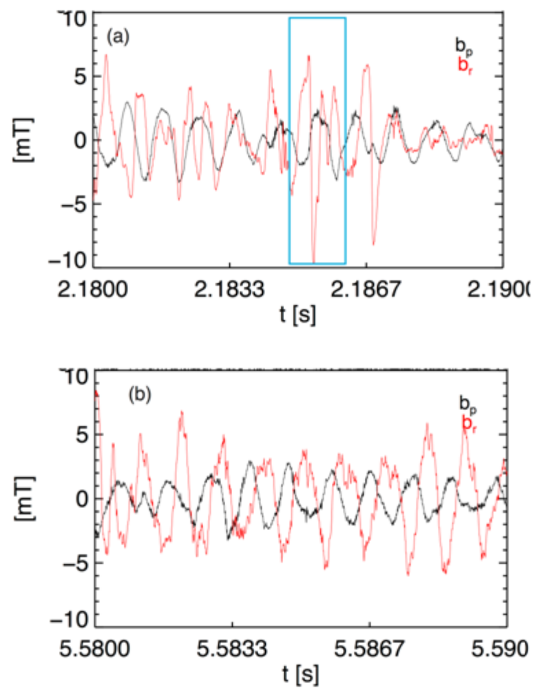

Fig 2.36: Radial and poloidal magnetic fluctuations in two time intervals (a) unmitigated phase, where clear signature of ELM filaments is highlighted in cyan box (b) mitigated phase, where coherent mode seems to dominate on the radial component

2.4.2 Edge Physics on TJ-II stellarator, COMPASS tokamak and TORPEX simple magnetized torus

Filamentary structures elongated in the magnetic field line direction have been detected in magnetized plasmas ranging from laboratory, including thermonuclear fusion devoted experiments, to astrophysical ones [martines09]. A special attention is paid to the study of turbulent features characterizing edge plasmas of toroidal devices for magnetic plasma confinement, where this represents a hot topic due to the role played by coherent structures in contributing to the transport of particles and energy. Recently an increasing interest has been devoted also to the study of the field-aligned features of these filamentary plasma structures, including both their electrostatic and electromagnetic properties.

New information is then provided beyond the standard cross-field characterization, and direct measurement of associated parallel current density, $J_{\parallel}$, and vorticity, $\omega_{\parallel}$, is added.

In this respect a strong experimental effort, coordinated by the Consorzio RFX in tight collaboration with the EPFL (Lausanne), CIEMAT (Madrid) is in progress [spolaore12], in order to provide accurate information on structure features and to gain insight on their dynamics and ultimately on their driving mechanisms. In particular a direct observation of current density filaments associated to the so called “blobs” or turbulent structures has been performed in the edge region of the RFX-mod reversed field pinch device [spolaore09], where drift kinetic Alfvén structures have been identified [vianello10].

Similar investigations are in progress, thanks to a specifically designed diagnostic tool [carralero12] installed last year, in the edge region of the TJ-II stellarator experiment, where a range of plasma beta and different plasma equilibria can be explored. A summary of the explored plasma condition is shown in fig. 2.37, in particular it is found that the filaments exhibit electromagnetic features only for the highest local electron beta.

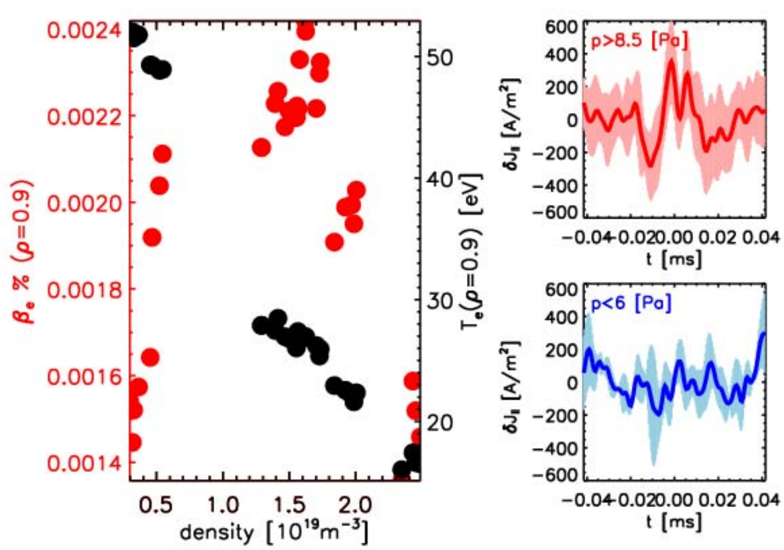

Fig. 2.37: (left) Summary of plasma conditions explored in TJ-II for the current density filament investigations; (right) average current structures detected at two local electron beta.

Similar filaments have been observed also in the TORPEX experiment, simple magnetized toroidal plasma, where blobs originated by ideal interchange waves.

In this last case, for the first time the cross-field map of the parallel current density in the filaments has been revealed [furno11a, furno11b] and the associated pattern up to the 3D details, both on $J_{||}$ and $\omega_{||}$, was measured this year, see the example shown in fig. 2.38.

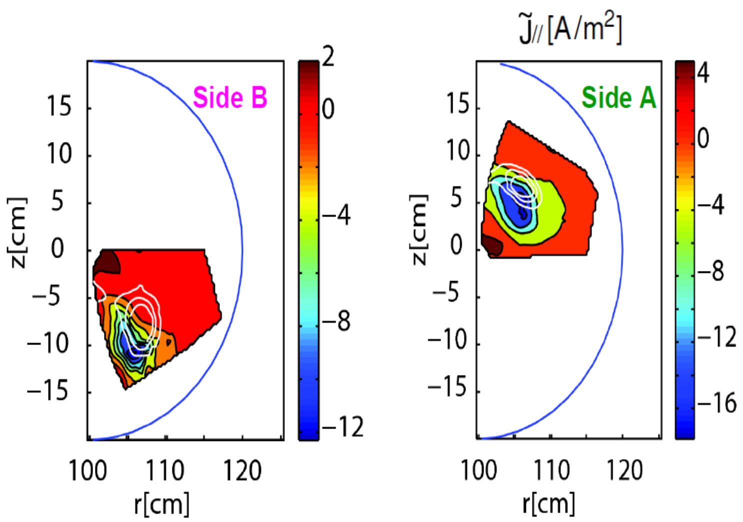

Fig. 2.38: Current density filament pattern in the cross-field plane measured at the two sides of the limiter in the TORPEX experiment, the white contours indicate the associated density pattern.

A first attempt of comparing electromagnetic properties of turbulent structures, exploiting the complementarity of different magnetic configurations: TORPEX, characterized by open field lines, and the hotter plasmas of fusion devoted experiments represented by the TJ-II stellarator and RFX-mod, which can be operated with both reversed field pinch and ohmic tokamak, is shown in fig 2.39. The measured trend highlights the important role of the local β_e [spolaore12].

It is worth mentioning that a special relevance for fusion devoted experiments is ascribed to current density associated to ELMs phenomena, observed in the edge of magnetic confinement fusion devices.

An analogous joint collaboration is in progress with the IPP Prague association in order to perform, in the COMPASS tokamak, the investigation of ELMs and turbulent structure current density filaments. In this case a probe head similar to the U-probe used in RFX-mod was realized during 2012 [Weinzettl12], see picture 2.40, and is planned to be installed on the diagnostic port at the LFS above mid-plane and commissioned in the 2013.

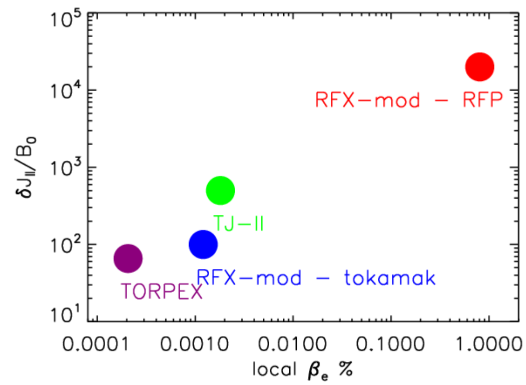

Fig.2.39: Comparison of the $\delta J_{\parallel}/B_0$ fluctuations of the current density filaments, vs local electron beta, as measured in the four different magnetic configurations explored.

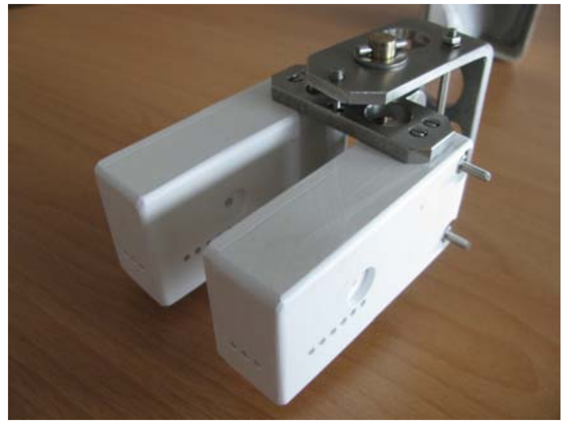

Fig.2.40: Picture of the probe head designed for the investigation of ELMs and turbulent structure current density filaments in the edge region of COMPASS tokamak.

2.4.3 JET

Electrostatic turbulence fluctuation analysis was carried out on JET analysing data collected with the reciprocating Langmuir probe during Ohmic discharges at different fraction of the Greenwald density. In particular we were able to determine the typical shape of blobs as seen on ion saturation current and poloidal electric field as shown in Fig. 2.41, showing that this shape does not depend on the density of the discharges. Work is now in progress on the so-called M-Mode, a global mode recently observed in ILW experiments at JET associated to the appearance of a pedestal in the density gradient but with a moderate or weak pedestal on the temperature. This mode can be seen in a variety of diagnostics, as for example on the Dα looking at the divertor, as shown in the spectrogram in Fig. 2.42. Work is now in progress in order to understand the nature of this mode which could be somehow related to some Geodesic modes so far not observed at JET.

Regarding tungsten transport issues, we highlighted the impact of the centrifugal forces on W, which in beam heated discharges shows a poloidally distribution strongly asymmetric, with an emission peak of the soft X-rays (SXR) on the low field side.

We revamped the use of the SXR tomography which is essential to photograph the asymmetries of the impurity density in the plasma core, and also we urged the upgrade of the JETTO/ SANCO post-processor UTC in order to be able to compare synthetic and

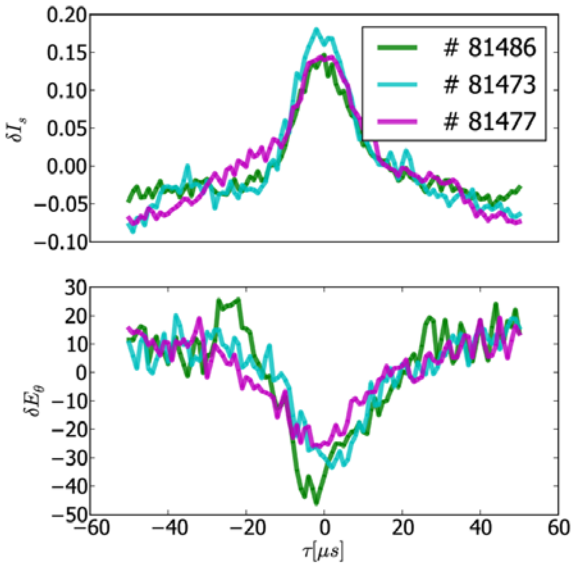

Fig 2.41: Top. Typical shape of a blob identified on the ion saturation current as measured in 3 different plasma discharges (#81486 n/n_G=0.3, #81473 n/n_G=0.42 and #81477 n/n_G =0.73) Bottom: poloidal electric field fluctuations associated to ion saturation current blobs

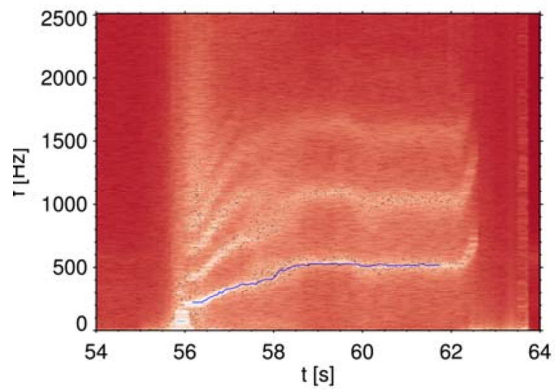

Fig 2.42: Spectrogram of the D_a signal with highlighted the evolution of the dominant frequency of the M-mode

experimental SXR emissions in presence of W. The request to have the same thickness for the Be filters on all of the SXR cameras was also put forward. The analysis of a couple of hybrid discharges has shown the need to further modify the JETTO/SANCO code in order to incorporate in a correct manner the term for the description of the centrifugal force. The implementation of the latter changes will require time but could hopefully be ready before C31 starts. In addition we have emphasized the need to procure or develop tools for a 2D simulation of the W behavior. The main result of the simulation analysis is that W contributes mainly to core radiation and to the SXR emission, while Zeff, typically around 1.5, is due mainly to Be. Quantitatively simulation of the core SXR is quite in agreement with the W concentration independently estimated by means of wavelength resolved spectroscopic structures. Fig. 2.43 shows the comparison between simulated and synthetic SXR emission.

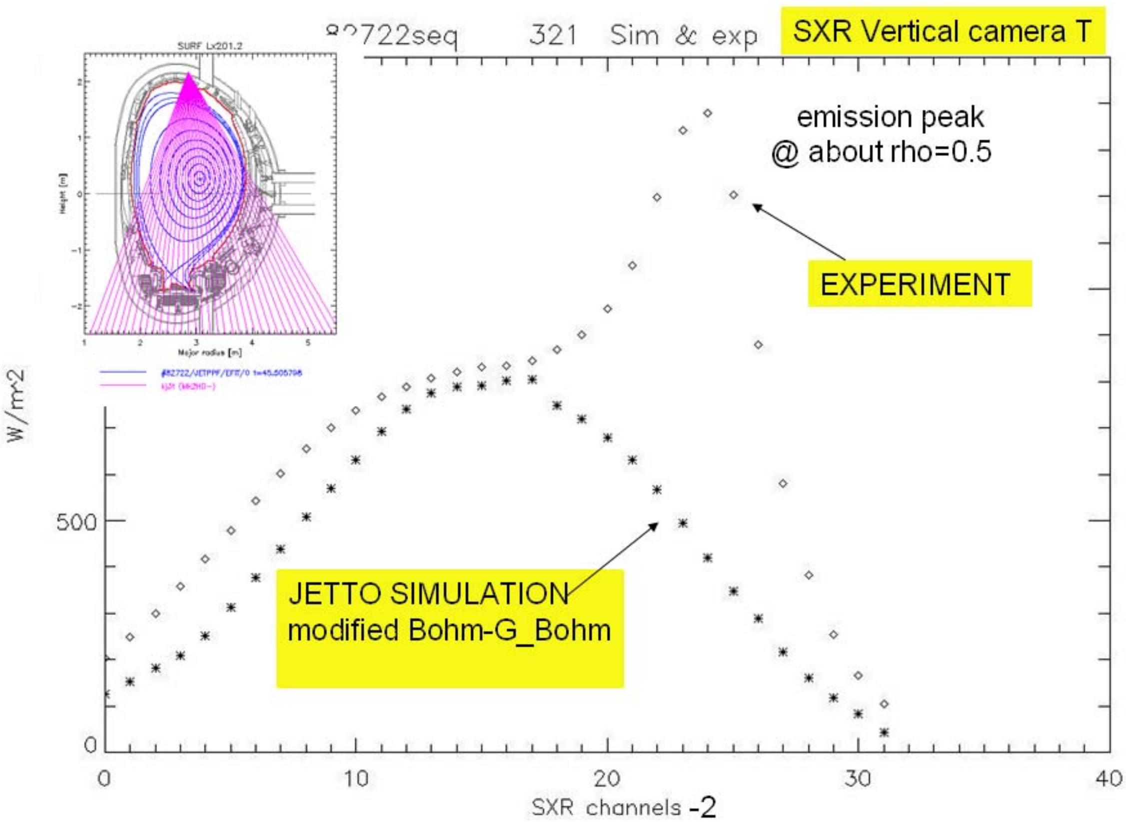

Fig 2.43: Comparison between simulated (stars) and experimental (diamonds) SXR vertical camera of a JET discharge. The emission peak on the Low Field Side is due to centrifugal forces. Simulation of the latter effect is in progress.

2.4.4 TCV

A systematic investigation of the influence of the divertor-leg-length on the L-H transition at TCV tokamak has started. This activity is justified by the widely observed, but not well documented, L-H power threshold dependence on the spatial position of the X-point. Examples of this dependence have been highlighted in different machine: in JET an increase of the power threshold PLH with X-point height has been seen [Andrew2004], on the contrary a decrease of PLH with X-point height has been reported in C-Mod [Meyer2011]. The extremely flexible shaping capability of TCV allows planning a systematic investigation of this influence foreseeing to move the X-point both vertically and radially.

The experimental procedure foresees to perform different discharges in Lower Single-Null (LSN) configuration at different vertical positions, keeping main plasma parameters and shape as constant as possible. In each discharge the ECRH power is increased and measured in order to precisely track the power at which the L-H transition occurs. A further density scan for each position will give the possibility to track the X-point height influence on the international multi-machine PLH scaling [Martin2008].

First experimental sessions have proven the feasibility of the investigation method and provided first confirmation. In Fig. 2.44 the comparison of two shots with different X-point height is reported. The quality of the plasma shaping match is evident. As starting point the density dependence of PLH was investigated while maintaining fixed the plasma position. The well known non-monotonic curve characterizing Tokamak devices, see for example [Ryter2009, Andrew2006], has been recovered, as can be seen in Fig. 2.45.

The change in X-point positioning seems to confirm the JET observation: reducing the X-point height the PLH decreases. Further investigation is needed to complete the systematic investigation and to reveal what physical parameter is hidden behind the X-point height variation.

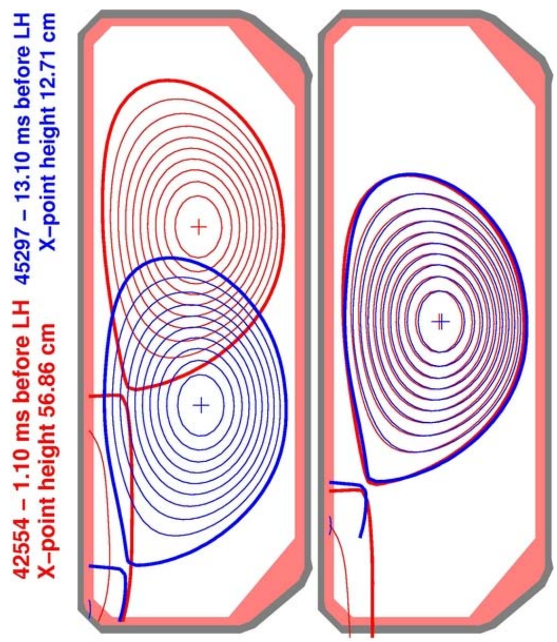

Fig 2.44: Comparison between two shots with different X-point height on TCV. (LEFT) The performed shots with the real positioning inside the vacuum chamber. (RIGHT) Plasma shifted to highlight the high quality match of the plasma shaping

2.4.5 DIII-D

A team of RFX-mod scientists in collaboration with a wide international team has been awarded the 2012 Torkil Jensen Award "for innovative and potentially transformational experiments in DIII-D", the largest American tokamak based at General Atomics, San Diego, USA. The proposal was based on results previously obtained in RFX-mod, that demonstrated the possibility to run a tokamak with edge safety factor $q(a)<2$. This was considered for a long time an impassable limit for tokamak operation and was overcome both in RFX-mod and DIII-D thanks to magnetic feedback control of MHD stability. The experiments performed in DIII-D were successful maintaining q95 below 2 for about 0.5 seconds (see Fig. 2.46) and showing that the above limit can be overcome even in D-shaped plasmas at high plasma current up to 1.7MA. This result opens new interesting perspectives for further experiments in DIII-D and other large tokamaks, to explore the physics and the robustness of this new type of operation as a reactor-relevant scenario. Further experiments have been proposed, which aim in particular at extending this scenario to H-mode and to even lower safety factor values.

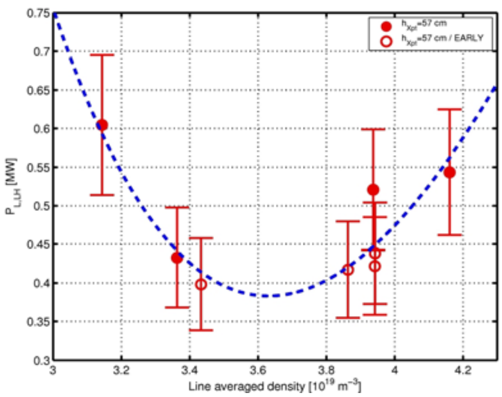

Fig 2.45: H-mode power threshold versus line average density.

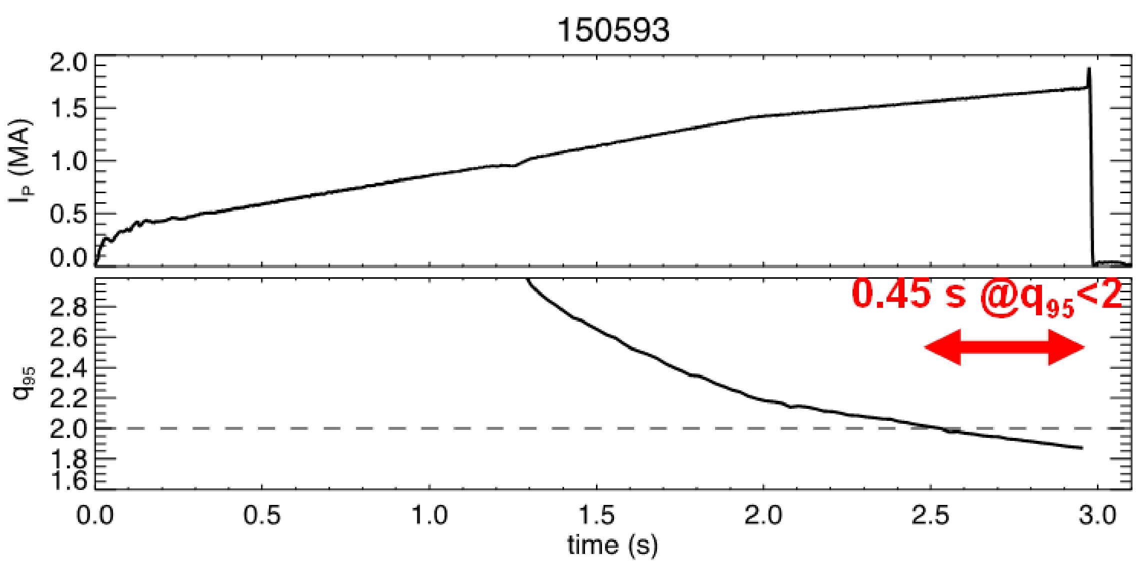

Fig 2.46: Example of DIII-D discharge where q95 is brought below 2 for about 0.5 sec, much longer than the shell constant time of 2ms and of the energy confinement time of about 100 ms.

2.4.6 JT60-SA physics

Consorzio RFX actively contributes to the European efforts in support to the preparation of JT-60SA scientific exploitation coordinated by EFDA/F4E. These efforts complement the contributions to the Broader Approach agreement that are described in chapter 6 . Consorzio RFX participation is concentrated in key areas of its general program such as MHD stability and control, diagnostic development and integrated scenario modeling with NBI as main additional heating and current drive source. Consorzio RFX is also coordinating the European contributions on MHD stability and control and has one representative in the recently launched EU-JA Data Working Group, which will address important issues related to the way experimental data from JT60-SA will be made available for analysis.

The specific areas in which Consorzio RFX is contributing are:

a. MHD stability and control: during 2012 a formal agreement between Consorzio RFX, CCFE and JAEA was signed on RWM stability studies with the inclusion of kinetic effects; Consorzio RFX is providing the European coordination of these specific studies. First results have been presented in [Bolzonella 12] and are mentioned also in the following paragraph 4.4 “Resistive Wall Modes studies”. Preliminary considerations on active feedback stabilization of RWM by means of external coils also started in 2012. One further topic where Consorzio RFX contributed is the control of NTM by ECRH in JT60-SA; first results of this study, developed in collaboration with CNR-Milano have been presented in [Sozzi12].

b. Diagnostics development: Consorzio RFX is participating to the optimization of the Thomson Scattering diagnostic optics and started a collaboration on the design of a polarimetric system for JT60-SA.

c. Integrated scenario modeling: Consorzio RFX is contributing to scenario development through predictive simulations with particular interest in the modeling of heating and current drive sources (NBI in particular). Recent results have been presented to the last IAEA-FEC conference in San Diego, see [Giruzzi12, Ide12]. A critical analysis on how present tokamaks could contribute to the validation of JT60-SA scenarios lead to interesting considerations on the role of the aspect ratio parameter in scaling laws; some conclusions from this effort have been presented in [Orsitto12]. This activity is organized in the framework of the EFDA Integrated Tokamak Modeling (ITM) Task

Force and is also mentioned in the following paragraph 3.5.3 “Plasma-beam interaction”.

References

[Agostini12] M. Agostini, A. Scaggion et al., Plasma Phys. Contr. Fusion **54**, 065003 (2012)

[Andrew2004] Y. Andrew et al, Plasma Phys. Control. Fusion **46**, A87 (2004)

[Andrew2006] Y. Andrew et al, Plasma Phys. Control. Fusion **48**, 479 (2006)

[Auriemma07] F. Auriemma, RFX Sci&Op meeting, 2007

[Baruzzo12] M. Baruzzo et al., Nucl. Fusion **52**, 103001 (2012).

[Brezinsek12] S. Brezinsek et al., “Fuel retention studies with the ITER-like wall in JET”, 24th IAEA Fusion Energy Conference, San Diego 8-13 October 2012, paper EX/4-1 (2012)

[Bolzonella12] T. Bolzonella et al, “Recent studies in support to MHD stability and control on JT-60SA” 39th EPS Conference & 16th Int. Congress on Plasma Physics, 2012 Stockholm, Sweden, P4.025

[Canton2012] A. Canton et al. 20th ICPSI, Aachen 21-25May 2012 –P3-73, tbp on J. of Nucl. Mat.

[Carralero12] D. Carralero PhD Thesis Universidad Politecnica de Madrid, 2012 http://oa.upm.es/11485/

[Cooper11] W.A. Cooper *et al.*, Plasma Phys. Control. Fusion **53** 084001 (2011)

[Dal Bello11] S. Dal Bello et al., Fusion Eng. Des. **86**, 772-775 (2011)

[Furno2011a] I. Furno et al. Phys. Rev. Lett **106** 245001 (2011)

[Furno2011b] I. Furno et al., Plasma Phys.. Control. Fusion **53** (2011) 124016

[Giruzzi12] G. Giruzzi, J. Garcia, N. Hayashi, M. Schneider, J.F. Artaud, M. Baruzzo, T. Bolzonella et al., “Model validation and integrated modelling simulations for the JT-60SA tokamak”, 34-TH/P2-03, IAEA FEC 2012 S. Diego

[Gobbin11] M. Gobbin, D. Bonfiglio et al. Phys. Plasmas **18**, 062505 (2011).

[GobbinEPS12]M. GOBBIN et al 39th European Physical Society Conference on Plasma Physics Stockholm, Sweden 2012 P4.094

[Guo01] S.C. Guo, M.S. Chu, Phys. of Plasmas **8**, 3342 (2001)

[Hanson09] J.D. Hanson *et al.*, Nuclear Fusion **49** 075031 (2009)

[Hirshman83] S.P. Hirshman and J.C. Whitson, Phys. Fluids **26** 3554 (1983)
[Ide12] S. Ide, N. Aiba, T. Bolzonella, et al., "Optimization of JT-60SA plasma operational scenario with capabilities of installed actuators", FTP/P7-22, IAEA FEC 2012 S. Diego [Manduchi12] G. Manduchi, L. Marrelli, et al., "Development of MHD active control in the RFX-mod RFP", Proceedings of the 24th IAEA Fusion Energy Conference, paper EX/P5-38, San Diego, USA (2012).
[Manduchi2012b] G. Manduchi et al., submitted to Fusion Engineering and Design (2012).
[Marchiori12] G. Marchiori et al., "Extended characterization of RWM active control system in RFX-mod", Proceedings of the 39th EPS Conference & 16th Int. Congress on Plasma Physics, paper P1.060, Stockholm, Sweden (2012).
[Martin2008] Y.R. Martin et al, J. Phys.: Conf. Series **13**, 012033 (2008)
[Martines09]E. Martines et al. Plasma Phys. Control. Fusion **51,** 124053(2009)
[Martines10] E. Martines et al., Nucl. Fusion **50**, 035014 (2010).
[Martines11] E. Martines et al. Plasma Phys. Control. Fusion 53, 035015 (2011)
[Meyer2011] H. Meyer et al Nucl. Fusion **51**, 113011 (2011)
[Moyer12] R. A. Moyer, *et al.* Nucl. Fusion **52**, 123019 (2012).
[Munaretto 2012] S. Munaretto et al. Nucl.Fus 52 023012 (2012)
[Neto10] A. Neto et al., IEEE Trans. Nucl. Sci. **57** (2010).
[Olofsson12] K.E.J. Olofsson et al., "Subspace identification analysis of RFX and T2R reversed-field pinches", submitted for publication to Control Engineering Practice (2012).
[Orsitto12] F P Orsitto, K Lackner , T Bolzonella,G Giruzzi, "Physics driven scaling laws for similarity experiments", 39th EPS Conference & 16th Int. Congress on Plasma Physics, 2012 Stockholm, Sweden, P2.154
[Pereversev02] G. Pereversev, P. N. Yushmanov, and Max Plack Institut fur Plasmapshysik, Report IPP 5/98, Garching, February, 2002
[Predebon10] I. PREDEBON et al., Phys. Rev. Lett. **105**, 195001 (2010)
[Puiatti09] M.E. Puaitti et al., Nuclear Fusion, 2009
[Ryter2009] F. Ryter et al, Nucl. Fusion **49**, 062003(2009)
[Sattin11] F. SATTIN and N. VIANELLO Plasma Phys. Control. Fusion 53, 025013 (2011) [Scarin2011] P. Scarin, N. Vianello et al. Nucl. Fusion **51**, 073002 (2011).
[Spagnolo11] S. Spagnolo et al., Nuclear Fusion **51**, 083038 (2011)
[Spizzo12] G. Spizzo, M. Agostini et al., Nucl. Fusion **52** 054015 (2012)

[Sozzi12] C Sozzi et al., " ECH and ECCD effects on NTMs stabilization by ECRF in JT-60SA tokamak ", presented at the 17th Joint Workshop on Electron Cyclotron Emission and Electron Cyclotron Resonance Heating (EC 17), 2012; to be published on http://www.epj-conferences.org/

[Spolaore09] M. Spolaore et al. Phys. Rev. Lett **102** , 165001 (2009)

[Spolaore12] M. Spolaore et al. EPS/ICPP 2012 invited talk I4.415, submitted to PPCF

[Suttrop11] Suttrop, W. et al. *Phys. Rev. Lett.* **106**, 225004 (2011).

[Terranova11] D. Terranova et al., 38th EPS Conference on Controlled Fusion and Plasma Physics, Strasbourg (France), 27 June-1 July 2011, P5.084

[Terranova12] D. Terranova et al., 54th APS Conference, 29 October -2 November 2012,

Providence, Rhode Island, JP8.00168 [Terranova10] D. Terranova *et al.*, Plasma Phys. Control. Fusion **52** 124023 (2010)

[Veranda12] M. Veranda, D. Bonfiglio, S. Cappello, D. F. Escande, L. Chacón, Varenna fusion theory conference 2012, submitted to Plasma Phys. Control. Fusion

[Vianello10] N. Vianello et al. Nucl. Fusion **50,** 042002 (2010)

[Vianello11] Vianello, N. et al. *Phys. Rev. Lett.* **106**, 125002 (2011).

[Vianello12] N. Vianello, M. Agostini, et al., 24th IAEA Fusion Energy Conference, San Diego, CA, USA paper EX/P8-02 (2012)

[Vianello12b] N. Vianello, G. Spizzo, et al. Nucl. Fusion, in preparation (2012)

[Weinzettl12] V. Weinzettl “Overview of COMPASS diagnostics” 4th COMPASS Programmatic Conference September 17-18, 2012

[Xanthopoulos09] P. Xanthopoulos *et al.*, Phys. Plasmas 16, 082303 (2009)

.

3. ITER

3.1 Introduction

Consorzio RFX is committed to the ITER Project, primarily for the development of the NBI system and then for the activity on the magnetic sensors, LIDAR system and ITER modeling. The NBI development is based on an Agreement between F4E and Consorzio RFX, for the period 2012-2019, which includes the realization of the Neutral Beam Test Facility (PRIMA Project) and regulates the mutual responsibilities between F4E and RFX according to the Memo of Understanding between ITER Organization (IO) and F4E. The activity aimed at the preparation of the local NBI Team has continued by specific training of RFX personnel on existing facilities at IPP (Germany) and NIFS (Japan) and by adding further experimental and numerical tools.

The international cooperation has been reinforced with the International, European and National Institutions involved in the project of the NBI.

3.2 NBI development

In 2012 several manufacturing activities started after the implementation of the two bilateral agreements signed at the end of 2011 between ITER Organization and Fusion for Energy (F4E), and between F4E and Consorzio RFX, and after the signature of five Procurement Arrangements between ITER Organization and the three Domestic Agencies (EU-DA, JA-DA and IN-DA) for the in kind contribution to the construction of the Neutral Beam Test Facility.

The status of the project and the main achievements of the year are described in the following sections.

The main areas of activity of the team are:

1. Design of plant systems, components and diagnostics towards the preparation of the documentation for the procurement activities.
2. Technical follow up of procurements from call for tender issued by F4E up to the acceptance of the manufacturing design. After this phase the follow up prosecutes with assistance to all the manufacturing phases up to the final acceptance tests.
3. R&D on prototypes of components and prototype of plant systems to confirm the design choices, to assess the reliability of the chosen technologies and to identify correct manufacturing processes.

4. Interface management between buildings-plant systems-components to guarantee the coherence of the overall design.
5. Modelling and experimental validation on existing facilities to support the design work of the ITER test beds in close collaboration with the Accompanying Programme.

3.2.1 PRIMA

3.2.1.1 Buildings

In September 2012 started the construction of the buildings to host the two experiments SPIDER and MITICA.

In fig. 3.1 the architectural view of the PRIMA buildings is shown,

Fig. 3.1: PRIMA buildings

In fig. 3.2 the internal layout showing the two testbeds hosted inside biological shields is shown.

Fig. 3.2: PRIMA buildings: internal layout of the two tesbeds

The actual status of the works in the building site can be seen on picture. More than half of the more than 400 foundation piles have been manufactured by the end of 2012 and the construction of the two water basins started.

In 2012 a significant work of revision of all the interfaces between the buildings and the different plant systems has been performed involving all the team in a further check of the consistency and coherence of the building design with all the plant systems. All three ITER domestic agencies have been involved in this work.

Fig. 3.3: PRIMA site buildings

3.2.1.1 Cooling Plant for SPIDER and MITICA

The procurement contract of the cooling plant has been signed in July 2012, and in October 2012 the kick off meeting has been held to officially start the activities. The first relevant milestone accomplished in the year has been the release of the Conceptual Design performed by the supplier on the basis of the Preliminary Design and Functional Specification developed by the team and used as the technical documentation during the call for tender activities. It is worthwhile to evidence that this is the most important auxiliary plant of the PRIMA facility since it has to handle and release to the atmosphere approximately 70 MW of thermal power. For safety reasons the design foresees independent cooling circuits for the different component and plant systems and for each cooling circuit a three stage power handling system. Moreover to minimize the costs of the atmosphere release system a heat capacitance system based on two water basins has been designed.

3.2.1.2 Vacuum, gas injection and gas storage for SPIDER and MITICA

The tender activities have been completed in November 2012 with the award to the company. The signature of the contract has been performed by the end of 2012 and the kick off meeting is scheduled within January 2013. So that to start the manufacturing activities.

The injector systems are very demanding in terms of pumping speed requirement for the vacuum systems since both the plasma source and in particular the gas neutraliser inject a huge amount of gas in the respective components, but at the same time the base pressure in the accelerator and in all the beamline has to be maintained as low as possible to minimize beam-neutral particle interactions to minimize charge-exchange and reionization phenomena and therefore loss of beam particles and generation of secondary charged particles.

Therefore the requirements of the vacuum systems are very demanding and the necessity of extensive use of liquid and gas He-cooled cryopumps is mandatory.

3.2.2 SPIDER

3.2.2.1 SPIDER vacuum vessel, beam source and beam dump

The procurement contract for the manufacturing of the vacuum vessel, the beam source and the beam source handling tool was signed in September 2012, and in the beginning of November the kick off meeting gave the start to the manufacturing activities.

In this year the main work dedicated to these items has been the technical follow up of the call for tender during the negotiation between F4E and the bidding consortium of companies lasting more than 6 month only in 2012.

In fig. 3.4 the SPIDER vacuum vessel is shown on the left whereas in the same figure the beam dump to be delivered by Indian Domestic Agency and installed in the front lid is shown on the right side. In Q2-2012 the final Built to Print design review was performed and the procurement activity soon after started.

During 2012 the main activity has been the update of the interfaces between the Beam Dump (form INDA) and the front lid of the vessel (from EUDA) and the verification and revision of the Technical Specifications developed by INDA and used for the procurement call for tender.

In fig. 3.5 the beam source is shown completely assembled inside a semi-transparent electrostatic shield and also an exploded view of the main components is given.

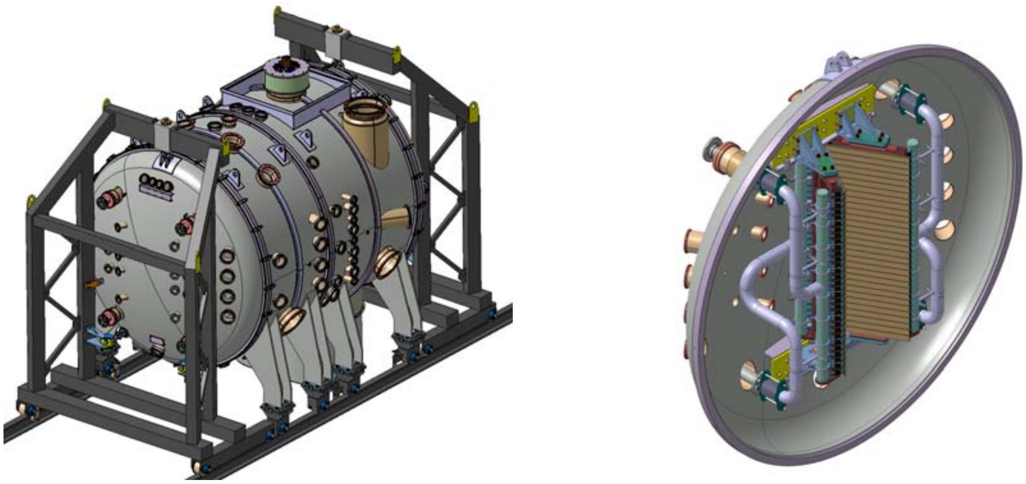

Fig. 3.4: SPIDER vacuum vessel and beam dump installed on the front lid

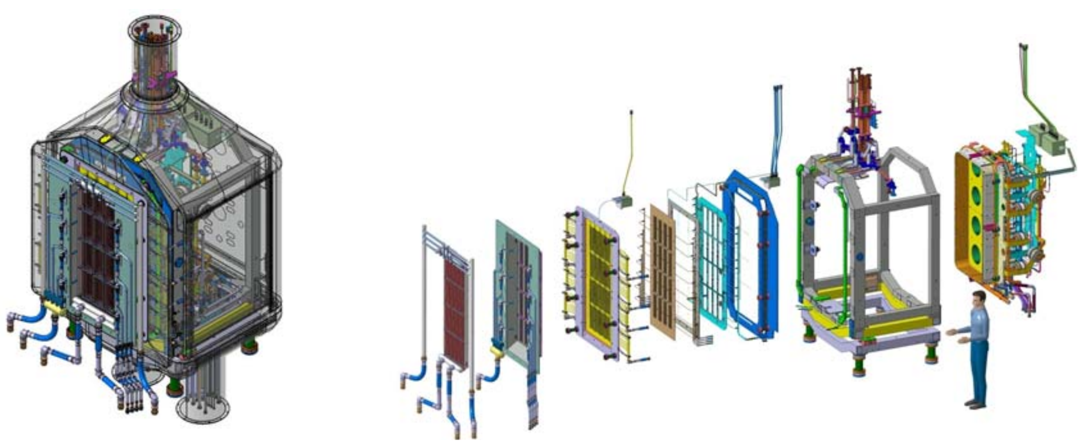

Fig. 3.5: SPIDER beam source: assembled and exploded view (without electrostatic shield)

3.2.2.2 SPIDER power supplies: ISEPS, 100 kV accelerator power supplies, High Voltage Deck and Transmission line

The contract for the procurement of the Ion Source Power Supplies resumed to full time work in May 2012 after a long period of financial troubles of the company, whereas the second part of the in kind contribution of Indian Domestic, the 100 kV AGPS (Acceleration Grid Power Supplies) also started the manufacturing activities.

In 2012 the manufacturing design developed by the supplier has been revised and formally approved. After this, the manufacturing phase is started and in conjunction with the start of this activity also the follow up is now switched to witness the construction phase. A significant work has been dedicated to the revision of the interfaces with the control and data acquisition system, since the original requirements were developed in 2008/09.

With regard to the work with INDA for the procurement of the 100 kV AGPS the interfaces with the other PS system (ISEPS), with the buildings, with the Control and Data Acquisition System, with the high voltage deck and with the cooling system have been revised and updated.

Moreover the Technical Specifications used for the Indian procurement have been checked and revised.

The scheme in fig. 3.6 shows the scheme of the power supply system.

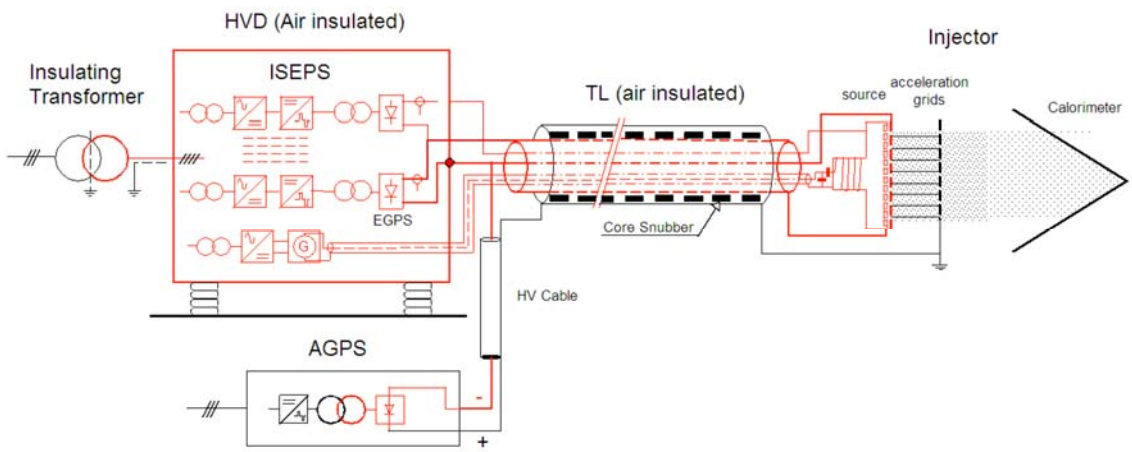

Fig. 3.6: SPIDER ISEPS and 100 kV AGPS supplied by INDA

In fig. 3.6 it is sketched the High Voltage Deck (HVD) insulated at -100 kV that hosts the ISEPS, all these power supplies being connected electrically to the beam source that through the AGPS is at the potential of -100 kV. A further relevant component in this figure is the Transmission Line (TL). Both these items are air insulated. These last two items are included in a procurement contract that is under completion. The signature of the contract is scheduled early in Q1-2013. In fig. 3.7 the layout of the HVD (yellow box) and TL (square shaped grey articulated channel) and of the AGPS (INDA procurement) inside the buildings are shown.

In this year the work has been concentrated to the technical follow up during the negotiation phases with the potential bidders.

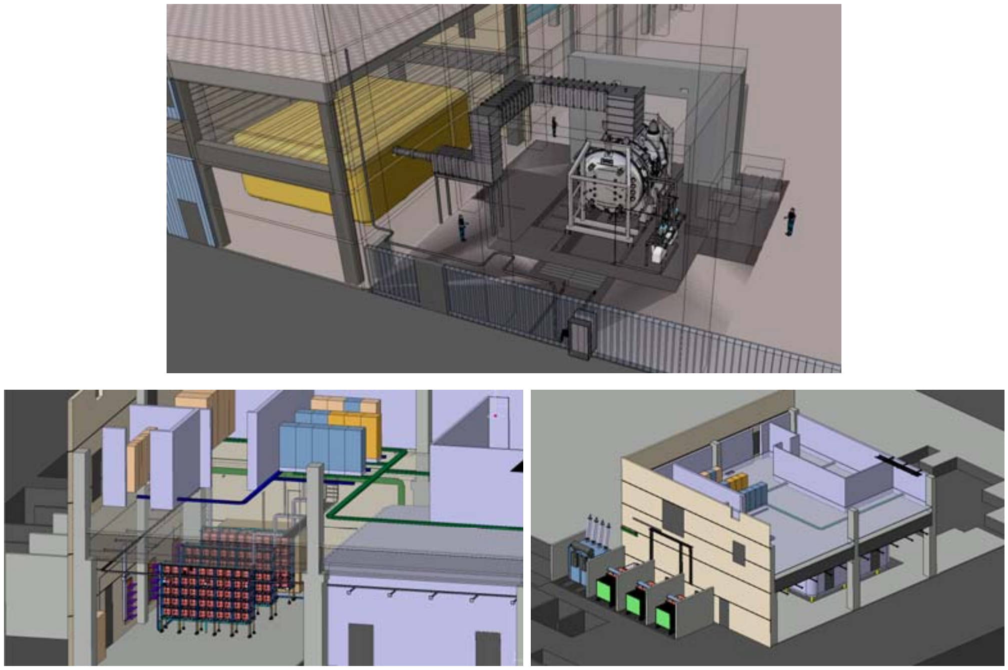

Fig. 3.7: SPIDER air insulated High Voltage Deck (HVD) and Transmission line (TL)

In 2012 further revision and refinement of the integrated electrical model to study the transient behaviour of the overall electric system has been performed by introducing updated parameters following the development of the project realization in all the involved items. Many studies on the effect of breakdowns, on fault condition propagation and parametric studies for the insertion of protection elements have been performed. In fig. 3.8 the overall system that has been modelled with the integrated

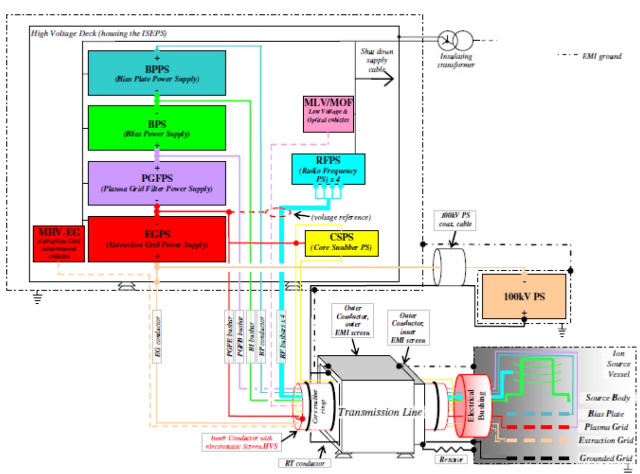

Fig. 3.8: SPIDER system that has been modelled in the integrated electrical model

electrical model is shown, whereas in fig. 3.9 an example of the propagation of the breakdown between Extraction Grid and Grounded Grid is shown in two position of the electric system.

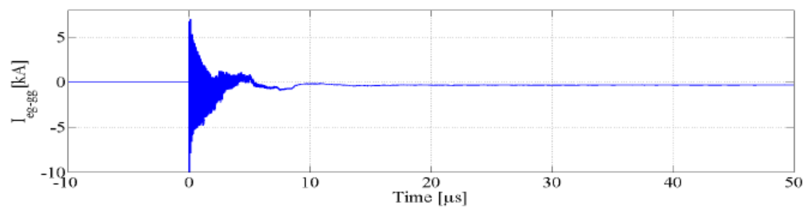

Figure 12: Breakdown current between Extraction and Grounded Grids

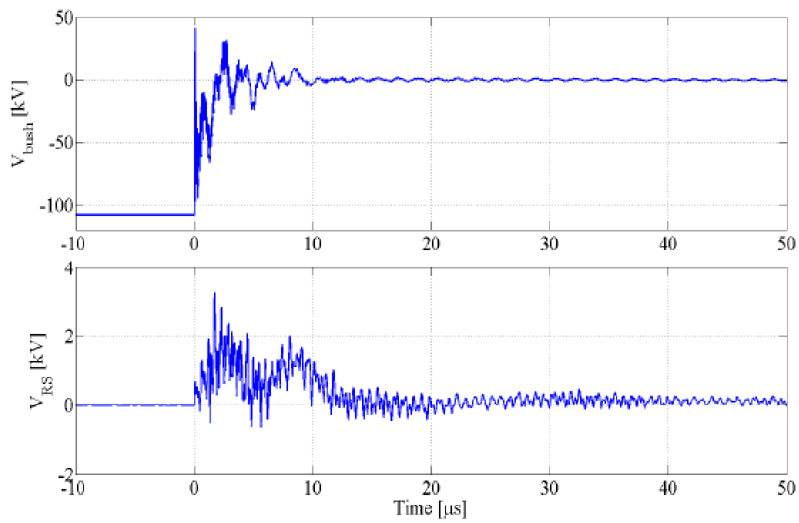

Figure 16: Voltage stressing bushing ring (top) and the termination resistors between TL outer and inner screen (bottom)

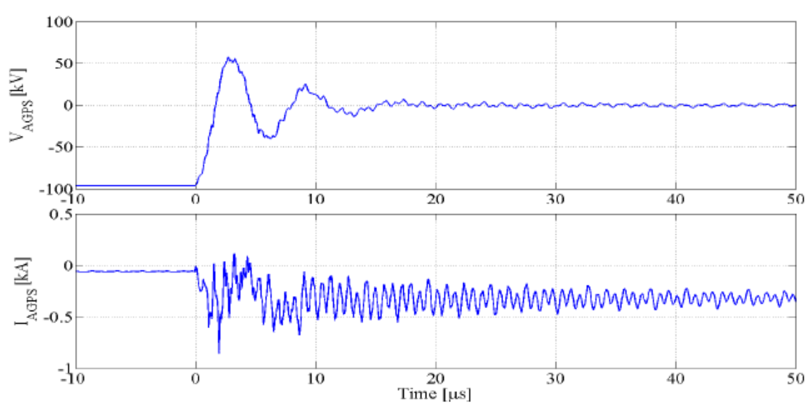

Figure 22: AGPS output voltage and current at the HVD level

Fig. 3.9: SPIDER breakdown between EG and GG and the effect seen on

3.2.2.3 SPIDER diagnostics

In 2012 further development of prototypes and qualification of components has been continued to identify the most appropriate components and to overcome technological issues. In addition to the thermocouples for calorimetric purposes and thermal survey of surface temperatures, the electrostatic probes used to qualify the plasma parameters in the plasma source, and the electrical and vacuum measurements, the main diagnostic systems foreseen in SPIDER are:

- Optical emission spectroscopy
- Cavity ring down spectroscopy
- STRIKE - Diagnostic calorimeter
- Beam tomography
- Neutron diagnostic on the rear side of the Beam Dump.

As an example of all the R&D activities carried out during this year, it is shown here the construction and results of the tests of a small size diagnostic calorimeter installed in the beam source BATMAN at IPP-Garching. In fig. 3.10 the layout of SPIDER STRIKE diagnostic calorimeter is shown together with the expected footprint of the IR image of one beamlet group of 5x16 beamlets, among the overall 16.

.

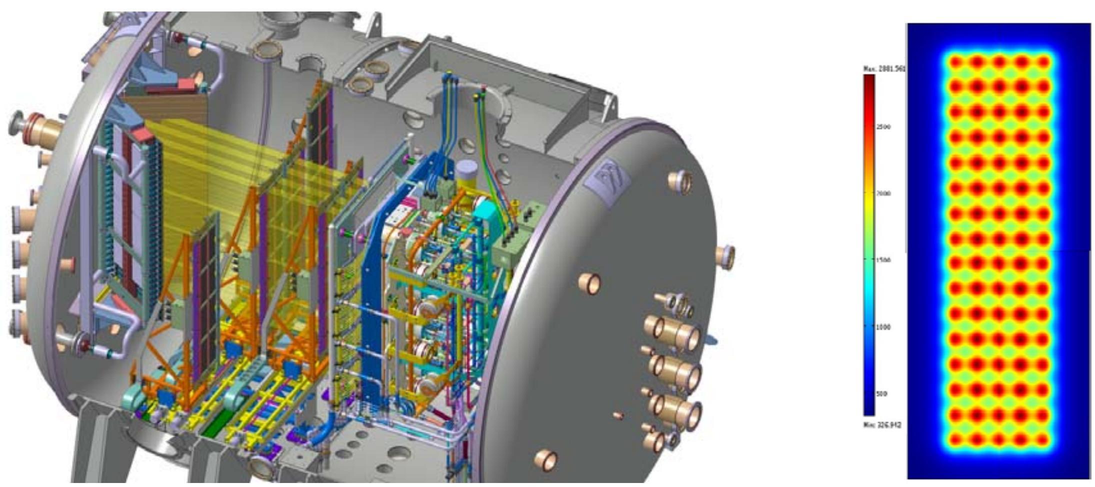

Fig. 3.10: SPIDER diagnostic calorimeter STRIKE: layout and expected footprint of one beamlet group

In fig. 3.11 the picture of the prototype diagnostic calorimeter (mini-STRIKE) installed in BATMAN is shown, together with an infrared image where the footprint of the sampled portions of the beam are clearly visible.

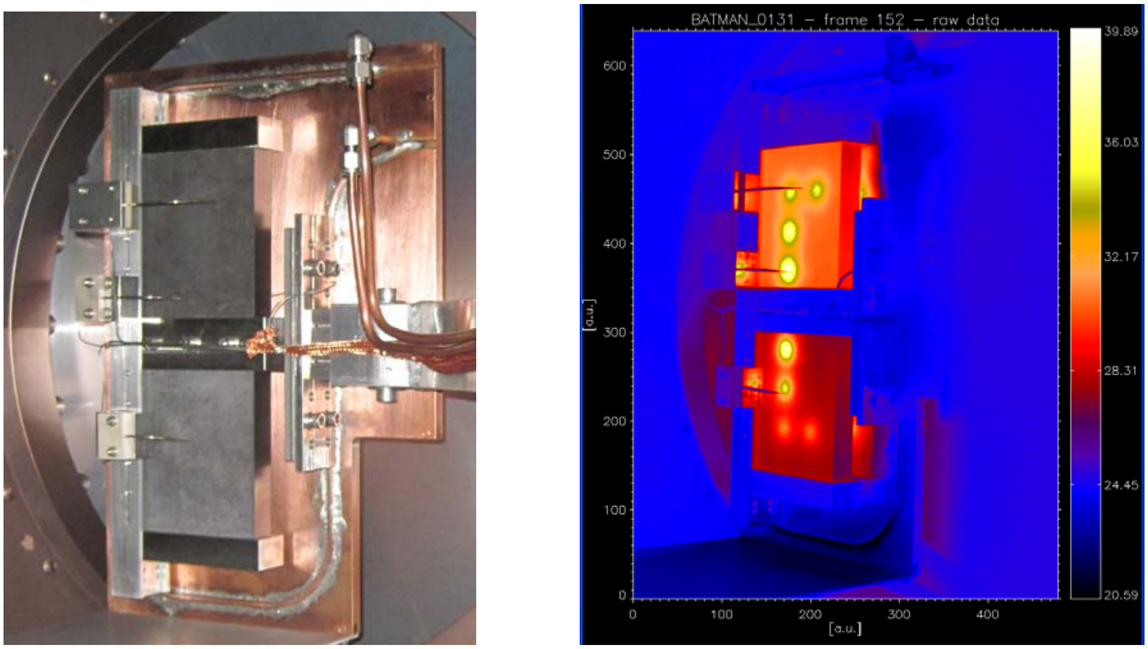

Fig. 3.11: mini-STRIKE installed in BATMAN and infrared image

In fig. 3.12 the reconstruction of the beamlet Gaussian footprint from experimental data is shown. The apparent elipticity is due to the inclined view of the infrared camera with respect to the perpendicular line to the CFC surface.

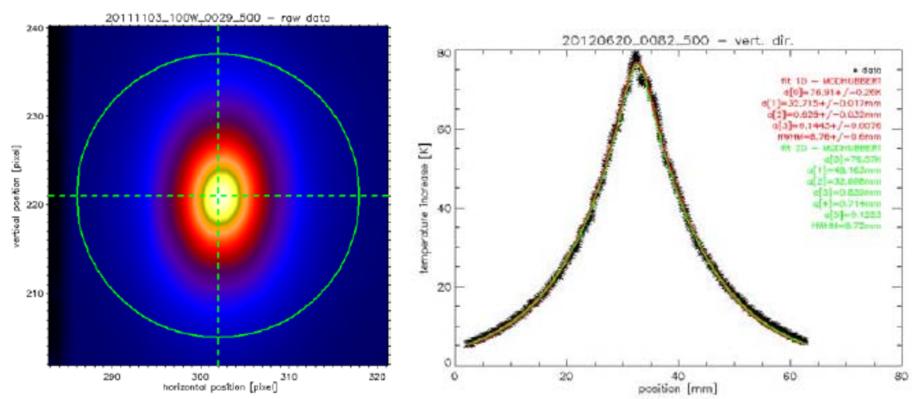

Fig. 3.12: reconstruction of the Gaussian distribution derived from the infrared image of the footprint of one beamlet in Mini-STRIKE during the tests performed in BATMAN at IPP (Garching)

A second example of development of diagnostic systems for SPIDER is the construction and the tests of thermocouples and electrostatic probes that have tested in the BATMAN (IPP-Garching) negative beam source. The RF electromagnetic field and the Cs plasma environment of the plasma source was a concern for the correct measurement of both these type of transducers. The tests performed in 2012 on prototypes installed in BATMAN have demonstrated that a correct design of the transducers and a proper signal transmission and conditioning allows to have robust signals. In fig. 3.13 the SPIDER prototype of thermocouples and electrostatic probes manufactured for the use in BATMAN is shown, whereas in fig. 3.14 the signal acquired during the operation of BATMAN for both thermocouples (left curve) and electrical characteristic I-V of the electrostatic probe is shown on the right of the same figure.

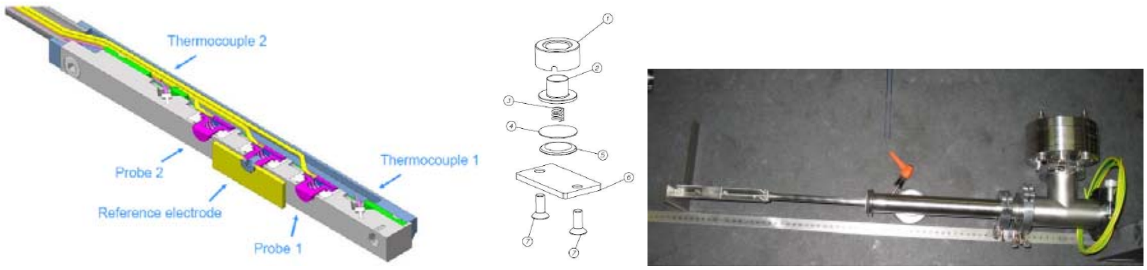

Fig. 3.13: prototypes of the thermocouples and electrostatic probes used in BATMAN (IPP-Garching)

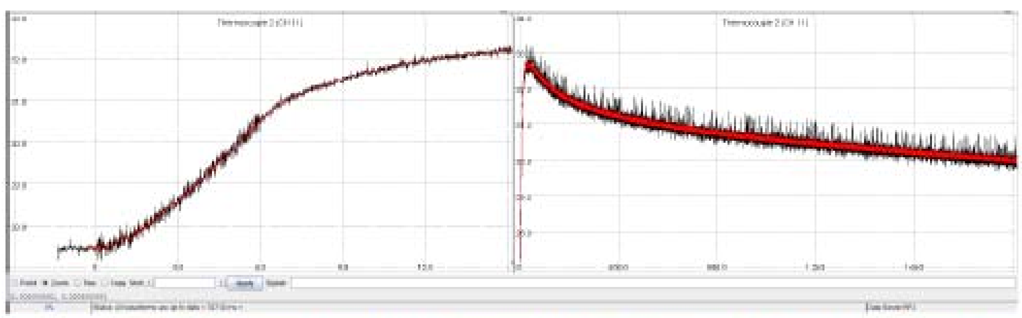

Figure 16 Raw and software filtered signals acquired before, during, and after BATMAN pulse 87508 for a total duration of about 30minutes

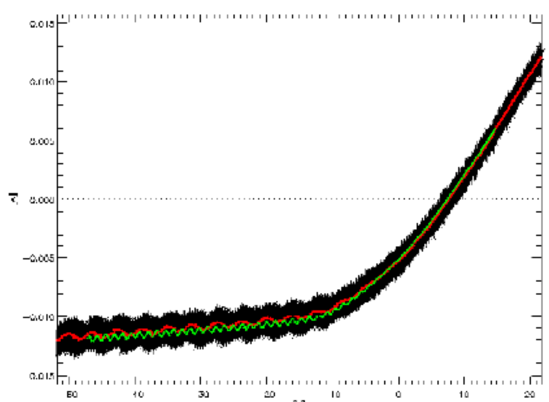

The I-V characteristic of the probe 2. Raw data (black) are compared with data filtered at 10 kHz: probe 2 (red) and probe 1 (green). Plasma condition (a): magnetic filter field drifted far from the probes and no bias on PG applied.

Fig. 3.14: TOP curves: thermocouple signal & BOTTOM curve: I-V characteristic of the electrostatic probe measured in the plasma of BATMAN (IPP-Garching)

3.2.2.4 SPIDER control system (CODAS) interlock and safety systems

A full prototype system of the control system (CODAS) has been developed having all the relevant Hardware to be installed in SPIDER and later on in MITICA and having all the Software tools developed and integrated to assess experimentally the performances of the overall control system.

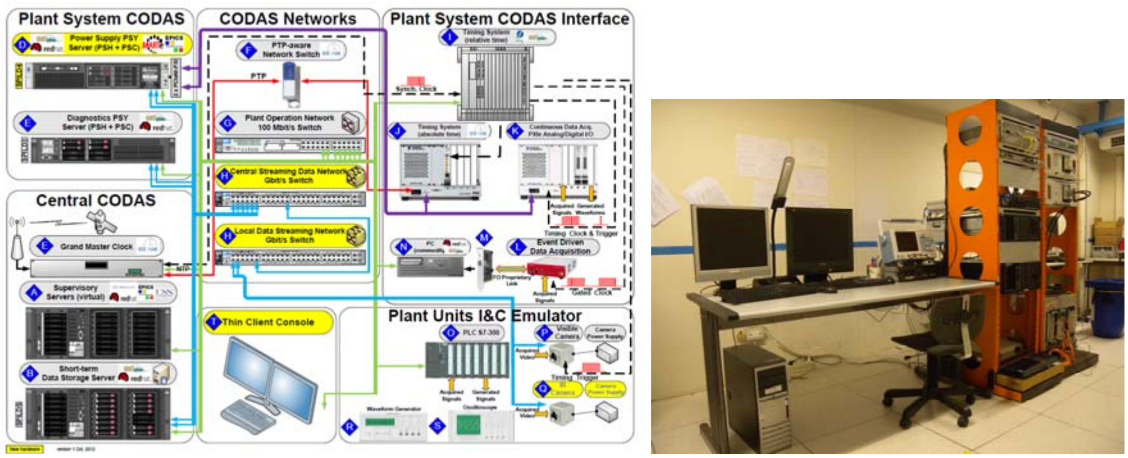

Fig. 3.15: SPIDER: prototype of CODAS and picture of part of the Hardware used for the test

The tests performed on the prototype have been witnessed by F4E and ITER Organization and also INDA has demonstrated the interest on the prototype implementation. This is the first experimental implementation of the control system architecture foreseen also for ITER. The results have demonstrated that the system is able to acquire, handle, elaborate and store the signals expected to be available in SPIDER and in particular in MITICA where the control system will be the same system to be used in ITER.

The main requirement that has been achieved has been the 1 hour of operation with 100 GByte of total data acquisition and up to 200 MByte/s peak sustained data throughput.

The interlock system design has been revised along the year in subsequent steps and the full documentation ready for the procurement has been prepared.

For the SPIDER safety system the activities started in the second semester and a preliminary version of the system requirements have been prepared. During the work performed in this year the following tasks have been performed:

- Safety criteria have been identified
- Safety system conceptual design has been developed

- Main risks in all the plant systems and area of work and operation have been identified

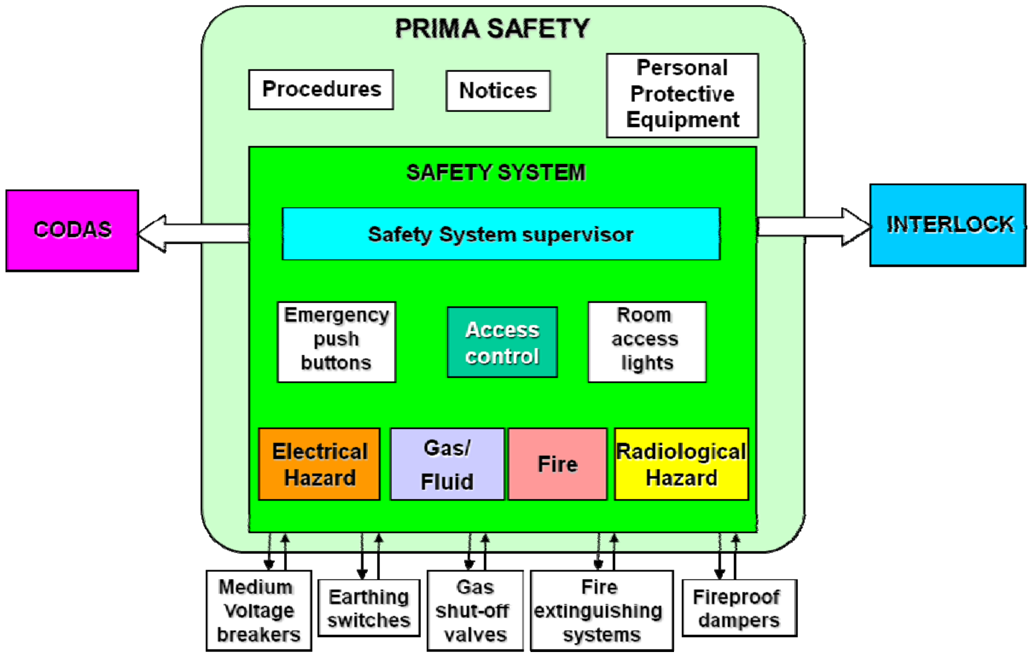

Fig. 3.16: SPIDER: SAFETY system blocks and interaction with other sub systems

3.2.3 MITICA

During 2012 the work has been focused on the design of the vessels, of the beam source, of some of the beam line components, of the residual magnetic field coils, on the finalization of the design of the AGPS ground voltage, and on the support to the finalization of the design of the HVD1 hosting the MITICA ion source power supplies and of the high voltage bushing between HVD1 and SF_6 insulated transmission line.

Moreover during this year the integration of the items to be delivered by Japan Domestic Agency has progressed with regard to the integration of the AGPS overall system including both ground voltage (EU-DA part) and step up transformers including rectifier diodes and filter system (JA-DA part) and with regard to the integration of the SF_6 transmission line in the PRIMA building. In particular, progress has been made on the integration and interface definition of the high voltage bushing between SF6 and on vacuum environment installed on the top of the beam source vessel.

3.2.3.1 MITICA beam source and line vessels

In March 2012 the PDR (Preliminary Design Review) was performed in ITER Organization and, from the outcome of the panel works, the design has been finalised up to the production of the final 3D model, the relative 2D drawings, the technical specifications ready for the call for tender and the final report on the analyses developed in support to the design work.

In fig. 3.17 the drawing of the two vessels is shown. The figure also shows the support structure of the vessel itself and of the HV bushing.

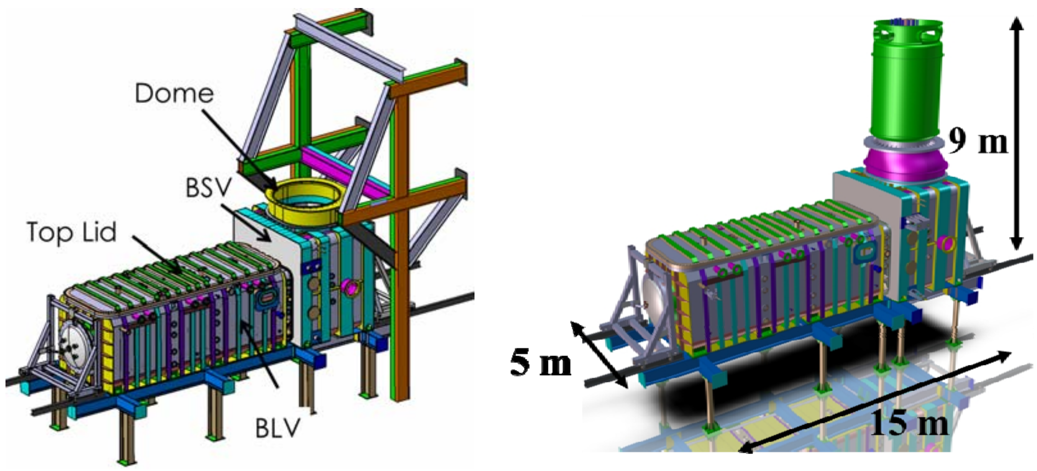

Fig. 3.17: MITICA vacuum vessels and support system for both vessel and high voltage bushing

All the final documentation was delivered at the end of 2012 ready for the FDR (Final Design Review) in ITER Organization scheduled in the second week of 2013.

An example of design verification results derived from one of the eight combination of the twenty-five different load cases is shown in fig. 3.18.

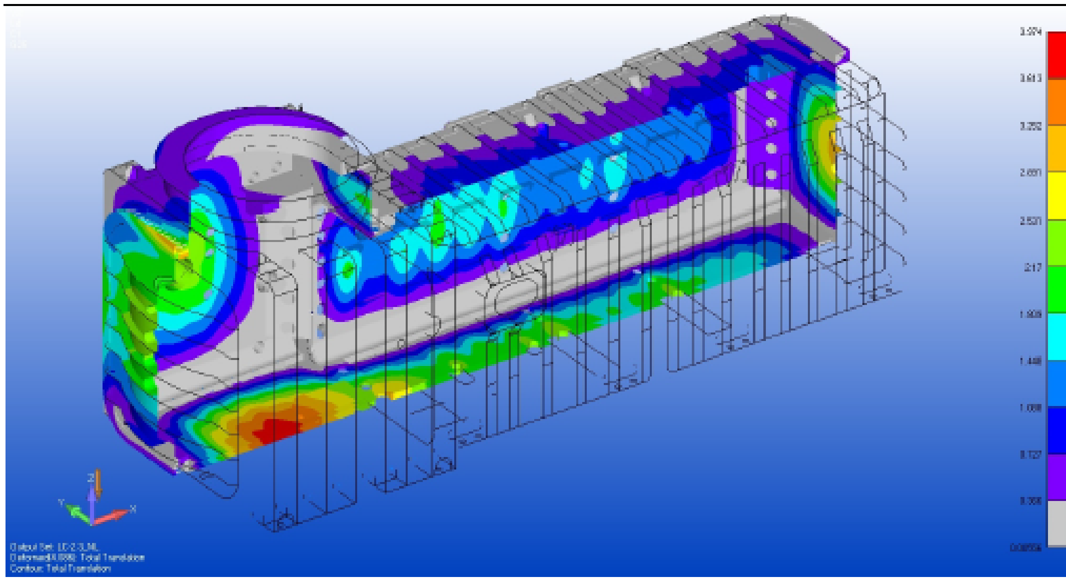

Fig. 3.18: MITICA vacuum vessel displacement for one of the relevant load combination among the 25 load cases identified for this component.

3.2.3.2 MITICA beam source

The MITICA beam source design has progressed significantly in many areas and the design at the end of 2012 is ready for the PDR (Preliminary Design Review) in ITER Organization that will be also held on the second week of 2013.

Some R&D activities were initiated in 2012 with regards to the design and manufacture of ceramic post insulators, critical mechanical component due to the torque mainly manufactured with ceramic material not capable to withstand tensile stresses.

Moreover the R&D on the heterogeneous joint between copper and stainless steel has been carried out. This was done with the test of electron beam welding mock-ups reproducing the joint of the stainless steel cooling pipes of the grid with the copper grids themselves.

Finally the order to manufacture a full scale prototype beam source copper back plate coated with a 1 mm Molybdenum by using the explosion bonding technique was launched.

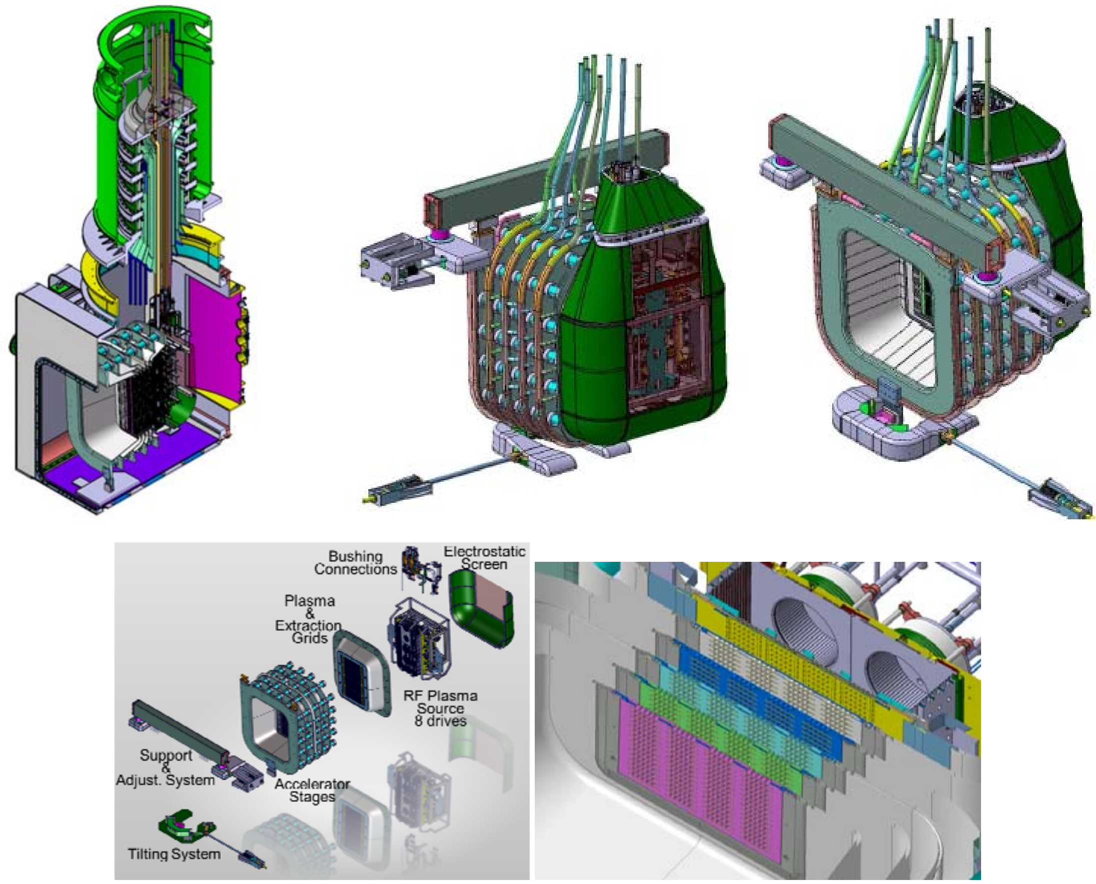

Fig. 3.19: MITICA beam source

In fig. 3.19 the actual drawings of the whole source and some details are shown.
In fig. 3.20 the design of the ceramic post insulators used to support each step of the accelerator stages and to support the plasma source is shown. This design has been developed following the development of the R&D activities performed along the year.

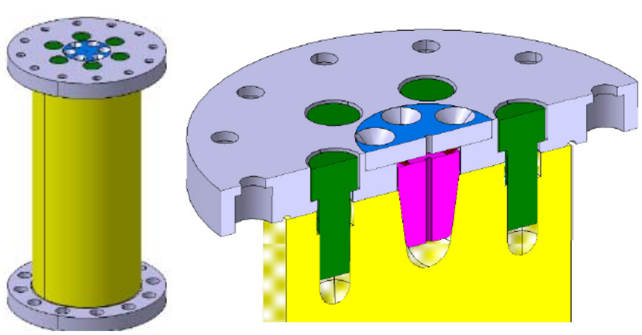

Fig. 3.20: post insulator design as resulting from the R&D work performed in 2012

In fig. 3.21 the first prototypes of electron beam welding between Copper and SS have been manufactured to develop the heterogeneous joint between the two materials that will be used in the acceleration

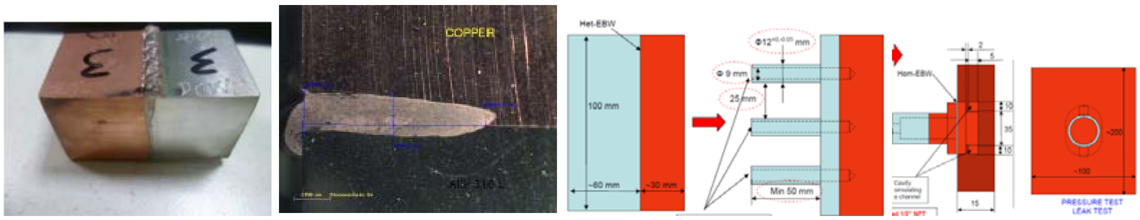

Fig. 3.21: sample of Cu-SS EBW and detail of the welded zone on the left side, whereas on the right side two examples of possible joints resulting from machining of the metal pieces after the welding

A relevant design effort has been dedicated to increase the vacuum voltage holding strength up to the required nominal value of 1 MV. This was done by using the discharge probability code developed in the Consorzio RFX which has been benchmarked with some experimental data and that will be further assessed in the HVPTF (High Voltage Padova Test Facility). In fig. 3.22 an example of horizontal electric field map and probability discharge and particle path is presented.

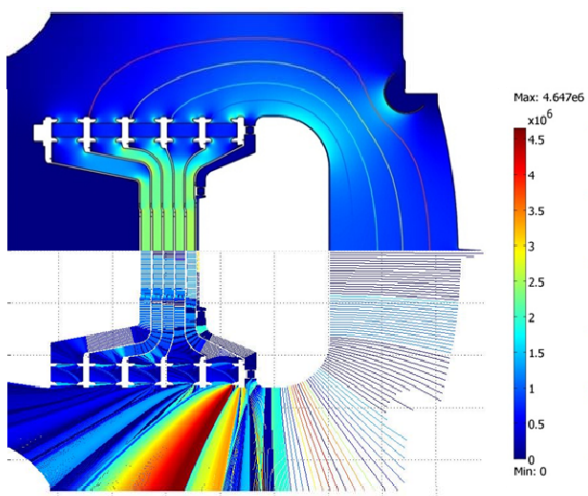

Fig. 3.22: MITICA horizontal 2D electrostatic field map, probability discharge and particle path

A further relevant optimization in the design of the source was the minimization of the neutral particle profile in the accelerator region. This was reached through the implementation of an original code developed at Consorzio RFX. The fig. 3.23 shows an example of the neutral particle profile in the accelerator region.

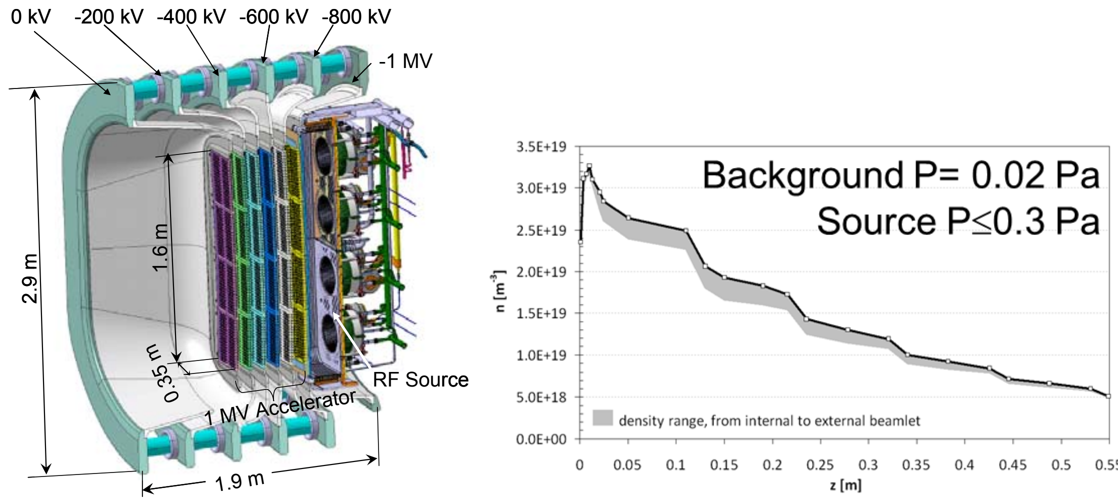

Fig. 3.23: MITICA vertical cut view showing in different colours the accelerator stages and the neutral particle profile starting from the plasma source (right side in the left figure) up to grounded grid (last purple grid on the left figure)

3.2.3.3 MITICA beam line components

The PDR (Preliminary Design Review) in ITER Organization of all the beam line components in 2012 was held in March 2012. In fig. 3.24 is shown a scheme of the components.

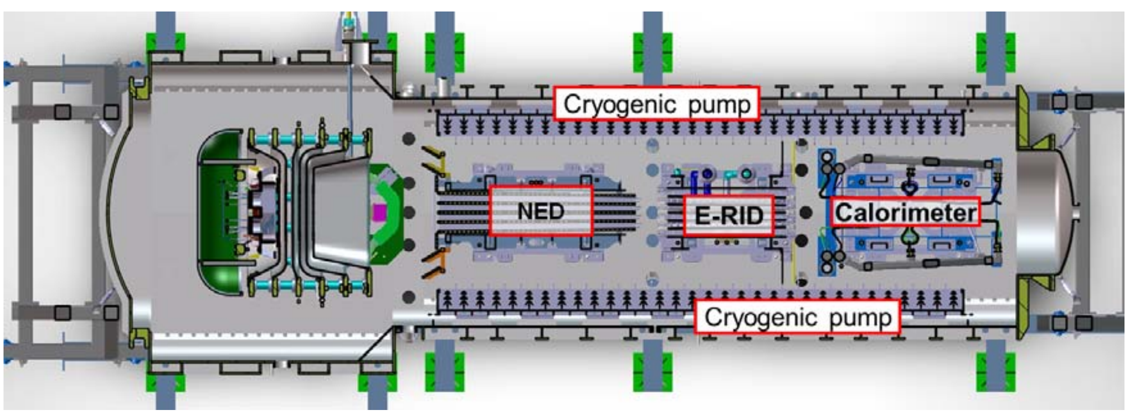

Fig. 3.24: MITICA beam line components installed inside the vessels

The beam exiting from the accelerator is composed not only of D-/H- particles, but a not negligible fraction of electrons are present. The presence of a uniform magnetic field used to dispose the electrons within the accelerator implies a subsequent deflection of the electrons, a detailed analysis of the areas in which these electrons will impinge was performed. In fig. 3.25 an example of the trajectories of this population of electrons is shown.

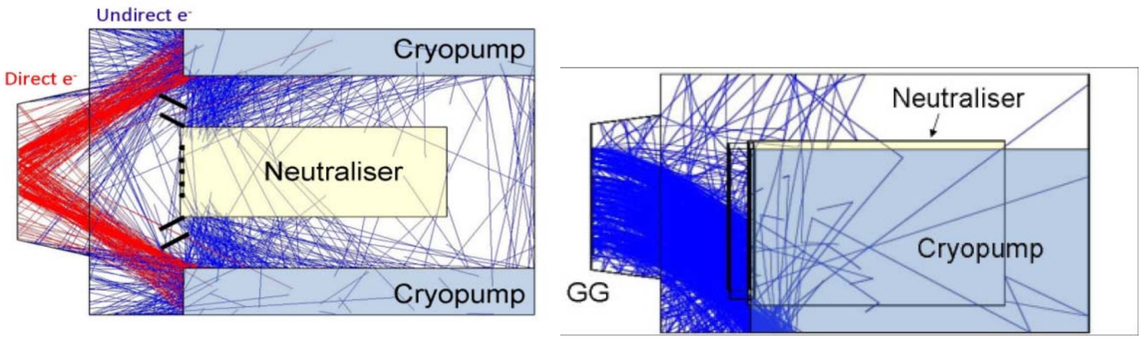

Fig. 3.25: electron trajectories downstream after the exit from the accelerator (upper and lateral view)

From the outcome of the panel works, the design has been finalised up to the production of the final 3D model, the relative 2D drawings, and the technical specifications ready for the call for tender. A final report was prepared on the analyses developed in support to the design work developed by Consorzio RFX on the Neutraliser and the Electron dump (fig.3.26).

A preliminary Final Design Review in ITER Organization of this component will be given in the second week of 2013.

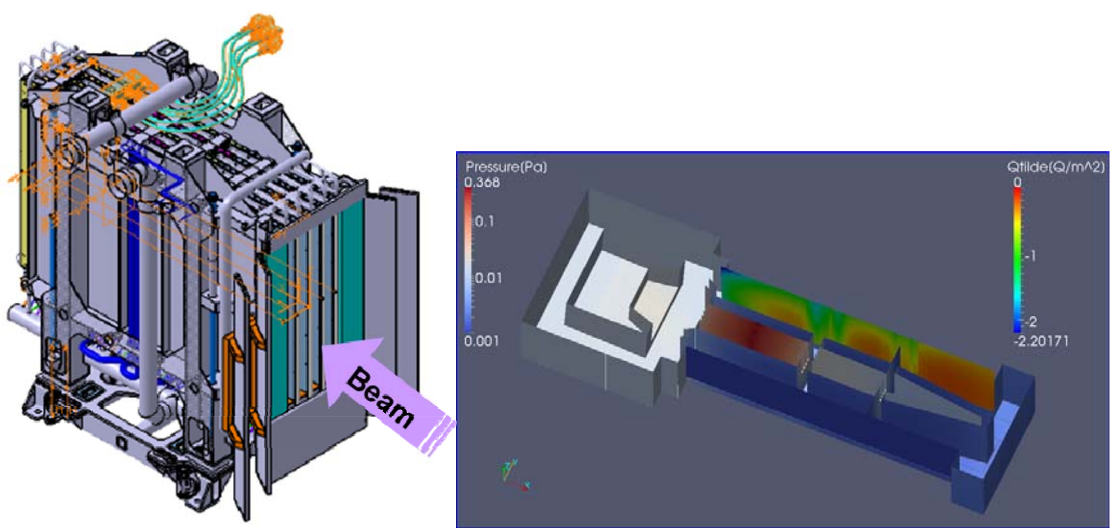

Fig. 3.26: MITICA neutraliser and electron dump; pressure profile and throughput in the beam line vessel

In fig. 3.27 some result of the thermo-mechanical behaviour of one panel of the Neutraliser is shown in which it is visible the cooling temperature of the water, the panel temperature map of both sides and the amplified bowing of the panel due to the uneven heating of the two sides.

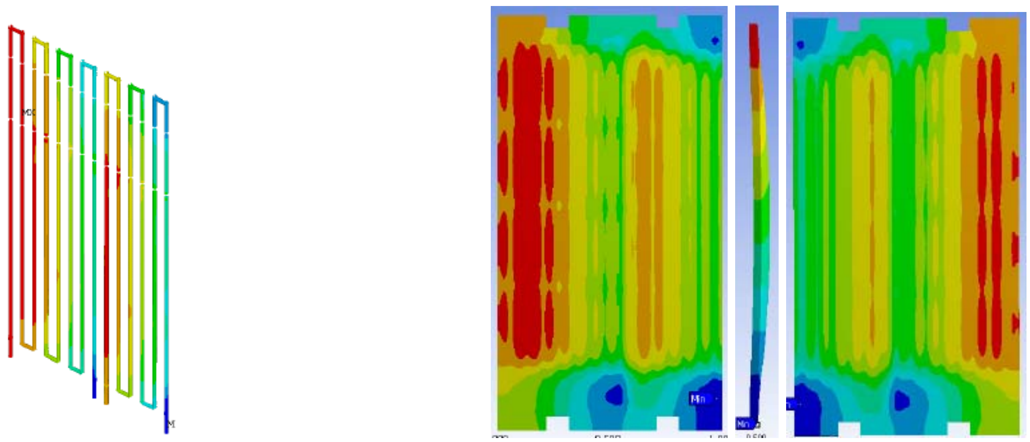

Fig. 3.27: coolant temperature (left figure), temperature maps on both side of one neutraliser plate and out of plane deformation (right figures)

Some relevant R&D have been carried out for the verification of the alignment of the deep drilling of the cooling channels on the CuCrZr panels and in the development of the vacuum and radiation compatible thermocouples of this component (fig. 3.28 and 3.29). The results obtained in the development of the deep drilling have been found to be useful also for the Electrostatic Residual Ion Dump (ERID) so that the outcome of this last development will be applied also to the other two beam line components and to the beam source.

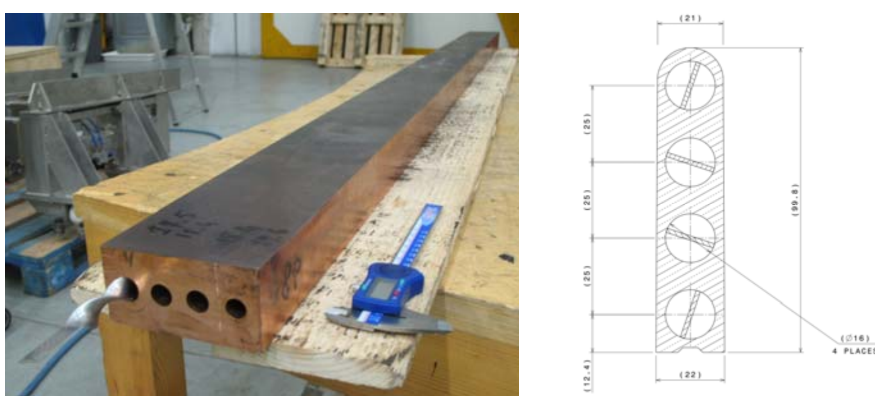

Fig. 3.28: MITICA deep drilling of Cu-Cr-Zr panels that are used both in the Neutraliser and in the E-RID

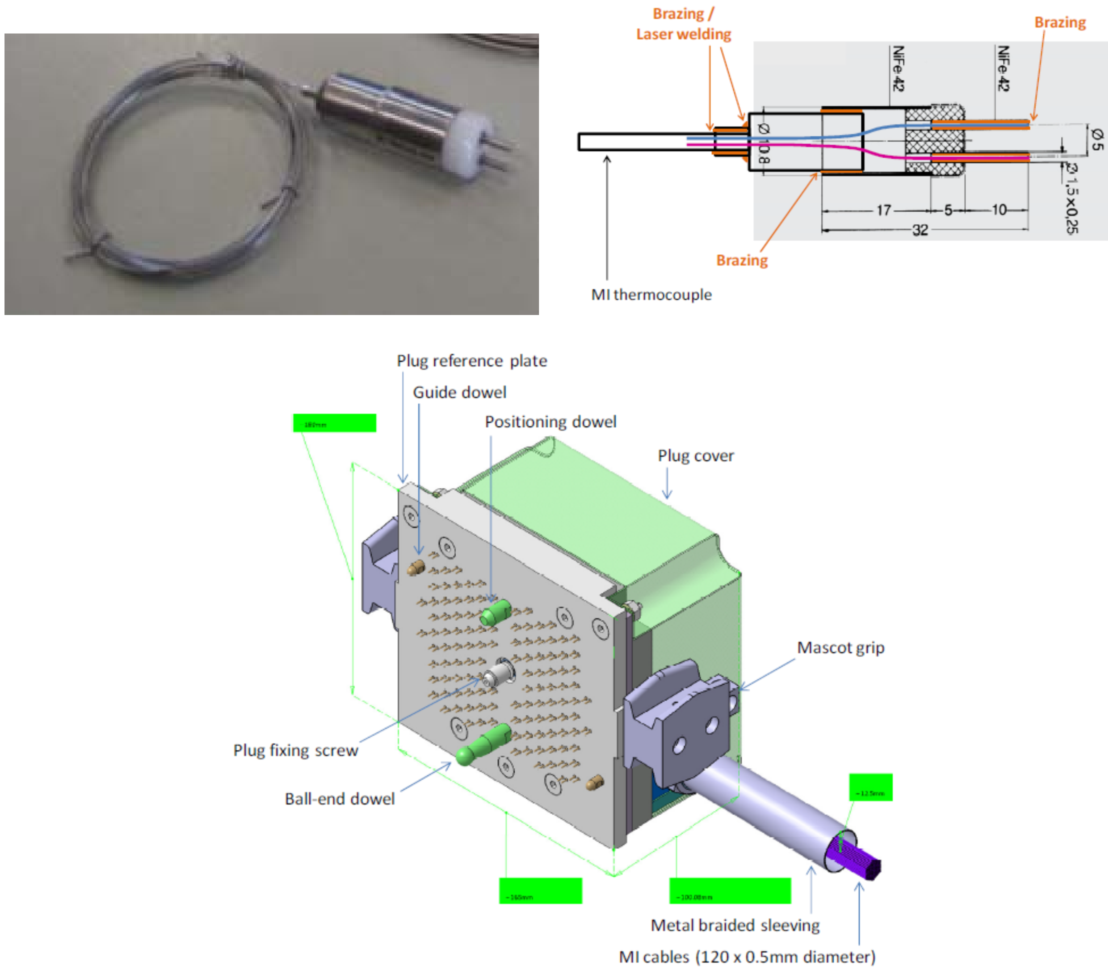

Fig. 3.29: MITICA thermocouple prototype vacuum and radiation compatible manufactured in three different diameters (here is shown only the 0.5 mm diameter) and plug RH compatible

For the ERID (fig. 3.30), due to the reduction in interest and manpower from CCFE the activities remained on hold after the Preliminary Design review held in March 2012. Nevertheless the completion of the design for the Neutraliser and the progress in the design of the Calorimeter have allowed solutions to be found to the issues that were in common between all three beam line components.

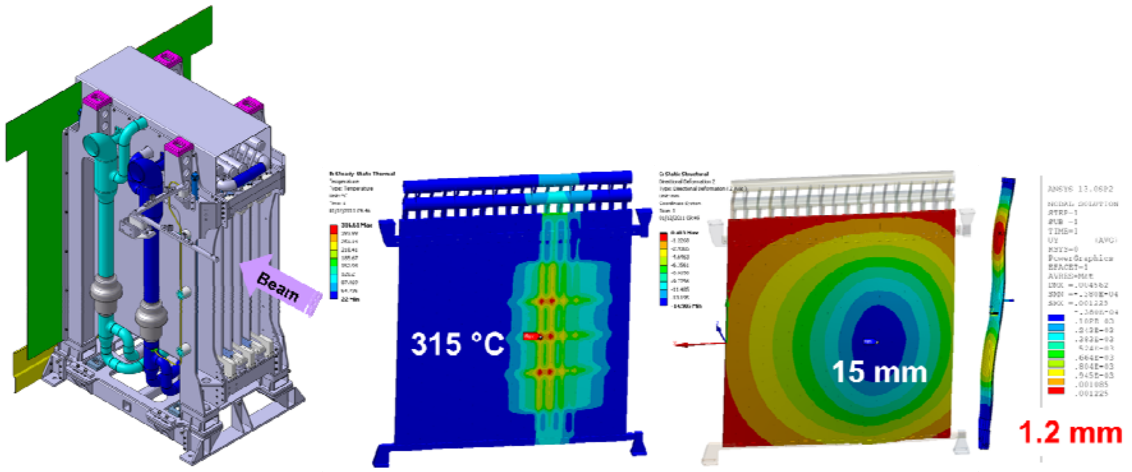

Fig. 3.30: MITICA ERID

After the Preliminary Design Review, the activities for the completion of the design of the Calorimeter (fig. 3.31) have progressed in the last quarter of the year with the collaboration of the CCFE. The most relevant issues originated at the PDR have been analysed and solved during this year, so that the design is nearly completed.

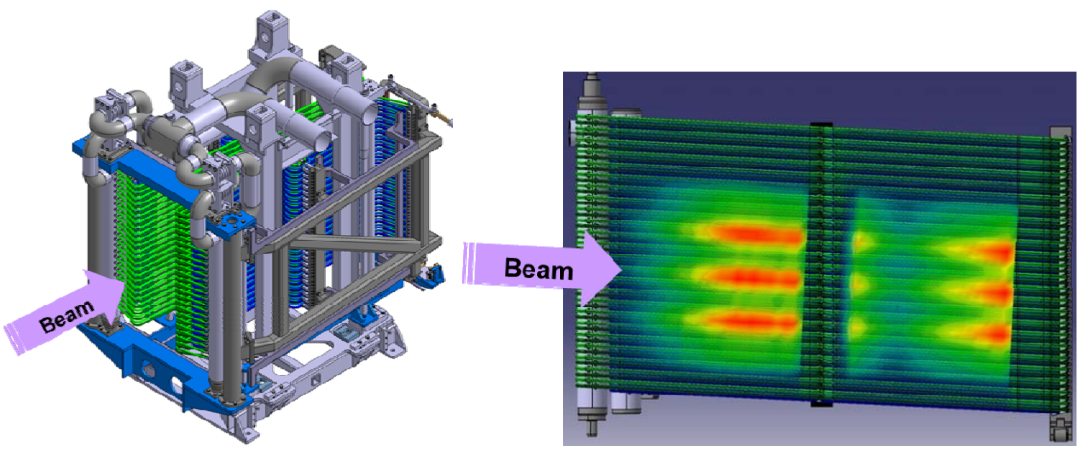

Fig. 3.31: MITICA calorimeter

This year, an R&D activity was developed to assess the issue of the manufacturability of the CuCrZr tubes used with the required bending precision (fig. 3.32). Tests on the insertion of stainless steel swirl tape inside the CuCrZr before the bending process were performed to identify the most suitable length and to assess the issues on both length and width of the tapes. The obtained results confirmed the design choices and allowed to identify a viable manufacturing process.

Turbulence promoter inserted inside the tube

Fig. 3.32: MITICA calorimeter single CuCrZr tube prototype

3.2.3.4 MITICA Residual Magnetic Field Coils (RMFC)

The requirements in terms of magnetic field required to reproduce in MITICA the stray field of the ITER-HNB was defined in 2011, as well as a configuration of coils suitable to guarantee a sufficient flexibility to vary the field strength and distribution and to discriminate the influence of the field in different region of the injector. As a consequence, the Power Supplies requirements to the new identified exploitation needs have been defined.

The power supplies rating was confirmed in Q3-2012, and in the last quarter the design work of the coils and their integration in the MITICA vessel and in the MITICA support frame started. The design of the RMFC has been performed (fig. 3.33) and a first version of the Technical specification, drawings and design report has been delivered by the end of 2012 for the Preliminary Design Review performed in ITER on the second week of 2013.

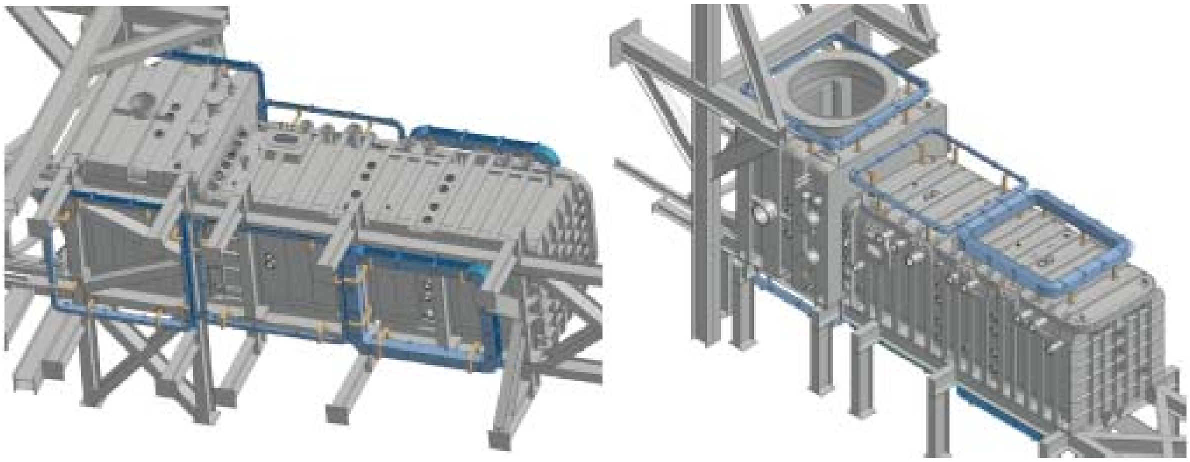

Fig. 3.33: MITICA RMFC layout and installation on the vessel support frame (bottom coils) and the vessel itself (upper coils)

The magnetic field induced in three different relevant regions of the injector are evidenced in fig. 3.34, whereas in fig. 3.35 a 2D thermal analysis of one coil section is shown. The internal turn of the coil are cooled by a plate connected to a water cooled pipe. The overall single coil is inserted inside a cable duct.

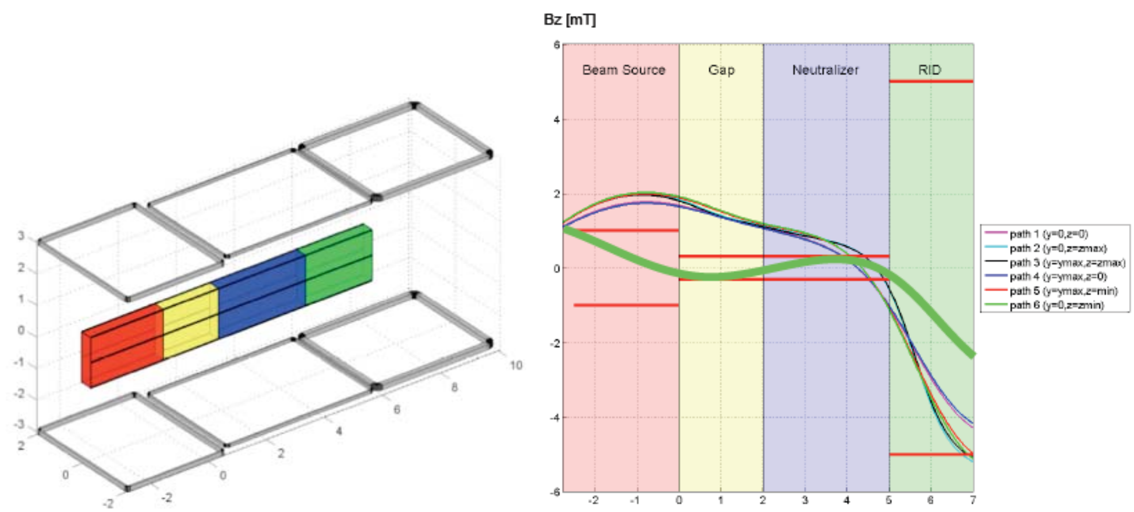

Fig. 3.34: RMFC magnetic field produced in the coloured relevant regions and comparison with the expected stray field in ITER injector (green gross line)

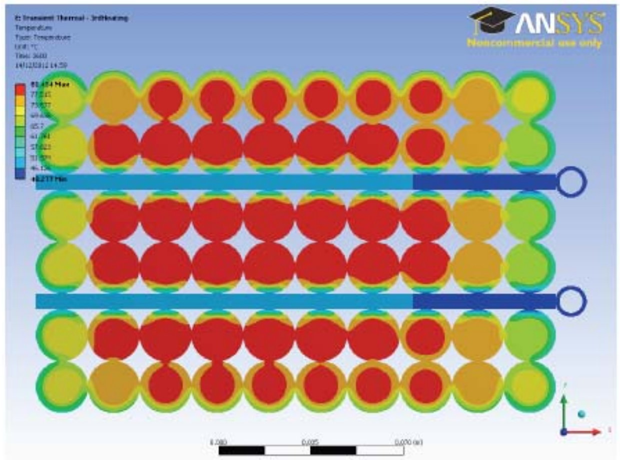

Fig. 3.35: Temperature contour plot of the section of one RMFC coil

3.2.3.5 MITICA Power supply systems

The power supply system of MITICA includes a set of PS that feed the active components of the source like in SPIDER and therefore share the same name ISEPS at a potential of approximately –1MV and the most relevant system of power supplies necessary to accelerate the beam in five stages of -200 kV each. This last system is shared between JADA and F4E and a complex integration activity is necessary both on mechanical and electrical aspects.

In fig. 3.36 it is shown the layout of the high voltage transformers with on top the rectifier diodes supplied by JADA as well as the SF6 (6 bar) insulated transmission line also supplied by JADA. In the system are also integrated two High voltage decks: HVD1 delivered by F4E dedicated to host all the electrical PS belonging to ISEPS and HVD2

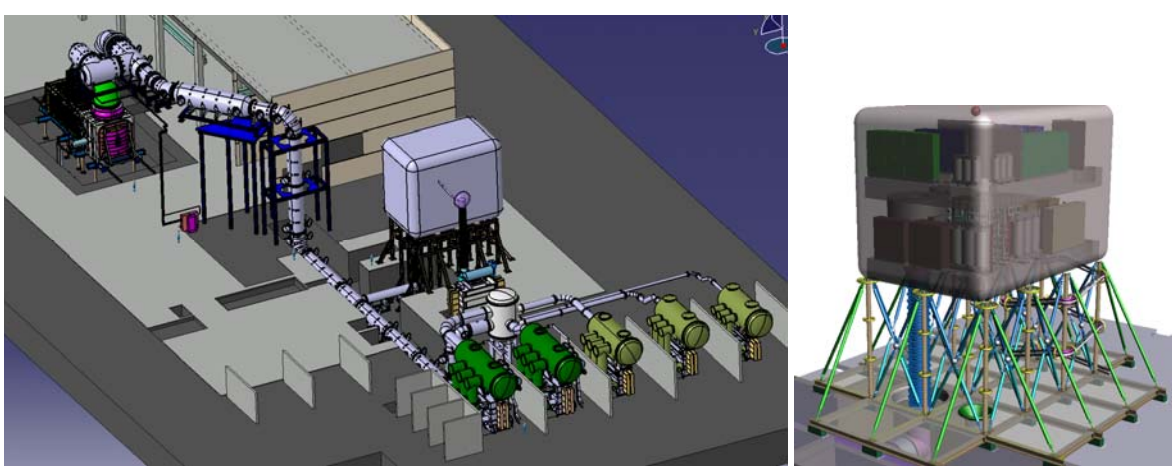

Fig. 3.36: MITICA power supply system layout and detail of the HVD1

delivered by JADA dedicated to feed the source and the intermediate voltage stages with cooling water and with the operating gases.

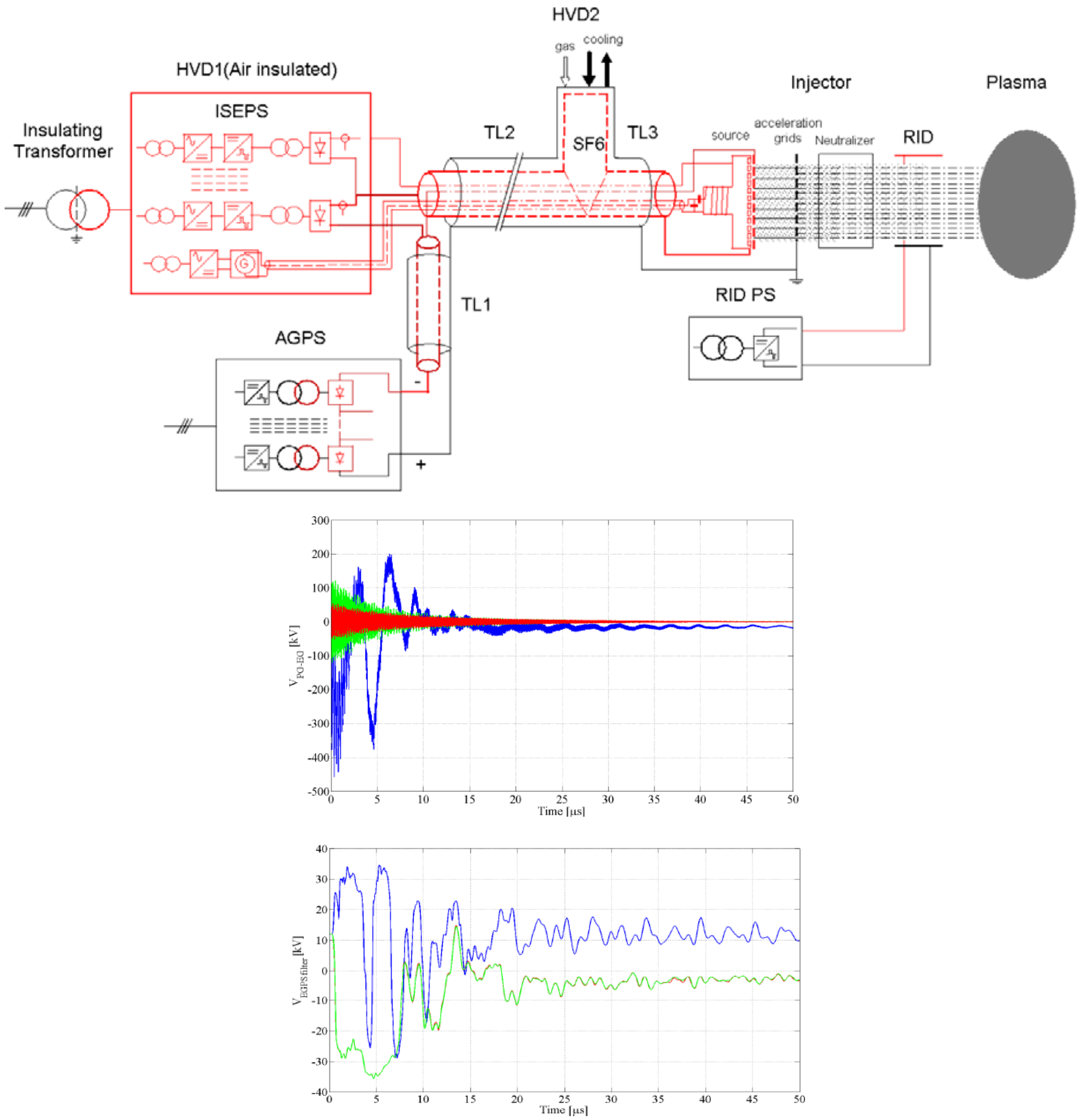

Fig. 3.37: MITICA integrated modelling result: example of one typical breakdown between EG and GG and the propagation up to the EG power supply

Also for MITICA an integrated electric model has been developed including all the active and metallic part of the injector to study the evolution and the propagation of breakdowns and other fault in the individual part of the system. He model was further updated in 2012 with the progress of the design and in fig. 3.37 there is the example of a breakdown between EG and GG and the propagation of this up to the EG power supply installed inside the HVD1.

3.3 NBI accompanying programme

3.3.1 HV Holding

The 2012 experimental activities focused mainly on the issue of the high voltage tests with magnetic field. Several experimental campaigns aimed to study the possible displacement of the Paschen curve by magnetic field were carried out. The MITICA accelerator is designed to work with a background gas pressure lower than 0.05 Pa in the region surrounding the electrostatic accelerator. Being the geometric maximum gap length about 1.4m, the maximum product p*d (pressure x distance) is 0.05*1.4=0.07 Pa*m, which is lower than 0.1-0.2 Pa*m which corresponds to the limit of the Paschen curve left branch in hydrogen. Following a request from ITER, it has been investigated if (and how) the magnetic field can shift such branch.

Since the left branch of the Paschen curve is relatively steep, it has been noticed that such an effect can be studied at relatively low voltage (U <100 kV). Based on this observation, the experimental campaigns at the HVPTF during 2012 have been carried out at relatively low voltage. In fig. 3.38 is shown the Paschen curve obtained with and without magnetic field and with different distance of the electrodes. It has been observed that the distance determining the onset of breakdown is the distance between the electrodes and the vacuum vessel and that the presence of a strong magnetic field can shift that curve in a way that breakdown can occur in a region that was free from breakdown without magnetic field.

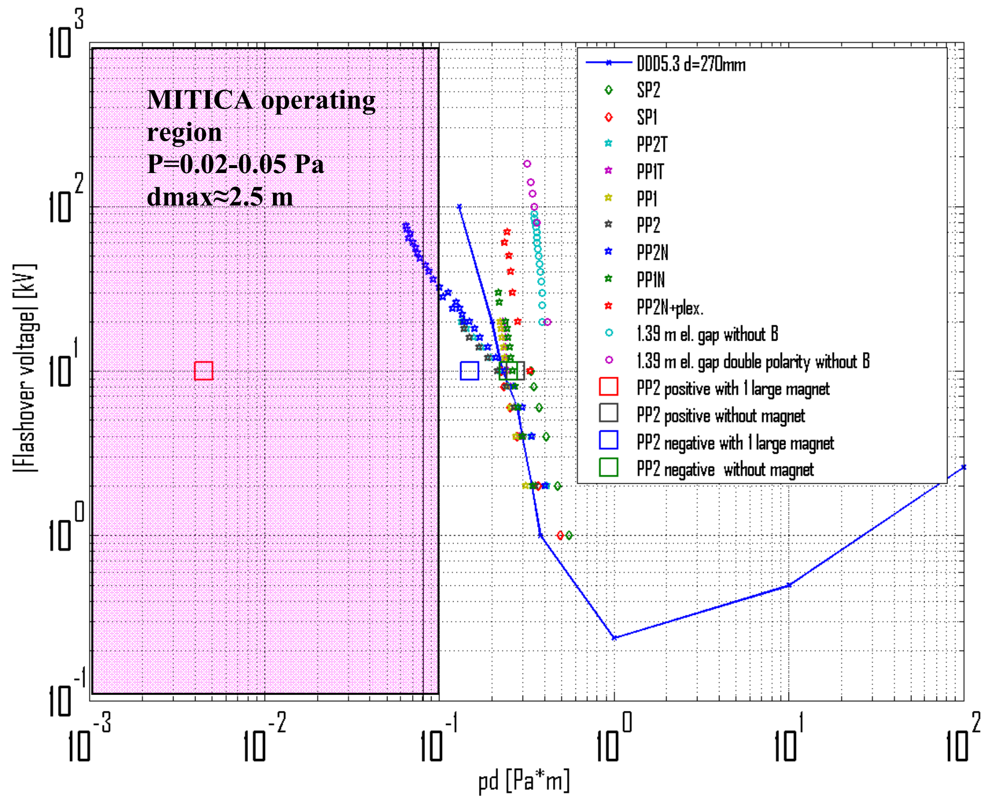

Fig. 3.38: Paschen curve with and without magnetic field

3.3.2 NIO1

During 2012 the procurement of the NIO test facility proceeded in the framework of the funding provided by “Fondazione della Cassa di Risparmio del Veneto”.

Specifically, the company that received the order issued at the end of 2011 for the construction of the NIO1 source realized most of the components. As an example, the components of the RF coil are shown in Fig. 3.39.

The following items were procured: high voltage power supplies, high current power supplies, insulating ceramic cylinders, most of the items for vacuum and gas injection system, optical fibres, photomultipliers, and some other items for emission spectroscopy. The order for the high voltage transformer was issued. The layout of the site was defined; the configuration of the cooling systems is being finalised.

Fig. 3.39: Components of the RF coil of the NIO experiment.

Simulations of spectroscopic signals were carried out to assess the expected range of the measurements, as well as and the suitability of the available spectrometers and cameras. In Fig. 3.40 the spectra expected along horizontal and vertical lines-of-sight are shown.

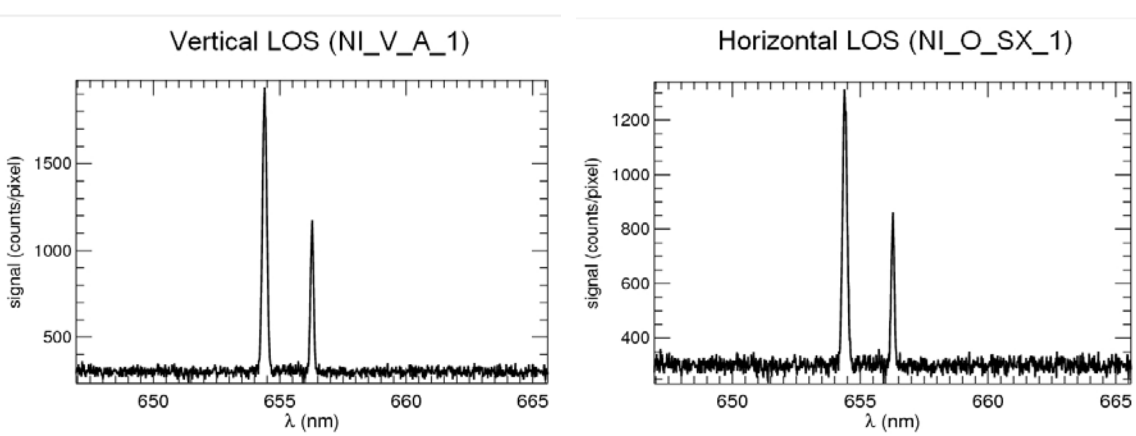

Fig. 3.40: Spectra of the light collected by the vertical (left) and horizontal (right) lines-of-sight.

3.3.3 Modelling

Within Grant F4E-2009-GRT32-PMS-H.CD several design options were identified, tested and compared (equal vs different grid gaps, horizontal vs vertical magnets, ferromagnetic material etc.) with the objective of guaranteeing the optimal ion beam optics, while reducing the complexity of the grids.

Some modifications and improvements were proposed during RFX internal meetings. In addition, after the distribution of these results to the NBI community, RFX co-operated with personnel from CEA, ITER IO, IPP and JAEA.

The most promising design concepts have been compared, in terms of:

- Beam optics (beamlet divergence, beam aiming, compensation of electrostatic repulsion). Regarding this aspect in fig. 3.41 the repulsion of the side and corner beamlets in one beamlet group (8x16) is shown.

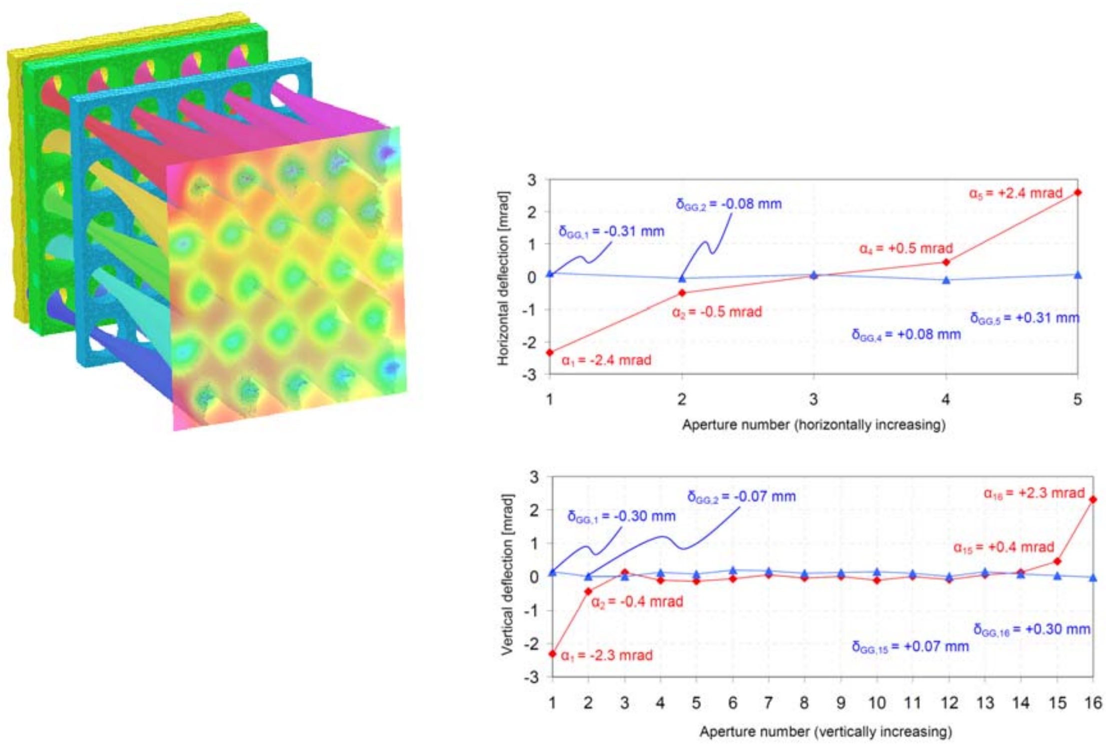

Fig. 3.41: Electrostatic repulsion of side and corner beamlets in one beamlet group (5x16)

- Capability to dump the co-extracted electrons and the ones generated by stripping (Fig. 3.42)

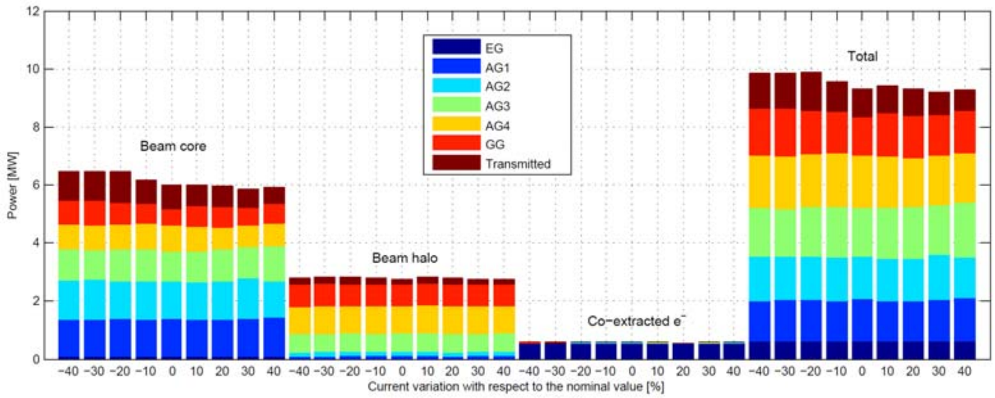

Fig. 3.42: Dumped and transmitted power with EQ_GAPS_33 geometry, CESM+ESESM+PG_8 magnetic configuration and the PG current varying in the range [-40%,+40%] around the nominal value.

- The EQ_GAPS_33 geometry, with the magnetic configuration #18, was found to be the best performing design solution (fig. 3.42). Hence, this solution is proposed as the reference one. The main features of this solution are:
    - Equal acceleration gaps to increase the voltage holding capability.
    - Specific PG and EG shapes, following the suggestions by JAEA and CEA.
    - Optimized diameters of the accelerator grids permitting fair sharing of the heat loads.
    - Uniform long range magnetic field produced by the PG current acting both in the plasma source to remove electrons form the front of the PG and on the accelerator region to dump the stripped electrons on the accelerator stages to prevent their acceleration through subsequent stages. (fig. 3.43)
    - Horizontal permanent magnets embedded in the EG and in the accelerator grids combined with the long range field to have good performance of the accelerator with reduced grid heat loads. (fig. 3.43)

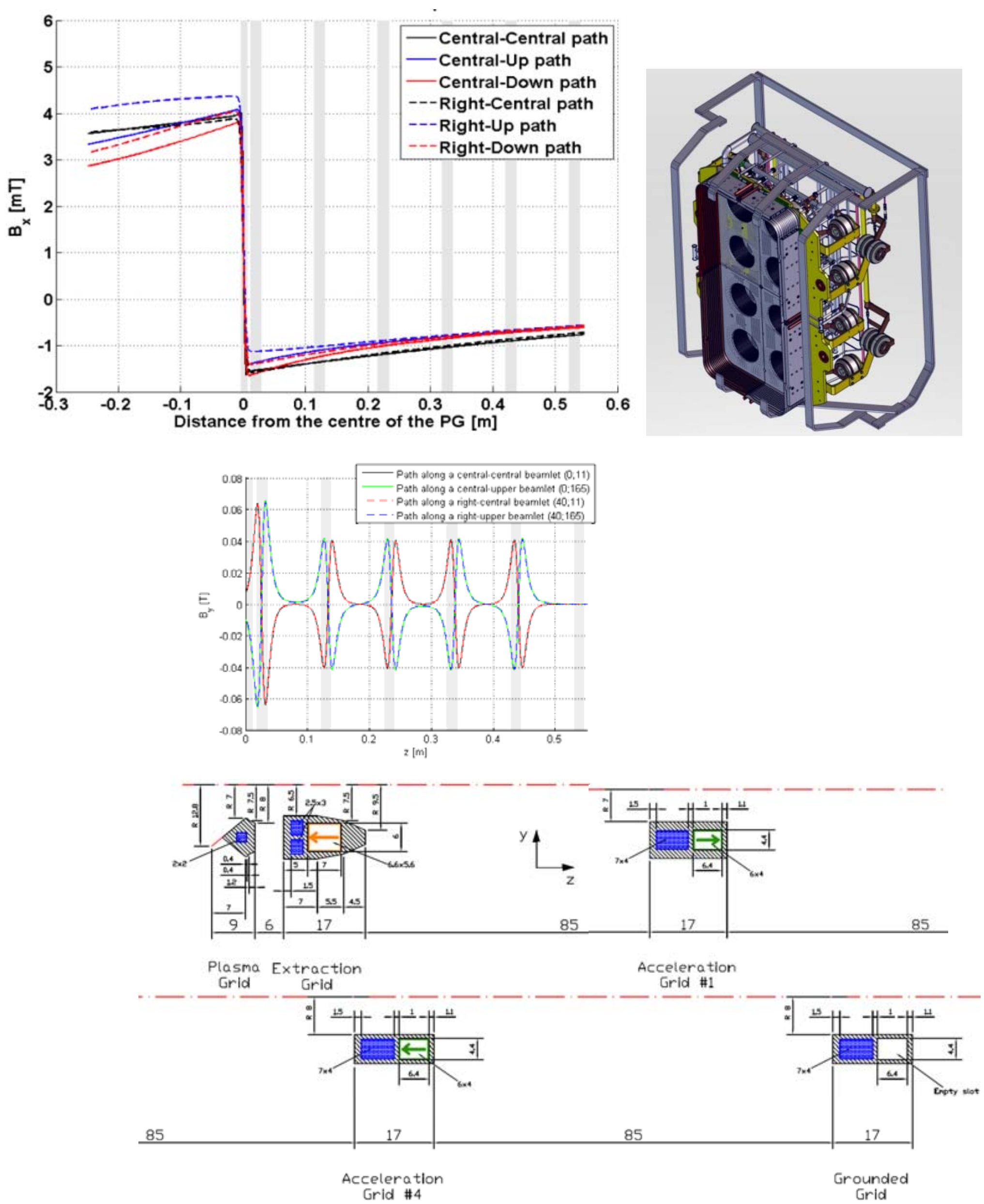

Fig. 3.43: long range and local magnetic field along the ideal linear beamlet trajectory in the accelerator. The shape of each grid highlighting the cooling channel and the permanent magnet position it is also shown. Please note that Grid 1 & 2 are identical as well as Grid 3&4.

- Thermo-mechanical behaviour of the grids (stress, strain, deformation, fatigue life) as shown as an example for one individual grid segment in fig. 3.44. Each grid is composed of four segments horizontally cut and covering four beamlet groups.

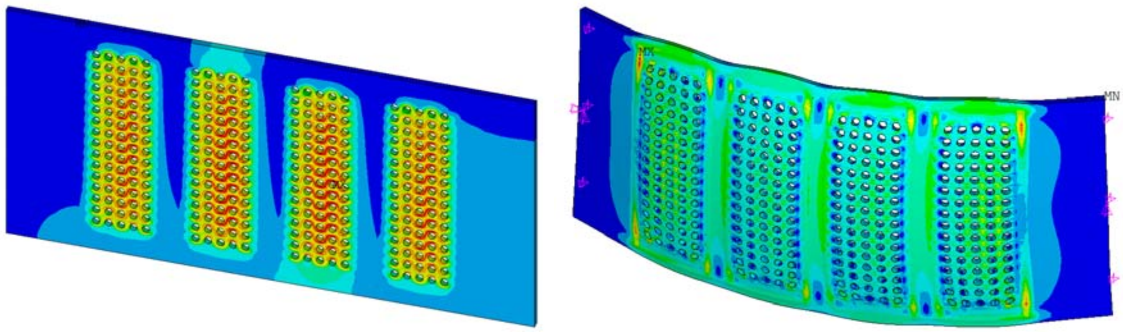

Fig. 3.44: temperature map of one segment of one grid on the left figure, mechanical stresses and deformation on the right figure.

- Thermo-mechanical assessment of the components located downstream of the beam source (neutralizer, ion dump, cryopumps, vessel). This has been already shown in section 3.2.3.3.

The neutral gas density profile was computed by means of the AVOCADO code (Fig. 3.45), which was improved with respect to previous versions in order to take the temperature into account. The code gives the profile in the three dimensional space in any position inside the accelerator and models the real geometry.

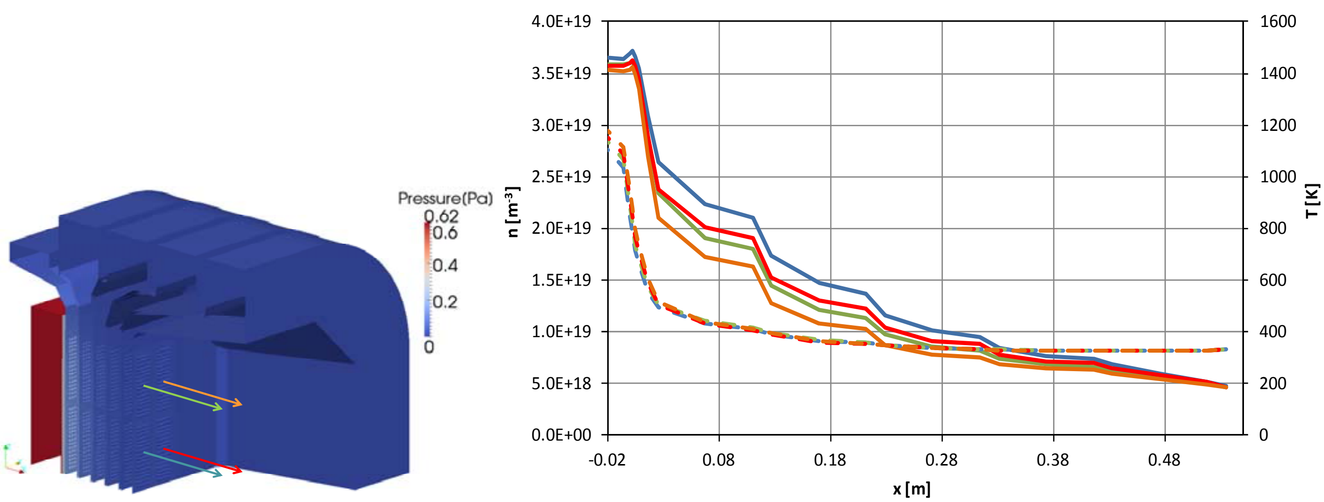

Fig. 3.45: Density profiles and gas temperature calculated with Avocado code in four positions,.

The vacuum environment of the MITICA injector was modelled, considering updated dimensions of the first two beam line components. This model was simulated using AVOCADO code. The results have been compared with previous researches, with which the average density profiles are fully compatible. Unlike the previous models, AVOCADO allows the determination of the density profile across the beam (Fig. 3.46).

The Adaptable Rarefied Instrumented Atmosphere for Neutral iNjection Applications (ARIANNA) experiment has been set up as complementary service in the beam source modelling activity, supporting the development and validation of the AVOCADO code for molecular flow and density distribution analysis.

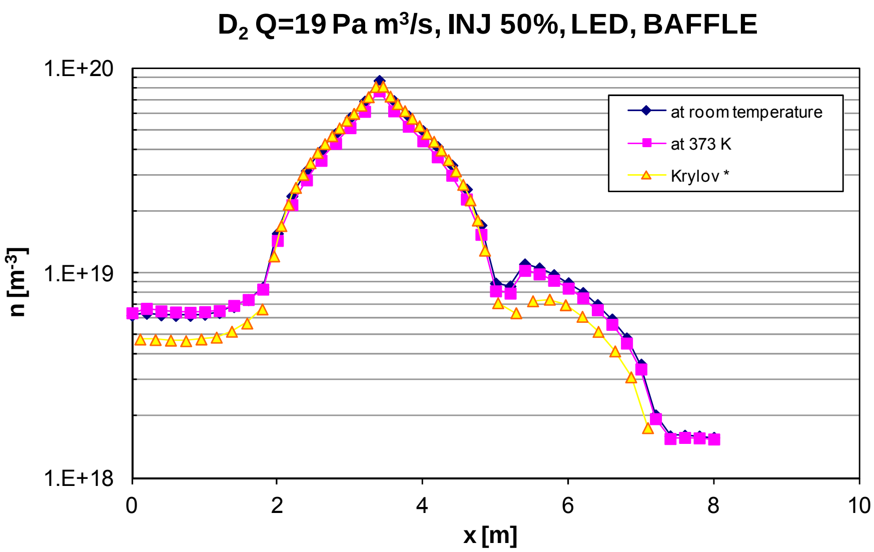

* no GG pit, baffle at the RID entrance, room T

Fig. 3.46: Density profile along the beam path, downstream of the GG; the Avocado results are obtained applying 0.001 Pa uniformly at the cryopanels. Krylov results do not consider the Lateral Electron Dump.

The BACKSCAT 3D code was used to evaluate the heat loads due to the electrons exiting from the Accelerator. This is a 3D particle tracking code developed in COMSOL environment, that uses as main inputs the geometry of the components located downstream of the accelerator and the particle exiting from each aperture (output of the EAMCC code). The trajectories of particles exiting from each aperture are calculated until they hit a component. Then a backscattering effect is included with an ad hoc model, and the power deposition is evaluated and mapped for each of component mentioned. The inclusion in this simulations of the long range magnetic field induced by the current flowing in the plasma grid, showed a different trend with respect to the previous simulations. An unacceptable power deposition was found on the vessel floor (Fig. 3.47) and a high amount of electrons reached the surface of the cryopumps. A novel design was proposed for the Electron dump, in order to minimize these effects (see also the previous section dedicated to Neutraliser and Electron Dump).

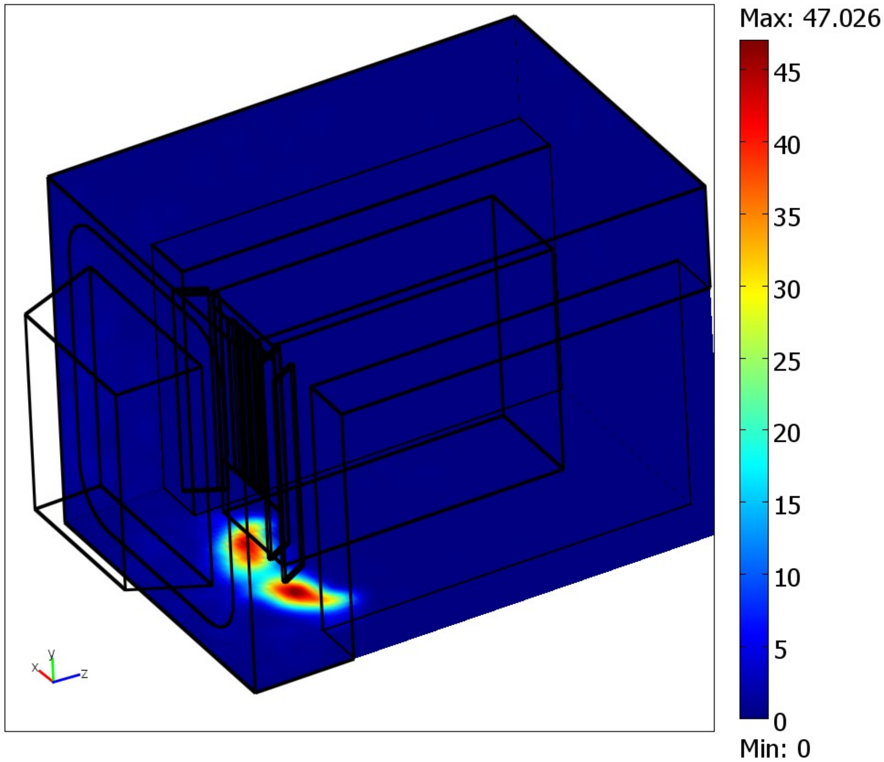

Fig. 3.47: Power load (kW/m^2) distribution on domain exit, vessel floor and left side.

After the acceleration stage, beam transport at reduced divergence is possible only thanks to space charge compensation of the beam. An investigation of this phenomenon was performed, aiming to characterize the spatial extension of the charge-compensated region. A 2D particle-in-cell code was used and modified to include the very last part of the accelerator. Realistic primary beam density profiles can also be implemented, and matching to the ray tracing codes used in accelerator modeling was performed (Fig. 3.48). The influence of a repeller electrode was also considered, both on the field topology in the region and on the slow particles motion.

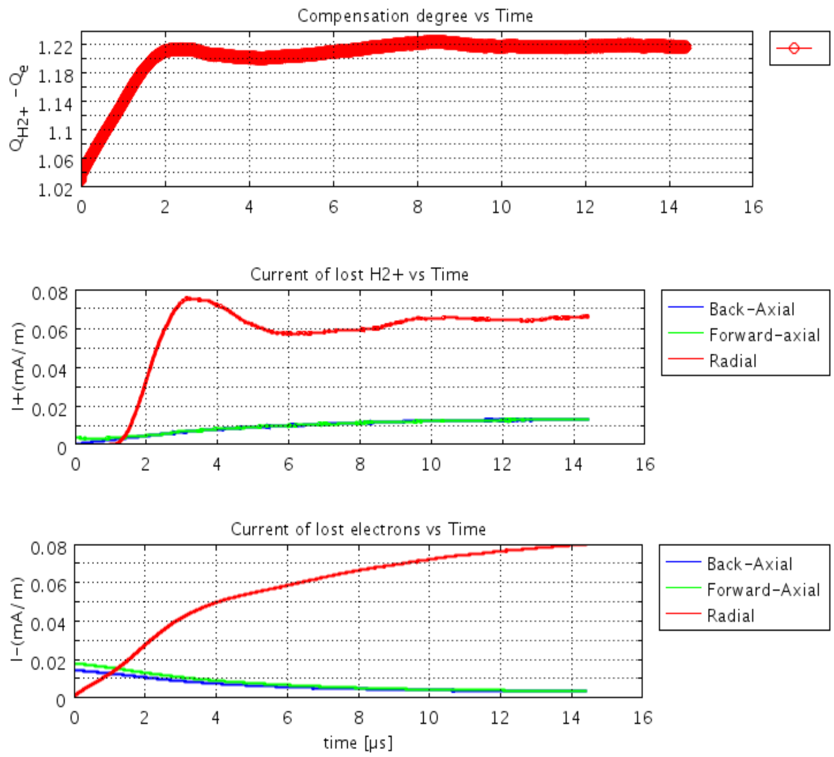

Fig. 3.48: Temporal evolution of space charge compensation and related losses, for the case with trapezoidal profile and $n0 = 2{\cdot}10^{12} m^{-3}$.

3.3.4 Participation to operation of Ion sources and Neutral beam injectors at other facilities

During 2012 several researchers participated at IPP, Garching (D) to the operation of BATMAN experiment and to the commissioning of ELISE experiment. Key tests of calorimetric and electric measurements were successfully completed. During the same year an intensive collaboration on beam optics simulations started with NIFS (Japan). A researcher was sent by NIFS at RFX to be trained on the use of numerical codes to simulate the beam optics in hydrogen. Following this visit researchers fro RFX have been sent to NIFS to apply the same numerical codes to interpret experimental results from the negative NBI in operation in the experiment LHD.

3.4 ITER Diagnostics

3.4.1 ITER Magnetic Diagnostics

During 2012 the activities related to the design of electro-magnetic sensors for ITER progressed with a contribution from Consorzio RFX articulated in two Grants supported by Fusion for Energy.

The first Grant (F4E-2009-GRT-047), started in 2010 in collaboration with CREATE, ENEA (UTFUS) and CCFE, is aimed at the optimisation of the ITER magnetic diagnostic system through the development and exploitation of numerical tools for performance evaluation of the magnetic diagnostics in achieving the target technical requirements.

During 2012 the activities were focused on the improvement of the method, started in the previous year, for the evaluation of performance and the optimization of the halo current diagnostic system for ITER. The capability of reconstruction of the halo current distribution on the first wall components was studied in some representative vertical displacement events simulated with a simplified plasma model (Fig.3.49) and adopting an interpolation algorithm operating on the measurements from the set of Rogowski sensors presently foreseen in the magnetic diagnostics. The results obtained so far show that the present set of Rogowski coils and the reconstruction algorithm are able to meet the required performance for the identification of the halo currents in test cases consistent with the actual pattern expected in ITER (Fig.3.50). A thorough assessment of the system capabilities as well as

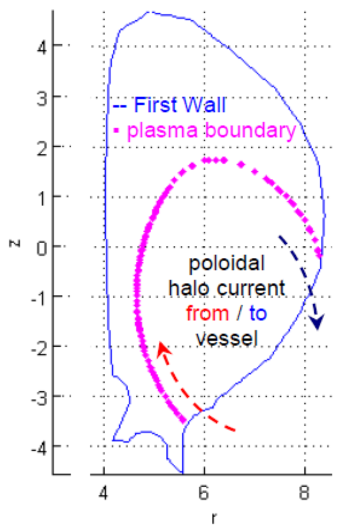

Fig.3.49: Projection of plasma boundary onto a poloidal plane for a VDE

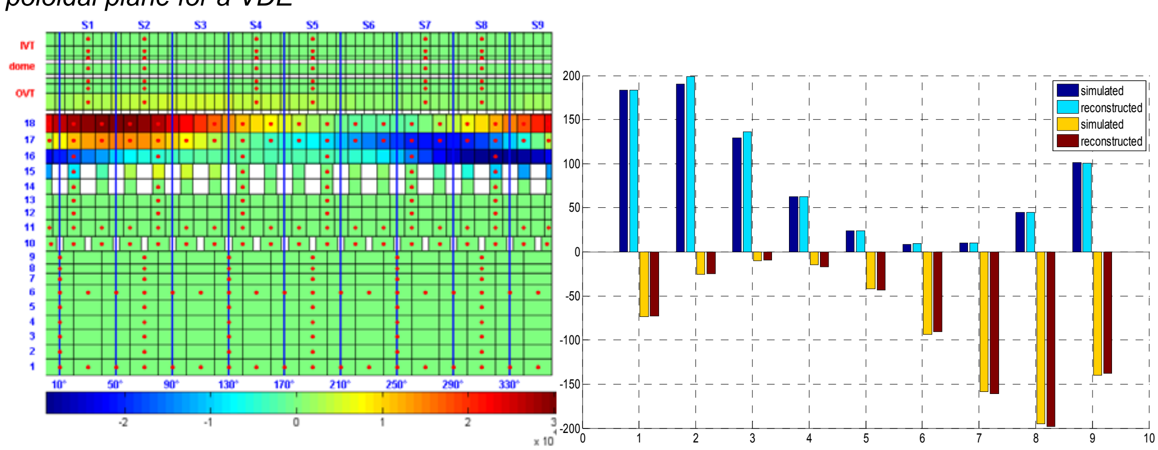

Fig.3.50: Left hand side: Identification of halo current on a 2D projection of the First Wall components for an asymmetric VDE (red bullets represent Rogowski sensors). Right hand side: comparison of simulated and reconstructed distribution of poloidal halo currents exchanged between plasma and wall in the 9 sectors

optimization of the set of sensors is still in progress by using a systematic and wide input data set, also considering the implementation of further magnetic measurements.

The second Grant (F4E-2010-GRT-155), launched in the second half of 2011, is aimed at the achievement of the detailed design of the ITER in-vessel magnetic sensors for plasma control and equilibrium reconstruction.

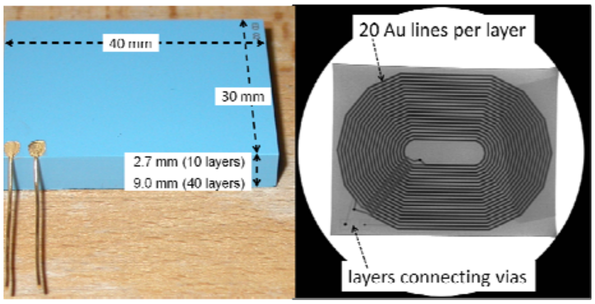

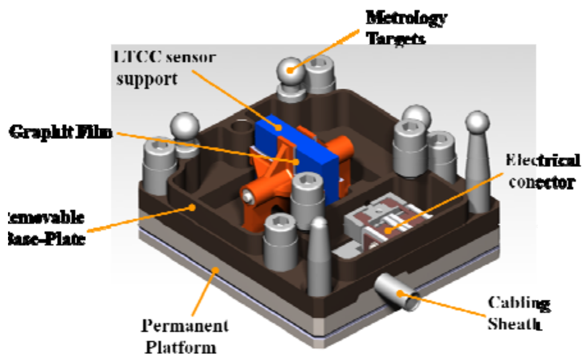

Fig.3.51: Prototypes of LTCC magnetic sensor: overall dimensions (left), X-ray image (right)

Fig.3.52: Magnetic sensor assembly

The activities during 2012 were mainly dedicated at the assessment of the conceptual design of the magnetic sensors, based on Low Temperature Co-fired Ceramic (LTCC) technology (Fig. 3.51), and the relative support and connection system, conceived to be replaceable by remote handling (Fig.3.52).

The sensor design progressed by means of thermo-mechanical and magnetic FEM analyses, to confirm the achievability of functional and operational requirements, and on nuclear analyses, performed in collaboration with SCK·CEN in order to estimate the effects of parasitic voltage induced by radiation on the sensors. Technical specifications for the manufacture and testing of new prototypes were produced and will be implemented during 2013.

3.4.2 ITER core LIDAR Thomson Scattering (TSCL)

The Framework Partnership Agreement with F4E originally expected in May 2012, was delayed to 2013. In the meantime RFX continued to define details of the NIR detector design and contacted potential detector manufacturer. A preliminary study of feasibility of a 1 cm diameter hybrid NIR photodetector with a TTS (transit time spread) below 100 ps was successfully carried out.

3.5 ITER Plasma Modelling

3.5.1 Integrated Tokamak Modelling Activity

The contribution to the Integrated Tokamak Modelling (ITM) EFDA taskforce concentrated in 2012 in two areas i.e. the Infrastructure and Software Support Project (ISIP) and the ITER Scenarios Modelling (ISM).

The ISIP activity in 2012 was mainly devoted to refinements in the low level and high level UAL interfaces in order to improve performance and to solve bugs reported by users during the usage of the UAL.

The integration of Complex Numbers in the UAL has also been carried out and is now under test. This required both an extension of the low level interface and the change in the XSL translation schemas for all supported high level languages.

In the framework of the ISM group of ITM EFDA Task Force, an activity aiming at the implementation of the JT-60SA H&CD configuration (NBI in particular) in the CRONOS transport code continued. This activity is part of a wider collaboration with CEA-IRFM colleagues on NBI-plasma physics studies and tokamak scenario modeling. In 2012 the foreseen JT-60SA beam configuration was integrated in two of the main reference scenarios, namely the ITER-like inductive and the steady-state ones. In the second case equilibrium reconstruction of high-beta normalized plasmas was found to be a critical issue for a proper modeling of the scenario.

3.5.2 Disruption modeling

The activity on nonlinear modeling of tokamak disruptions and VDEs in collaboration with PPPL in Princeton and MIT in Boston continued in 2012.

In particular the 1 MY F4E grant (GRT-334) signed in September 2011 was completed in October 2012. The study has mainly regarded the validation of the M3D code against experimental data of JET and Asdex. This study showned that high spatial definition simulations require further development in order to be able to satisfactory match the experimental behavior during disruptions. In particular a realistic thermal quench phase is difficult to be reproduced, since, in simulations, the thermal quench happens simultaneously with the current quench, while in experiments it clearly precedes the current quench. The study contains also a first attempt to obtain a realistic simulation of the effect of halo currents produced during disruptions on the ITER wall. The M3D calculated halo structure was, in fact, passed to the code CAFÉ, a quite sophisticated 3D electromagnetic model of the ITER wall and blankets. The resulting resistive distribution of currents on the wall were calculated, at a given time, allowing the evaluation of forces and stresses on the wall. A follow up and continuation of these activities was envisaged for 2013.

3.5.3 Plasma-beam interaction

Starting from the interest in modeling ITER plasma-beam interaction and in full synergy with the technological skills developed in the framework of the ITER beam test facility, in the last years a very fruitful activity developed at Consorzio RFX investigating the role of NBI in fusion plasmas of present and future devices. Modeling results on different devices (i.e. not only ITER) are collected here to underline the coordinated approach followed on this subject in Consorzio RFX. This activity includes important collaborations with CEA-IRFM Cadarache and with IPP Garching groups, and in 2012 it has been awarded with several EFDA task agreements contracts. Numerical tools used have been the 2D Fokker-Plank code RISK and the SPOT Montecarlo code, with the additional possibility of using their outputs as input in the CRONOS suite of codes for full integrated scenario modeling.

In the framework of the EFDA ITM ITER scenario modeling group, Consorzio RFX participated to the implementation of the JT-60SA H&CD configuration in EU transport codes with a specific activity on the NBI system. This led to the first EU simulations of NBI-plasma interaction in JT60-SA, where this system is particularly relevant for both heating and current drive; this study in the case of the 2 lines at 0.5 MeV energy is very relevant also for its implications on ITER.

A new activity on plasma-beam interaction started in 2012 in the framework of the EFDA-PPPT department. As part of the DEMO European studies, it has been coordinated also with the activities of the Energetics Program (see Chapter 7). The activity aims at validating the physics scenarios implemented (or to be implemented) in the European System Codes, with particular interest on the role that NBI systems could play. In 2012 the case of a pulsed DEMO was taken as a reference. This case assumes 100 MW of NBI as main H&CD system. Consorzio RFX took the responsibility of implementing different NBI configuration in the modeling tools used to study the sensitivity of the DEMO results to some of the main beam parameters such as energy and geometry of the beam. RISK code was used instead of SPOT for the injected ions population evolution in the study. The performed 2D Fokker-Plank calculation is much faster than the one performed by a full Monte Carlo code as SPOT. Despite being less accurate in modeling NBI transient regimes, SPOT and RISK results were compared in some test cases and we demonstrated that for large devices with high magnetic field, such as DEMO, the two compare well. A first NB Injectors scheme and geometry has been created for DEMO keeping it similar to the ITER case for size, energy and divergence. The final simulated NBI parameters are Einj=1 MeV, Pinj=100MW Rtang=7.687m. The effect on target plasma of different injection angles has been studied, eight different injection angles have been simulated as single source runs with NEMO and RISK. The eight injection angles were obtained by two different injector position in the (R,Z) plane, for each injector position four source tilting angles were simulated. The result of the final test geometry can be seen in fig. 3.53.

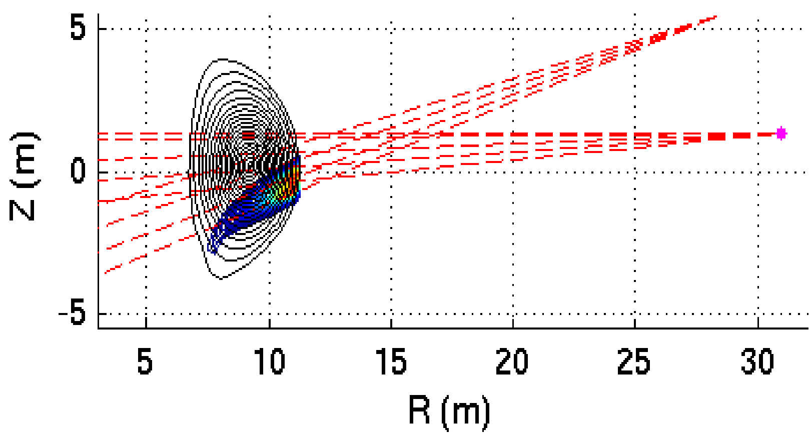

Fig 3.53: Fast ions birth profiles, poloidal view. The injection lines are numbered 1-8 from top to bottom starting from the most horizontal injector

The sensitivity of a given DEMO operational scenario on Neutral Beam parameters was also investigated self consistently by the METIS 0.5-D fast simulator code. The full scenario can be studied by this code so that the different choices on NBI parameters are directly reflected on the main plasma profiles and fusion products. On the other hand, the relevance of different plasma assumptions on NBI efficiency have been also studied, highlighting in particular the critical role of pedestal assumption (high, width, …), often not considered in system codes.

4. THEORY AND MODELING

4.1 Background

A large part of the activities described in this chapter is directly linked to the experimental program. From this viewpoint, a milestone in MHD simulations was the design of a successful experiment where helical equilibria were driven with imposed helicities. Other modeling activities were devoted to equilibrium reconstruction, to estimates of transport, and to the improvement of the feedback on MHD dynamics of both tokamak and RFP configurations. In the part of the program devoted to more fundamental issues, one should highlight the new MHD simulations on the HPC-FF facility at Juelich, which showed quasi single helicity (QSH) intermittency previously observed in toroidal low resolution simulations to be an artifact. Gyrokinetic calculations addressed several topics, and in particular they proved microtearing modes to exist even in the collisionless regime. Furthermore the trapped electron mode instability was compared in RFP and tokamak plasmas. An in depth comparison with the MARS-K code revealed different kinetic mechanisms to be at work for the resistive wall modes in the RFP and in the tokamak. A new method provides reliable error bars for the profiles of the transport coefficients calculated in experiments with periodic perturbations; applied to JET data, it exhibited the difficulties of classical transport codes when a source is present in the domain where transport is computed.

4.2 Extended magnetohydrodynamics modeling

4.2.1 Study of toroidal effects for the RFP

The nonlinear 3D extended MHD PIXIE3D code was installed on the HPC-FF facility at Juelich. The proposal for a dedicated project was accepted and dedicated CPU time has been allocated since June 2012. We immediately exploited this opportunity to study toroidal geometry effects, which can be handled by that code. As a result, we showed that the QSH intermittency previously observed in toroidal low resolution simulations (performed on the local facility) was an artifact. This further stressed the importance of using a proper numerical resolution, as already discussed in the nonlinear verification benchmark study of ref. [1]. The CPU time for this kind of simulation amounts to 80 hrs (using 512 processors, which corresponds to about half the allotted time per month at HPC-FF facility), which raises for the future the issue of code optimization (in particular with a preconditioner algorithm). Concerning the magnetic topology, perfectly conserved magnetic surfaces were shown to exist in such conditions. The major toroidal effect was the formation of a chain of m=0 islands at the reversal surface (they would be absent in cylindrical conditions due to the vanishing amplitude of the m=0 component). These studies were reported in ref. [2]

4.2.2 Study of the chaos healing properties of quasi helical RFP states.

The study has considered in particular the case of non-resonant dominant modes, relevant to the recent experimentation in RFX-mod in which a QSH generated by non-resonant modes was obtained through the use of external finite (non zero) references on the radial field at the edge, as it happens in MHD simulations with SpeCyl. In these simulations it has been shown that the level of chaos depends in a non-trivial way on the amplitude and phase of both the dominant and the secondary modes (first results presented in ref. [3]). Further analysis will be necessary in the future, in particular by using a method developed for computing the Fourier components of magnetic field in flux coordinates corresponding to the dominant helical structure. This is an algorithm complementary to the approach undertaken for experimental analysis [see section 2].

The benchmark between NEMATO and ORBIT was also addressed in the framework of this study. The agreement between the two codes was found to be good for fully 3D MH cases, both qualitatively (comparison of Poincaré surfaces of section), and quantitatively (estimate of correlation lengths). A paper is in preparation [4].

4.2.3 Closer comparison of the nonlinear MHD dynamics in RFP and tokamak experiments

In 2011, an experimental activity was proposed inspired by the markedly different features of chaos development in numerical cases characterized by resonant or non-resonant QSH states, in favor of the latter. The idea was to exploit the natural tendency of the first internally non-resonant modes to be linearly excited by the presence of a resistive wall (as resistive wall modes) or a vacuum layer (as resistive kink mode) [5]. Indeed linear stability calculation (MARS code) performed on the initial Ohmic equilibrium shows that the first internally non-resonant mode is strongly unstable, as is observed in nonlinear MHD simulations. Then, recent equilibrium theory highlighted that a finite radial magnetic field at the edge favors a helical equilibrium [6]. With the available capabilities of the CMC control system at RFX in mind, an experiment was proposed aiming at building up a non-resonant helical equilibrium by tuning the boundary magnetic field ("reference field"), so as to keep at suitable amplitude the internal resistive (RWM) mode (set to vanishing amplitude in standard operation). The experiment was successfully performed, in a first stage at the end of 2011, and in a second one during 2012 (Fig. 4.2) [see also Section 2.1]. In this frame, several new simulations of helical RFP's having a finite reference field with different toroidal periodicities were performed. This finite reference leads to *numerical states closer to the experimental ones* than with a vanishing reference, in particular as to the helical magnetic field and perturbations amplitudes. They are therefore expected to be more relevant for topological comparisons with experiments [7]. Presently, there is not yet a clear numerical recipe to convey the system into strongly robust chaos-resilient persistent states. However, these studies might help understanding recent experiments surveying the thermal properties of helical states as a function of the dominant mode (non-resonant and resonant ones). They showed the evanescence of thermal structures with the help of new diagnostics.

A study of the *nonlinear effect of MHD modes on the Tokamak sawtooth* dynamics was performed. The possibility of imposing a helical boundary condition for the radial magnetic field was implemented in PIXIE3D, both in cylindrical and in toroidal geometry. Tokamak simulations with toroidal geometry and helical boundary conditions are ongoing with PIXIE3D to give an interpretation of the experimentally observed effect of the 2/1 RWM on the amplitude and the frequency of the sawtooth cycle in RFX-mod tokamak

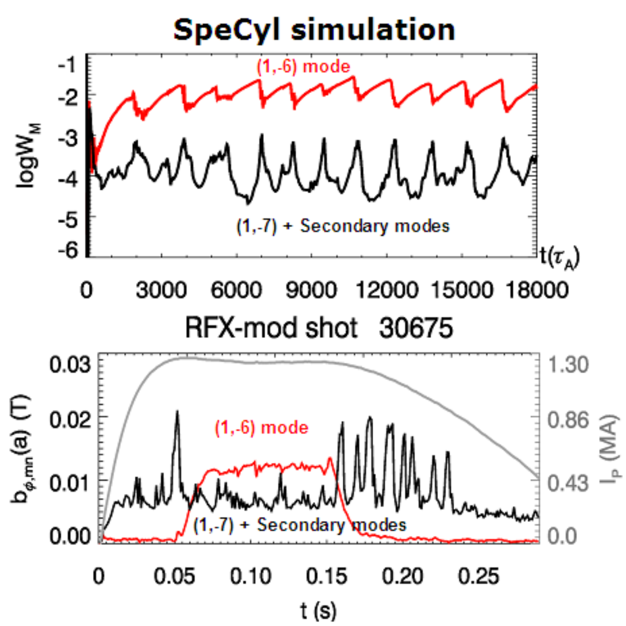

Fig.4.2: 3D nonlinear MHD and Experiment. SpeCyl simulation: Helical regime driven by edge non-resonant MagneticPerturbation (1,-6). RFX-mod discharge 30675: similar action is successfully applied by magnetic coils control system in order to stimulate helical regime different from the spontaneous one (the (1,-7) in RFX-mod).

discharges with q(a)<2 [see Section 2.1]. This topic was presented in [8].

4.3 Transport and microturbulence

In 2012 several topics were tackled by gyrokinetics. A part of the activity was devoted to investigating microtearing modes (MTMs) in collisionless regimes. While till now a finite collisionality has been thought to be a necessary condition for MTM destabilization, from GS2 linear simulations it turns out that collisionless MTMs may exist in particular plasma conditions, e.g., in high magnetic drift geometries or corresponding to flat density profiles. The results of this study were found to agree [32] with those provided by a slab drift kinetic model benchmarked with [31]. Due to the high magnetic drifts in such devices, RFPs and spherical tokamaks are found to be more prone to MTM turbulence than other configurations.

Nonlinear gyrokinetic (GS2) and gyrofluid (TRB) simulations were performed for ion temperature gradient (ITG) turbulence [33]: in two-species RFP plasmas, the ion conductivity turns out to follow a gyro-Bohm scaling. The gyrokinetic simulation displayed an up-shift (Dimits shift) of the critical ion temperature gradient with respect to the linear threshold, consistently with the picture given in tokamak plasmas: the turbulent-generated zonal flows lead to a reduction of ion heat transport also in the RFP configuration.

The GENE/GIST code package [34] was imported, and can now run on RFP VMEC equilibria. Preliminary linear simulations of ITG modes confirm the results previously obtained in axisymmetric geometry, i.e., an intrinsic high ITG stability threshold due to Landau damping. This activity is in collaboration with IPP Greifswald.

The features of the trapped electron mode (TEM) instabilities in RFP plasmas have been studied – in collaboration with Nankai University, China – in various parameter regions by solving the gyrokinetic integral eigenmode equation, and they were compared with those for the circular tokamak [33,35]. TEM instabilities are similar in both configurations, but the excitation of the TEM instability in the RFP requires a much steeper density profile, possibly because of the higher precession frequency and stronger ion Landau damping in the RFP. High electron temperature gradients can enhance the instability, but cannot largely influence the requirement on the density gradient. In addition, with the same approach the impurity mode instabilities were studied by means of broad parameter scans; the condition for mode excitation was extensively discussed in [36].

4.4 Resistive Wall Modes studies

In 2012, the study of the stabilization of Resistive Wall Mode by kinetic effects was completed. The work focused on the comparison of the results for the RFP with those for the circular tokamak and on the resulting physical interpretation. Several new modules have been added in the MARS-K code [41] for this analysis. In depth comparisons between RFP and tokamak plasmas reveal different kinetic mechanisms in MHD instabilities [43]. In the RFP, the RWM can be stabilized by the transit resonance of

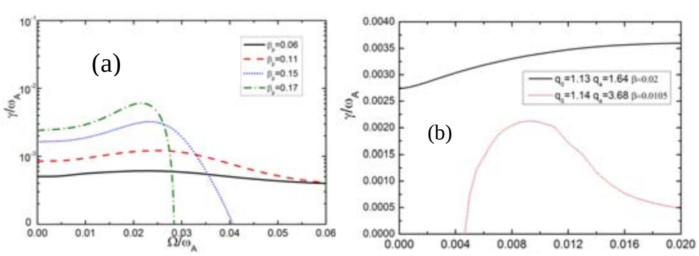

Fig.4.3: kinetic stabilization of RWM (a)in RFP for n=6 mode with various bp values (b)in tokamak for pressure driven RWM (q_a=3.68,dotted curve), the solid curve is for current driven RWM with q_a=1.64).

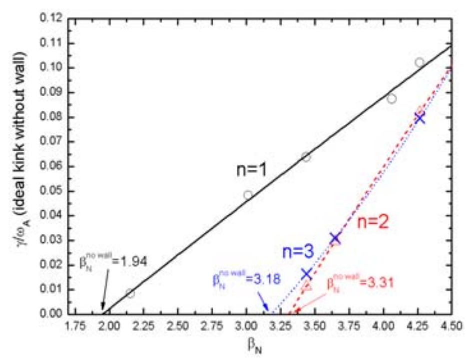

Fig.4.4

passing ions in the high beta region, and the critical flow rotation frequency required for the stabilization is in the ion acoustic frequency range [42]. This is much slower than previously predicted by fluid theory [46]. In the Tokamak, instead, the precession resonance of trapped particles can stabilize the pressure driven mode with very slow or even vanishing plasma rotation. The investigation of the MHD instabilities of non-circular RFP plasmas was carried out too. The effects of elongation and triangularity were taken into account. For RWMs it was found that the shaping of RFP plasmas can increase the growth rate and reduce the ideal wall beta limit. Although the kinetic resonant damping is stronger for shaped plasmas, no significant improvement was observed [44].

In the frame of the Europe-Japan collaboration program for JT60SA. the MARS code was applied to designed magnetic configuration of JT60SA. The no-wall beta limit of RWMs for JT60SA was calculated for n=1,n=2 and n=3 harmonics as shown in Fig.4.4 [45].

4.5 Transport

A code evaluating the susceptance matrix (i.e. the matrix relating fluxes and currents [Strand01]) from VMEC equilibria has been written, in collaboration with the CIEMAT theory group, and is now operational. An example of the radial profiles of the different elements of the matrix is shown in fig. 4.5. The susceptance matrix will be used for the simulation with the ASTRA code of the safety factor evolution induced by plasma resistivity. Numerical problems occurring when coupling the susceptance code with ASTRA are being solved, and a working version of the whole code system should be available in the first months of 2013.

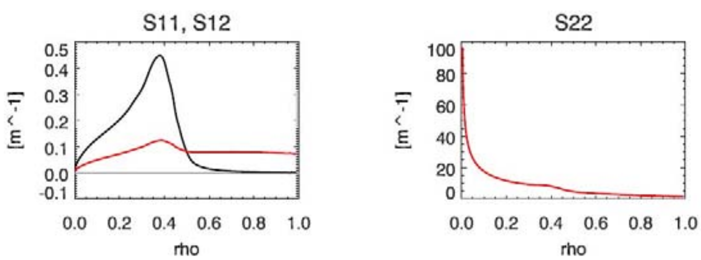

Fig.4.5: Radial profiles of the susceptance matrix elements evaluated from a VMEC equilibrium of a RFX-mod SHAx stat (shot 28218, t = 185 ms).

The Lithium transport code completed in 2011 was applied to simulate Li pellet injection experiments. The Li transport inside the plasma was well reproduced with the transport coefficients deduced in the past [Menmuir10] for Ni, Ne and intrinsic C and O. Li ionization simulations fit well the electron density time evolution, but the reproduction of the absolute enhancement of SXR signals is not yet satisfactory. The Li transport analysis will continue when the modified Li dropper will work on RFX.

To study light impurity transport, C solid pellets injection experiments were attempted, after the available C CR transport code had been modified to allow for a C source inside the plasma. Only preliminary results have been obtained, confirming the transport parameters deduced for intrinsic C. The solid pellet system was unable to inject small C pellets suitable for the impurity transport analysis: new experiments are foreseen after the planned improvements of the solid pellet injector.

The electron temperature profiles provided by DSX3, the new soft-x-ray diagnostic, were investigated from a statistical point of view and used as basic inputs to evaluate the thermal diffusivity in the barrier region with numerical tools like VMEC and ASTRA [Gobbin12]. This analysis allowed creating a large database which will be used to compare neoclassical predictions of transport with experimental results.

In contrast with traditional transport codes, the matricial approach published this year provides reliable error bars for the profiles of the transport coefficients in experiments with periodic perturbations [EscSatt]. This approach was used in 2012 to analyze already published JET data about the transport of angular momentum. The radial profiles of diffusivity, convection, and of other contributions to the flux, like the residual stress, were computed. In some cases they contradict those calculated with a transport code. The difficulty of such codes is due to the presence of the source in the domain where transport is computed, a problem evidenced theoretically in [EscSatt]. The results of this study were presented as an invited talk at the 2012 Stockholm EPS Conference [Sattin].

4.6 Equilibrium reconstruction

The SHEq equilibrium code was upgraded, so as to use a reconstruction of the helical component of the SHAx equilibria obtained for a generic μ profile (previously only profiles resulting from the $\alpha-\Theta_0$ model could be used). Its exploitation for studying the properties of helical equilibria with different current density profiles will take place in the course of 2013. Preliminary results indicate that the freedom in the choice of the μ profile is somehow limited, due to the constraints of having an appropriate level of toroidal field reversal at the edge and of obtaining a zero order safety factor profile with a resonance of the dominant helicity.

An iterative solution of Grad-Shafranov's equation in cylindrical geometry and helical symmetry was developed in order to study the QSH-like phases of the RFX-mod experiment. By using a back-averaging technique, and a linear combination with Newcomb's eigenfunction, convergence was reached. The final solutions fit the experimentally observed values of the radial and toroidal components of the perturbed magnetic field. A preliminary benchmark was carried out by running VMEC with corresponding assumptions, and showed a good agreement, as shown in fig.4.6.

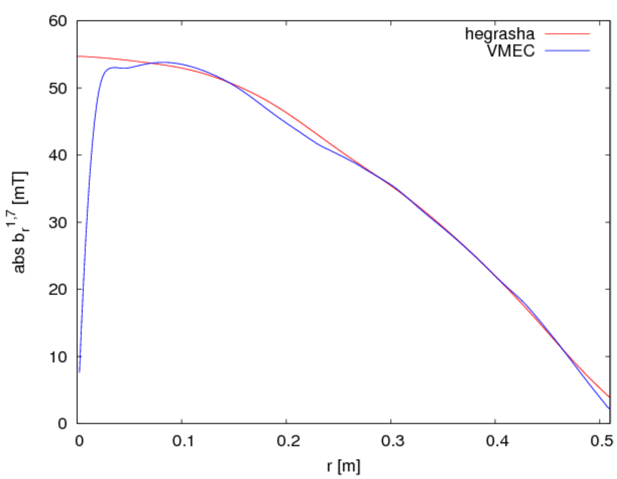

Fig.4.6: Absolute value of the radial component of the perturbed magnetic field as reconstructed by the helical Grad-Shafranov's solver (red) and the Variational Moments Equilibrium Code (blue).

4.7 Improving feedback efficiency

4.7.1 Dynamo modes control

A work in progress using the code RFXlocking [Zanca09] aims at assessing the RFXmod layout modifications, which could improve the feedback on the dynamo tearing modes. The main results of a thin-shell analysis [Piron12] with plasma, a vacuum-vessel, a shell and a mechanical structure set at the present radial positions are:

1) A shell time constant smaller than the present value τ_b=100ms implies an increase of both the edge radial field amplitude and the coils power request, without improving the slinky mode toroidal mobility. 2) However, for 100ms<τ_b<300ms the feedback performances do not vary appreciably, in agreement with a previous analysis based on a thick-shell model [Zanca09]. Therefore, there are no indications for modifying the present τ_b. 3). The slinky-mode mobility could be significantly increased by replacing the present stainless-steel mechanical structure sustaining the coils with an insulating support, as confirmed also by the thick-shell analysis [Zanca12]. Yet, this option is technically difficult and is not considered at the moment. 4) The reduced latency of the new control system is not predicted to imply a strong improvement.

The only way to significantly improve the tearing mode control is to reduce the distance between the plasma and the stabilizing shell, by placing the latter inside the vacuum-vessel. According to a recent (unpublished) analysis, a τ_b=50ms in-vessel copper shell would decrease by a factor 2,5 the plasma surface m=1 distortion, and would double the slinky-mode mobility with only a marginal increase of power request from the coil amplifiers. However, this arrangement is technically difficult with the present vacuum-vessel. Nevertheless, the possibility of transforming the mechanical structure into a new vacuum-vessel with the removal of the old one is under examination.

4.7.2 m=2, n=1 RWM control with radial sensors

Simulations performed with both cylindrical and toroidal models [ZancaMarchiori12] select the Clean Mode Control as the best strategy with radial sensors based feedback to suppress the m=2, n=1 RWM emerging in the RFX-mod q(a)<2 tokamak discharges. In fact both Raw Mode Control (the Fourier variant of the Intelligent Shell) and the Explicit Mode Control, where the aliased sidebands are removed by subtracting the entire vacuum coils field, are predicted to be affected by a growth rate limitation.

References

[1] Bonfiglio D., Chacón L. and Cappello S., Phys. Plasmas **17** (2010) 082501.

[2] S. Cappello et al. “Nonlinear Modeling for Helical Configurations in Toroidal Pinch Systems” TH/P2-16 IAEA FEC 2012 S. Diego

[3] Veranda M. et al “Helical features in nonlinear 3D MHD modeling of Pinch configurations” 39th EPS Conference & 16th Int. Congress on Plasma Physics, 2012 Stockholm, Sweden, P4.004

[4] Ciaccio G., Veranda M. et al paper in preparation

[5] Hender et al, Nuclear Fusion **29** 1279, 1989

[6] D. Bonfiglio, D.F. Escande et al, Nuclear Fusion **51** 063016, 2011

[7] Veranda M. et al Varenna Theory of fusion plasmas conference 2012, submitted to PPCF

[8] APS-DPP 2012 Conference, Providence, USA by D. Bonfiglio et al.

[31] N. T. Gladd et al. Phys. Fluids 23, 1182 (1980).

[32] I. Predebon and F. Sattin, 39th EPS Conference, Stockholm, P4.088 (2012)

[33] S. Cappello et al., Proceedings IAEA 2012

[34] P. Xanthopoulos et al., Phys. Plasmas 16, 082303 (2009).

[35] S.F. Liu, S.C. Guo, J.Q. Dong APS conference 2012.

[36] S.F. Liu et al Eur. Phys. Lett. 97, 55004 (2012).

[41] Y.Q.Liu et al PoP **15** (2008) 112503

[42] Z.R.Wang, S.C.Guo, Y.Q Liu and M.S.Chu, NF **52** (2012) 063001

[43] Z.R.Wang, S.C.Guo, Y.Q. Liu PoP **19** (2012) 072518

[44] S.C.Guo, Z.R.Wang, X.Y.Xu, Y.Q.Liu, APS Bulletin JP8 170 (2012)

[45] T. Bolzonella et al, EPS 2012

[46] S.C. Guo et al Phys. Plasmas 6, 3668 (1999)

[Strand01] P. I. Strand and W. A. Houlberg, Phys. Plasmas **8**, 2782 (2001).

[Menmuir10] S Menmuir et al, Plasma Phys. Control. Fusion **52**, 095001 (2010).

[Gobbin12] M.Gobbin et al, in Proceedings of the 39th EPS Conference on Plasma Physics, Vol. 36F, P4.094 (Stockholm, Sweden, 2-6 july 2012).

[EscSatt] D.F. Escande and F. Sattin, Phys. Rev. Lett. 108, 125007 (2012)

[Sattin] F. Sattin, D.F. Escande, Y. Camenen et al., Plasma Phys. Control. Fusion 54, 124025 (2012)

[Zanca09] P. Zanca, Plasma Phys. Control. Fusion **51**, 015006 (2009).

[Piron12] L. Piron, P. Zanca, internal documents NT FD/81, FD/82 (2012)

[Zanca12] P. Zanca, internal documents NT FC/84 (2012)

[ZancaMarchiori12] P.Zanca, G. Marchiori, L. Marrelli, L. Piron and the RFX-mod team, Plasma Phys. Control. Fusion **54**, 124018 (2012).

5. DIAGNOSTICS

Substantial budget cuts severely limited the completion of the 2012 Diagnostic development plan. For instance the Fast Reciprocating Manipulator project, the acquisition of new sources for the microwave reflectometer and the development of the Lithium neutral beam diagnostic, which are deemed to be very important for studying edge confinement barriers at high current, had to be once again transferred to the next year program.

Other activities proceeded as planned or with some delay. Among these, it is worth highlighting:

- The installation and commissioning of the Nd-YLF laser on the edge TS, which now routinely provides 10 temperature profiles per plasma pulse,
- The commissioning of two bands of the microwave reflectometer, which is now operating according to the full 3 bands design.
- The new multi pellet lithium injector commissioned in collaboration with Princeton Plasma Physics Laboratory, which was successfully tested and is now expected to reach the expected performance with some minor modifications.

Hence this chapter will focus on the activities where significant progress has been achieved in line with the 2012 plan.

5.1 FIR Polarimeter

The aim of the 2012 developments was to consolidate previous improvements and to extend the diagnostic time and spatial resolution. The following actions have been taken:

- A thorough analysis of the residual error on polarimetric measurements has been performed. The main source has been clearly identified as the vibration noise of the pyroeletric detectors. Preliminary vibration isolation tests have given promising results supporting the possibility to substantially reduce the measurement error.
- The effect of the laser tuning on beam polarization quality has also been analyzed, the results have shown that to perform good polarimetric measurements the fine tuning of both the optical pumping CO_2 laser and FIR

laser is required. To this end the design of a new real time feedback system for laser tuning was started.

- Half-wave plates optimized for the longer wavelength (185 μm) already successfully test in the past have been ordered and will be installed on all channels to reliably work at 185 μm.

5.2 Main Thomson Scattering

The diagnostic is routinely operating and the main development activities aimed at improving its reliability and availability. In particular 2012 work regarded essentially the feasibility study for the new Molybdenum beam dump and the setup of a remote control beam imaging system.

A laser damage test on a molybdenum mockup was performed in vacuum chamber, with satisfactory results. The new dump is now being manufactured (mid of November 2012) and its installation is foreseen in the December shutdown (80% done).

The remote control system for the beam camera has been designed and all its components tested; it is expected to be mounted at the beginning of next year (50% done).

5.3 Soft X-Ray (SXR) diagnostics

5.3.1 Horizontal SXR camera

This diagnostic was extensively used throughout 2011, although the noise level was slightly too high. Some tests had been performed to improve the signal-to-noise ratio but with no substantial changes. The observation that the noise had a switching pattern suggested to test the old SXR tomography amplifiers (differential ones) on the horizontal camera, replacing the existing (single ended) Femto amplifiers. One module of the 4 amplifiers was indeed tested on the SXR camera but the noise remained high, unless a substantial filtering of the data was applied (low-pass filter with a 2 kHz cut-off). This is not suitable in our case, since the SXR camera is very important for the analysis of the dynamics of the plasma and of the T_e profiles, requiring a bandwidth of at least 10 kHz. On the other hand, it has been found that, due to the very reproducible pattern of the noise, smoothing the data (using various software tools) is sufficient to eliminate most of the noise, in particular in high current plasmas where the SXR emission is larger and lower gains are used in the amplifiers. So it has been decided to use the SXR camera as it is for future RFX-Mod campaigns.

5.3.2 SXR Photodiodes

In collaboration with the MST group, a new SXR photodiode "shielded" to electromagnetic noise has been designed and tested at MST. The prototype was made of two diodes, one exposed to the plasma and the other blanked, with connections and wire paths as similar as possible. The signal from the blanked diode is used to subtract the noise component from the other diode. Actually the tests have shown that, even if the two diodes were spaced only 2 mm and similar cables and amplifiers were used, the noise signals on the two signals were different and not correlated, and the subtraction of the blanked diode signal from the exposed one did not reduce the noise.

This diode layout was also used to study the magnetic pickup noise in the SXR tomography, in particular for plasmas with rotating modes, with the important result that the pickup contribution is very small and can be neglected when amplifier gains lower than 10^8 are used.

5.4 Neutral Particle Analyzer

An order for new power supplies which have an interface for remote control was placed towards the end of the year. The setting up of the power supplies and the implementation of the remote control will therefore be performed in the first months of 2013. Tests were carried out in order to determine the best layout for magnetic field screening. Also this activity will continue during 2013.

5.5 Arcless power supply for ion saturation current measurements

This activity is quite important to improve the measurements of all of the edge probes, and had been postponed in previous years. Orders for all the needed parts were placed towards the end of the year, when funding became available. As a consequence, the first bunch of power supplies will be built and commissioned in the first months of 2013.

5.6 Revamping of the shot-to-shot probe insertion systems

This activity is quite vital for the functioning of this diagnostic, which is expected to be very useful also for future experimental campaigns on RFX-mod. Also in this case orders for all the needed parts were placed towards the end of the year, when funding became available. The work will be completed in the first months of 2013.

5.7 Edge Thomson Scattering

The Nd-YLF laser has been installed on the edge TS: a new cooling system and a new alignment system for the YLF laser have been built; the optical elements on the laser path have been changed according to the wavelength shift; the spectrometers interferential filter sets have been substituted, the spectrometers have been re-aligned and calibrated. The system is now fully operative returning 10 edge T_e profiles per discharge.

An example of the new measurements is given in fig. 5.1.

With the new setup the stray level is substantially reduced (which was unexpected); this means the grazing incidence metal mirrors which were planned to be installed are not strictly necessary. However, they are still being designed and built and they are expected to allow a small but significant gain in the signal level. Installation is planned for the next shutdown.

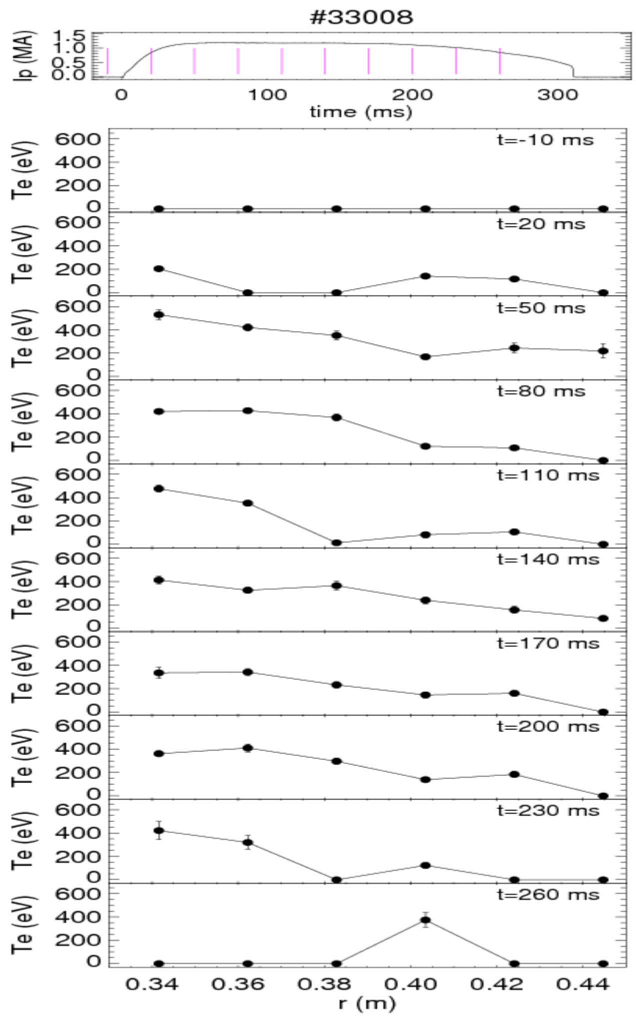

Fig.5.1: Example of the T_e profile measurements obtained with the re-commissioned edge Thomson scattering in a 1 MA pulse. Top graph: Plasma current with bars indicating the times of the laser pulses. Following from top to bottom: the 10 edge T_e profile measurements.

5.8 Diagnostic Neutral Beam Injector

A certain progress has been achieved in the field of the Motional Stark Effect, where for the first time a significant signal was acquired in discharges around 600 kA of plasma current. At this level of plasma current the combination of gas pressure and the intensity of stray fields generated by the field shaping coils in the region of beam duct close to the plasma does not annihilate the beam through re-ionization and subsequent prompt loss. Two examples are given in Fig. 5.2, where the Doppler shifted $H\alpha$ emitted by the beam is shown with and without a linear polarizer interposed between objective lens and plasma. The rotation of the polarizer was chosen in order to minimize the sigma component (central emission) and maximize the sensitivity of the magnetic field measurement, which in the case was evaluated to be 0.45 T. The field is in the right order of that expected in that type of discharge. An improved beam divergence would allow for a much better capability of resolving the π components on the sides of the spectrum. During the summer shutdown arrangements were taken in order to aim at the plasma center form a port on the equatorial plane. In this geometry fluctuations between π and σ component will be sought in order to describe the oscillations of the magnetic field in the core.

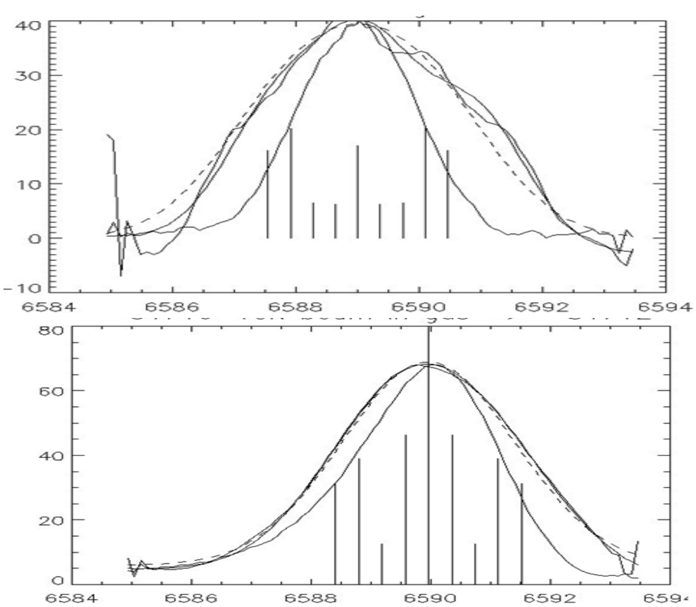

Fig.5.2: Doppler shifted H_α emitted at r/a=0.3 by the beam injected into a 600 kA plasma compared with the same emission of the beam, injected into RFX filled with gas, in absence of fields, together with a reconstruction of the Stark pattern and its overall fit (dashed line). TOP: with a polarizer. BOTTOM: without polarizer.

5.9 Microwave Reflectometer

The two new U (43-47 GHz) and V (54-58 GHz) bands have been set-up and commissioned. The reflectometer is therefore now working with 3 operational bands. The new configuration will allow a simultaneous monitoring of three plasma layers with electron density $n_e(Ka) \approx 1.2 \times 10^{19} m^{-3}$, $n_e(U) \approx 2.5 \times 10^{19} m^{-3}$, $n_e(V) \approx 3.8 \times 10^{19} m^{-3}$ with high time resolution ($\Delta t = 1 \mu s$). Tuning of the system and analysis of the first signals is presently under way.

5.10 CO_2 multi-chord interferometer

To improve the diagnostic reliability, which is vital for RFX-mod operation, in 2012 one of the two CO_2 lasers was replaced. The replacement will improve the diagnostic reliability because the new laser will have a higher stability. The replacement is also required because the old laser has been discontinued from repair in case of failure by the manufacturer. To improve the laser thermal stability, temperature sensors were installed on all CO_2 and CO laser and are now used for temperature control by feedback cooling. To improve the interferometer local and remote control and maintenance, the design and procurement of a new all digital interferometer control system was started.

5.11 Pellet injectors

5.11.1 Room temperature pellet injector

The room temperature injector was used extensively in 2011 for Lithium wall conditioning. Although at the end of the experimental campaign its reliability was satisfactory, some improvements were necessary in terms of injector diagnostics to provide a better remote control. The optical system for pellet speed measurement has been improved. The new set-up will allow measuring the speed of the smaller pellets used for impurity studies. The realization of the system to count in-loader sabots and to count sabots discharged after firing also started.

5.11.2 Multi pellet lithium injector

The loan of a multi pellet lithium injector from Princeton Plasma Physics Laboratory (PPPL) agreed in 2011 proceeded as planned. The commissioning was successfully done and the first experiments were performed, which achieved the injection 1 mm diameter pellets with a repetition rate of about 100 Hz.

Such frequency is smaller than the 400 Hz originally planned. The reason is to be ascribed to two phenomena: an insufficient production rate of pellets ready to be injected by the so-called pellet dropper, and a loss of pellets (pellets not entering in the RFX-mod vessel). The latter problem is mainly due to the fact that, in order to install the new system without venting the vacuum vessel, a pre-existing 40 mm gate valve had been used. Unfortunately the experiments showed that about 25% of the pellets did not enter such gate valve.

PPPL is now working to improve pellet production rate by modifying the dropper of the multi pellet injector. On the other hand, to reduce the number of lost pellet, a new vacuum interface between the injector and RFX-mod is being developed, that will use the full aperture of an equatorial port. The new interface was designed and is currently in the procurement phase.

6. BROADER APPROACH

6.1 Introduction and highlights

The activities of Consorzio RFX team to contribute to the JT-60SA project continued intensively in 2012 with particular effort addressed to the qualification process of the full scale prototypes of the Quench Protection Circuits (QPC), as described in the next paragraph. It is here underlined that, after the completion of the type tests on the individual components at manufacturer's premises, two wide test campaigns were carried out at Consorzio RFX facility on the whole TF and PF QPC prototypes. Big effort was performed to comply with the very tight schedule which required the prototypes ready in time for the two fixed time windows of the RFX-mod shutdowns. Several hundreds pulses have been performed in total during the whole test campaigns, at different current levels, many of them at nominal and higher values. The results allowed a comprehensive characterization of the operation and performance of the prototypes that proved the suitability of the design, the high margins assumed and the full compliance with the requirements. On top of this, positive fallouts derived from having performed the most significant tests at Consorzio RFX: the possibility to carry out additional tests to deeper qualify the prototype operation and to further improve the level of collaboration with JA colleagues and the opportunity to offer a very important occasion of training for our researchers and also for one Trainee of the EFDA Goal Oriented Training program, who selected the participation in these tests as his final specific training activity. Finally, it is mentioned that these results allow achieving the second milestone of the Procurement Arrangement between F4E and JA, which is the approval of the QPC factory type tests report, within 2012.

Steps forward was done also in the studies to finalize the design of the power supply system for RWM control, (the second system to be procured by CNR acting through Consorzio RFX), even if the JA sector coil design was modified again in summer. This obliged to revise and update all the analyses, as described in section 6.3, but will produce an optimization of the overall design in the end. Moreover, the impact is acceptable because this procurement is far from the project critical path.

The Consorzio RFX team participation in the general activities in the framework of the JT-60SA International Project Team continued in 2012 too, with a particular event, which was the organization of the 15th Technical Coordination Meeting (TCM-15) in Padova, at Consorzio RFX. These meetings are regularly held three times a year to discuss the development of the overall JT-60SA design and the interface issues in particular. The progress in the JT-60SA project, as a result of the overall team work, was presented at the IAEA Conference [Kamada].

6.2 Quench protection circuits

It is recalled that the QPC function is to protect the superconducting magnets in case of quench by quickly discharging the stored energy; three units are foreseen for the Toroidal Field (TF) circuit and ten for the Poloidal Field (PF) ones. The QPC scheme is based on a Hybrid Circuit Breaker (HCB) composed of two branches in parallel, a mechanical switch (BPS) and a static one, made of Integrated Gate Commutated Thyristors; the backup protection is assured by an explosively actuated breaker, called pyrobreaker (Fig. 6.1). Even if deep analyses and preliminary tests were carried out in the last years, it was decided to develop a full scale prototype within the procurement contract before proceeding with the manufacturing of the 13 units. The contract activities for the Quench Protection Circuits procurement were entrusted to the company Ansaldo Sistemi Industriali (ASI) on December 20th 2010; the detailed design phase was concluded in summer 2011 [Gaio1], the main QPC components were manufactured, and part of the type tests were carried out in the second half of 2011.

This year, the remaining type tests on the individual components and the main test campaigns on the whole QPC prototypes have been completed as scheduled; few remaining tests have been carried out within December 2012, a comprehensive report

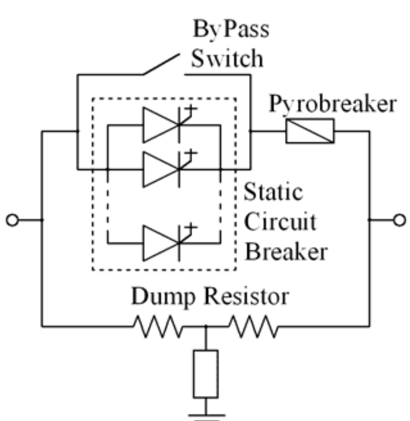

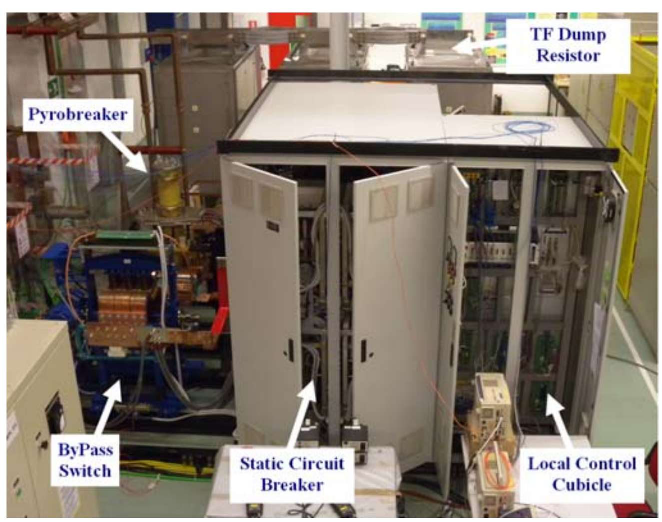

Fig.6.1: Quench Protection Circuit prototype for Toroidal Field Coil protection

have been prepared and revised by F4E and JAEA too, such that the second procurement milestone: the approval of the factory type tests report, which summarizes one year and a half work, has been successfully achieved.

The main type test campaigns results were the object of an oral presentation at the 27th SOFT conference [Gaio2] and subsequent publication on FED.

Some details follow: in January, this year, the remaining factory type tests on the ByPass Switch, consisting on temperature rise test, verification of the repeatability of opening-closing operation on 1000 pulses and the seismic tests, were successfully carried out at Siemens's, Ritter and AREVA premises, Germany.

In the same month, a test campaign on the second pyrobreaker prototype was carried out at EFREMOV Scientific Research Institute (Russia). The results highlighted pyrobreaker proper operation and the design margins with respect to the nominal rate in terms of voltage withstand and current interruption capability.

In February TELEMA, a subcontractor in charge for the design and manufacturing of the Dump Resistors for poloidal and toroidal circuits, completed the construction of the different items (four prototype rated for 70, 100 200, 350 MJ) and successfully tested them, including the seismic tests on vibrating table (Fig. 6.2).

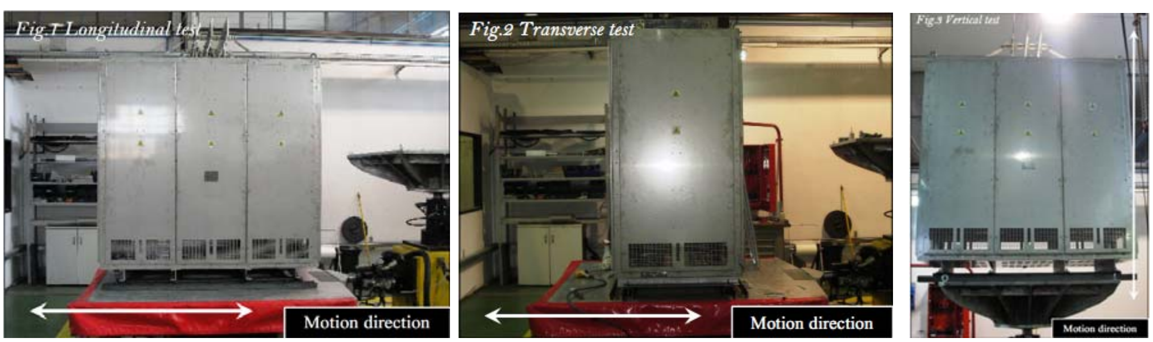

Fig.6.2: TF discharge resistors during seismic tests on vibration table

The tests were performed at Telema's premises, Piacenza, Italy.

The manufacturing of the Static Circuit Breaker, which is the newest device, was completed in January and preliminary tested at ASI premises, in Milano, Italy, in March.

Being quite high the power level necessary to perform a significant part of the type tests on the whole QPC prototypes, it was agreed to perform them at the Consorzio RFX laboratory; therefore, Consorzio RFX acted like Test Facility Host. The test circuit designed and set-up is shown in Fig 6.3; a control interface has been also developed by Consorzio RFX team to operate the QPC.

In April-May 2012, during RFX-mod shutdown period, after the prototype installation and commissioning, the contractual test campaign on the whole Poloidal QPC prototype has been executed proving that the Hybrid Circuit Breaker is able to interrupt and divert into the dump resistor a current up to values higher than the nominal one. The design margin of the SCB in terms of I^2t has also been verified with current 25% higher and with conduction time 25% longer than the nominal ones. An example of commutation test at full current is shown in Fig. 6.4.

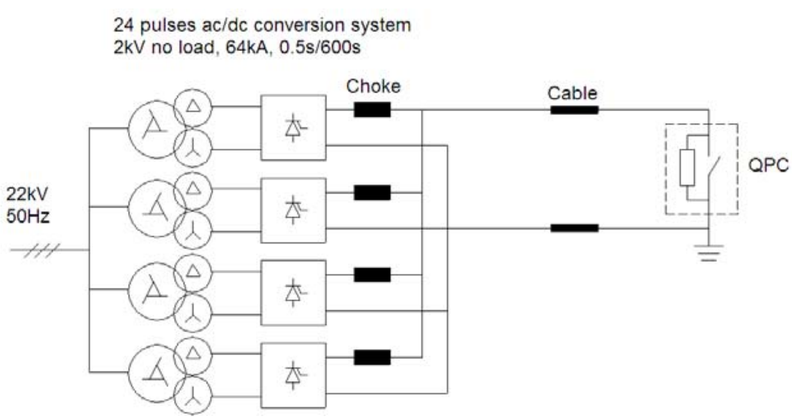

Fig.6.3: Simplified scheme of the circuit set-up at Consorzio RFX to test the QPC prototypes

The type tests on the Toroidal QPC prototype were carried out in August-September, during the next RFX-mod shutdown. Some issues related to the measurement of transducers, which arose during the first test campaign in April, were faced thanks to a strict collaboration with the manufacturer during the following months, so that during the next test campaign in August, they were proved to be solved.

After the successful conclusion of the specified and planned tests and the observation of the repetitive and reliable QPC operation, the confidence was enough to carry out additional tests with a big inductive load, (a spare part of the central solenoid coil of RFX-mod), even if the backup protection (pyrobreaker) was not operating (Fig. 6.5). In this way, the current was sustained by the inductive load for the time needed to reach the peak voltage on the dump resistors in a condition significantly close to the real one, proving that the transient overvoltage on the magnet remains within the specified limits.

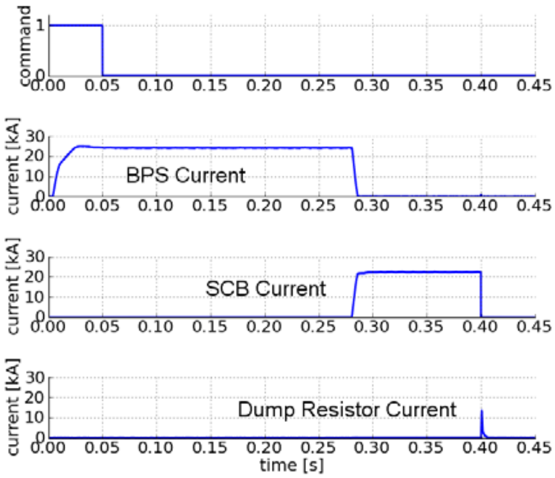

Fig.6.4: QPC current commutation test

Fig.6.5: Arrangement for the additional test with the big inductive load

In summary, the main specific Consorzio RFX activities during the year were: the analyses addressed to the detailed definition of the special type tests, the design and set up of the test facility at Consorzio RFX, including the relevant reconfiguration of the RFX poloidal circuit, the management and participation in the test execution and the first elaboration and analyses of the results; this last item however will be mostly object of the next year program.

Another significant work during the second test campaign has been the design and arrangement of a test bed to preliminary test the Reflective Memory interface between the QPC local control cubicle and the JT-60SA control system. This additional activity, not included in the original test plan, but made possible thanks to the test arrangement set-up at Consorzio RFX and the fruitful collaboration among all the partners (ASI company, F4E, JAEA and Consorzio RFX team), was agreed and carried out to gain confidence in advance on this matter and prevent possible future problems during the final commissioning in Naka; the results produced useful fallout also for the other power supply procurements.

6.3 Power supplies of the in-vessel sector coils for RWM control

The present design of the RWM control system of JT-60SA is based on 18 sector coils

(SC), six located in toroidal direction and three in the poloidal one, to be installed on the inner part of the stabilizing plate (SP), i.e. between SP and first wall. Beside a set of advantages, as in particular a lower shielding effect of the SP on the produced magnetic field, this solution implies a limited space for the installation of the coils. In particular, 2 turns per coil are foreseen by JAEA (Fig. 6.6) in the latest reference design included in the Plant Integration Document v. 3.0.

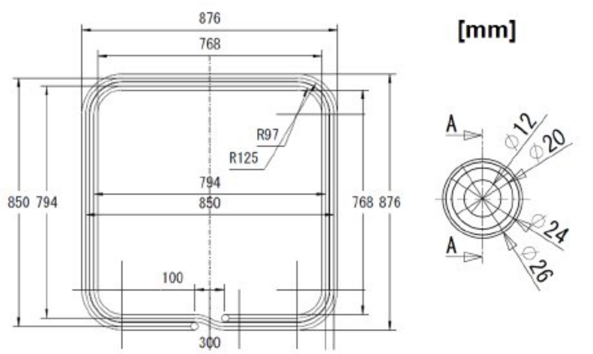

Fig. 6.6: Present reference design of RWM sector coils. On the left: coil geometry. On the right: MIC section.

Proceeding with the activities carried out since 2008, in 2012 Consorzio RFX finalized the electrical characterization of the coil with simplified FE analyses, basing on the reference coil design with 2 turns. In particular, the impedance as a function of frequency has been obtained, together with an estimation of the voltage induced in the coil in case of fast transients of plasma current. These results showed a good agreement with those achieved by JAEA. Possible useful connections among the coils in the toroidal direction have been studied, to verify the possibility to feed the 18 coils with a reduced number of PS, for example 9. However, to control all the RWM foreseen at very high β_N, 18 independent PS are required for the highest flexibility. These results have been presented at the 27th SOFT conference [Ferro1].

In parallel, progresses were achieved on the design of the Power Supplies (PS), which lead to the first release of the Technical Specifications, delivered to JAEA and F4E in May 2012. The reference design of the PS system has been developed, based on an ac/dc conversion system, a full bridge inverter for each coil and two dc-link capacitor banks, each feeding 9 inverters (Fig. 6.7).

The dynamic requirements of the inverters are quite stringent, in order to keep the RWM under control with the very low magnetic fields produced by 2.2 kAT only. In addition, the interface with the MHD Controller of JT-60SA has to be based on Reflective Memories, which is the standard chosen by JAEA for this experiment. These characteristics are not included all together in products already available in the market, thus an ad-hoc solution is necessary. To verify the interest of the industry and the feasibility of the system, an informal market survey has been carried out, which seemed giving a positive answer.

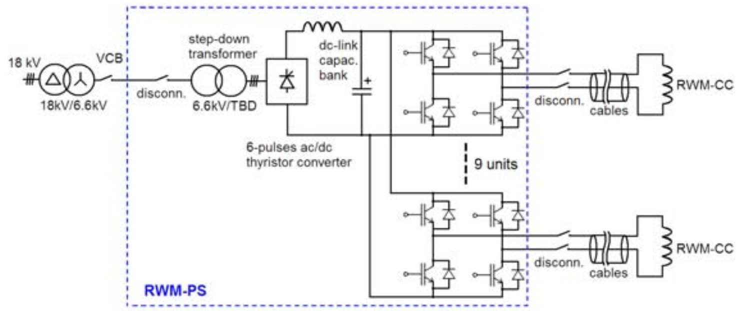

Fig. 6.7: Present reference design of RWM sector coils. On the left: coil geometry. On the right: MIC section.

An important drawback of the 2-turns solution is the low voltage (120 V maximum) and the high current (1.1 kA) required to the coil. As a consequence, the voltage drop in the feeders inside Vacuum Vessel and in the coaxial cables outside (2 in parallel) is even higher than the voltage drop in the coil. Therefore, the electrical efficiency of the system is quite low and the power switches have to be parallelized to share the current.

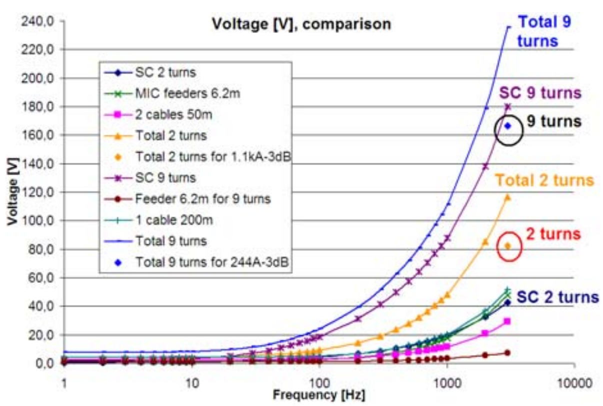

Fig. 6.8: Present reference design of RWM sector coils. On the left: coil geometry. On the right: MIC section.

Since summer 2012, JAEA has started a new revision of the coil design. The turn number is increased from 2 to 8 or 9, the exact number is not yet decided. Also the coil conductor is changed, from Mineral Insulated Cable to resin-coated copper cable with lower cross section. This change has been formalized at the 11th Design Rewiev Meeting on RWM PS, held on 23 July 2012.

Consorzio RFX performed a characterization of the load with the new coil design (with 9 turns, Fig. 6.8). Some differences have been found with respect to the JAEA preliminary results and the discussion is still on-going. However, the higher electrical efficiency of this design is confirmed. This implies a lower rated power for the PS system, about one half also with just one coaxial cable per coil. In addition, the new design allows installing the PS in more convenient places, far from the tokamak hall, for example in the Rectifier Building. Basing on the updated FE analyses and taking some margin, Consorzio RFX proposed a new set of electrical requirements for the PS (200÷240 V, 300 A). The Consorzio RFX activity is now addressed to the development of a first prototype of the inverter which will proceed during all 2013.

References

[Ferro1] A. Ferro, E. Gaio, M. Takechi, M. Matsukawa, L. Novello. “Studies on the requirements of the Power Supply system for the Resistive-Wall-Mode control in JT-60SA” under review for publication on Fusion Engineering and Design.
[Kamada] Progress of the JT-60SA project, 24th Fusion Energy Conference, San Diego, (CA), Oct. 2012
[Gaio 1] Gaio E., Maistrello A, Coffetti A, Gargano T, Perna M, Novello L, Coletti A, Matsukawa M, Yamauchi K. “Final Design of the Quench Protection Circuits for the JT-60SA Superconducting Magnets” IEEE Transactions on Plasma Science, vol. 40, p. 557-563, ISSN: 0093-3813
[Gaio 2] Gaio E., Maistrello A, Perna M, Coffetti A, Soso F., Novello L, Matsukawa M, Yamauchi K” “Full Scale Prototype of the JT-60SA Quench Protection Circuits”, oral presentation at the 27th Symposium on Fusion Technology, Liegi, Sep 2012 and paper accepted for publication on Fusion Engineering and Design.

7. OTHER ACTIVITIES

7.1 Energetic

Further developments of the FRESCO (Fusion REactor Simplified COsts) code, have been made to allow a more accurate modelling of mechanical loads on superconducting magnets, in order to achieve a better evaluation of extra costs due to inductive operation, to Improve the plasma physics routines, to calculate plasma parameters, to improve the computation of the poloidal magnetic flux and the relevant power supply necessary to achieve a full inductive mode in DEMO. First results aimed to the comparison of capital cost and cost of electricity of a D-T Tokamak fusion power plant operating in pulsed and steady state were obtained and published. These activities have been carried out under the EFDA TASK WP11-DAS, Design Assessment Studies

7.2 Biomedical applications

In the course of 2012 Consorzio RFX and Padova University reached an agreement with an Italian company producing medical instruments, which acquired the license for the patent on the atmospheric pressure plasma source used for treatment of living tissues. The agreement foresees that the company will develop an industrial level prototype of the source and, after obtaining appropriate licensing, will start clinical trials, with the aim of obtaining a commercial product.

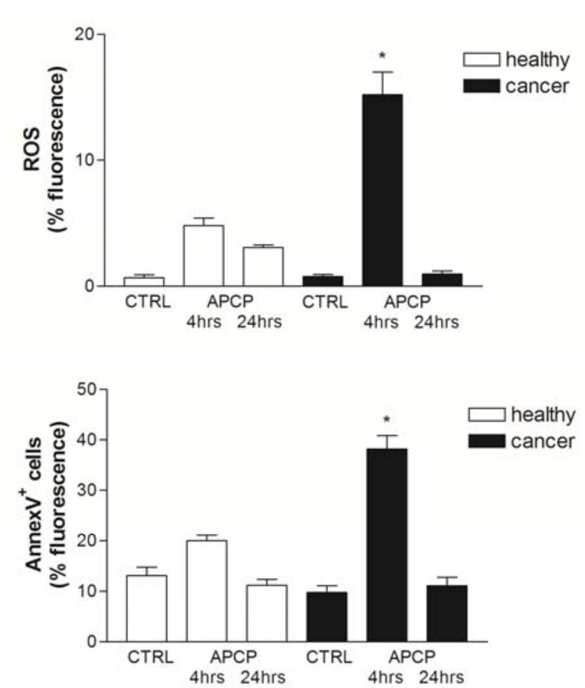

Fig.7.1: Top: ROS levels in healthy and cancer cells, for control, 4 and 24 hourse after treatment. Bottom: Expression of Annexin V for the same cases.

Meanwhile, experiments on cell cultures have been continued. Primary cells were isolated and cultured from both healthy and cancer human lung specimens and exposed to atmospheric pressure cold plasma for 2 minutes. To evaluate the intracellular pool of Reactive Oxygen Species (ROS), cells were loaded with 2,7-dichlorofluorescein diacetate, a probe specific for reactive oxygen radicals. As reported in fig.7.1 (top), plasma treatment significantly increased the ROS levels in cancer cells as compare to healthy cells ($p<0.01$) obtained from the same patient. The generation of ROS is transient since it disappeared 24 hours following the treatment. Indeed, the upswing in the ROS pool observed in cancer cells directly correlates with increased expression of Annexin V (fig.7.1, bottom), an inner membrane protein usually exposed to the outer leaflet of plasma membrane during the first stages of cell death. Using fluorescent activated flow cytometry, it was demonstrated that cancer cells are more susceptible to ROS-driven cell death compared to healthy cellular cultures ($p<0.01$).

7.3 Magneto-plasma-dynamic thrusters

The planned experimental campaigns on the newly built thruster have been postponed, due to the absence of a source of funding after the completion of the FP7 project HiPER. Some data analysis activity was performed with the aim of preparing the campaigns to be carried out when new funding will become available.

8. EDUCATION TRAINING AND INFORMATION TO THE PUBLIC (A. Buffa)

8.1 International Doctorate in Fusion Science and Engineering

In 2012, both the “Joint Research Doctorate in Fusion Science and Engineering” (by Padua and Lisbon universities), and the “European Interuniversity Doctoral Network in Fusion Science and Engineering”, among the same two universities and the Ludwig Maximilian University of Munich (Garching), continued under the responsibility of Padova University and of Consorzio RFX.

During 2012, over a total of 26 students participated to the doctorate, 13 performed here activity in Padova working at Consorzio RFX. Moreover 6 students completed their activity passing the doctoral final examination and obtaining the Joint International Doctorate Diploma. Of these, 1 student is working at ENEA (Frascati), a student is at Princeton with a postDoc grant and 4 students are still working at Consorzio RFX, with PostDoc grants.

For the Doctorate, during 2012, 3 specific Advanced Courses were organized, one in each university.

In particular, Padova organized the Engineering Advanced Course (12 – 23 November), of 52 hrs of frontal teaching and 8 hrs of student’s seminars.

The topics and the teachers of Course were:

1. Materials and plasma facing components for fusion reactors

The role of materials in fusion devices and structural materials (S. Dudarev, CCFE Culham), Plasma Facing components in ITER (M. Merola, ITER Cadarache), Supercoducting magnets for fusion applications (P.L. Bruzzone, CRPP Lausanne) Liquid metal for first wall (G.Mazzitelli, ENEA Frascati), Diagnostcs for material science (A.Carnera, Dip. of Physics Padova University)

2. Fusion Power reactors

Energy scenarios for the next century and the role of fusion (G. Zollino, RFX Padova), Power plant studies (D. Maisonnier, EU Commission Bruxelles), DEMO (D. Maisonnier, EU Commission Bruxelles).

3. Heating and current drive systems

Introduction to heating and current drive in fusion devices (A.Tuccillo, ENEA Frascati),

- NBI plasma heating and current drive (C. Hopf, IPP Garching), Physics challenges for the ITER NNBI (V. Antoni, RFX Padova), Mechanical challenges for ITER NNBI (P.L.

Zaccaria RFX Padova), Electrical challenges for the ITER NNBI(A:DeLorenzi/V.Toigo, RFX Padova), - - ECRH in fusion devices (G. Granucci, CNR Milano), ICRH and LHCD, electromagnetic issues and system integration (F. Mirizzi, ENEA Frascati), Antenna design for RF fusion systems (D. Milanesio, Politecnico Torino).

4. Fusion experiments, operation, management and communication

The role of engineering for the future of fusion (F. Gnesotto, RFX Padova), Structure, organization and tools for JET operation (A.Murari, JET Culham), Managing the design of a tokamak (P.Barabaschi, IPP Garching), Management and quality control for a large fusion engineering project (NBTF) (P.Sonato, RFX Padova), ITER vacuum vessel manufacturing preparation (P. Bonifazi,Walter Tosto SpA Chieti), The organization of the European fusion programme (D. Maisonnier, EU Commission Bruxelles), How to make an effective presentation (P. Martin, RFX Padova).

Teachers from RFX contributed also to the courses held in Lisbon and in Munich.

8.2 Other education activities

The other educational activities of Consorzio RFX on fusion related disciplines continued with a significant effort also in 2012.

In particular, the tutorial activity for development of bachelor and master thesis by RFX researchers continued as in the past.

Seven regular courses on fusion related disciplines, of Padova University, were given by teachers from Consorzio RFX.

Specifically:

- four for engineering students: ”Fission and Fusion Nuclear Plants”, “Thermonuclear Fusion”, “Industrial Applications of Plasmas” and “Energy Technology and Economics”;
- three for physics students: ”Introduction to Plasma Physics”, “Fluid and Plasmas Physics” and “Physics of Nuclear Fusion and Applications of Plasmas”.

The organization of short (1-2 months) summer stages at Consorzio RFX of secondary school students continued as in the previous years with direct involvement of RFX researchers.

In conclusion, RFX professionals were in charge of 16 PhD students, preparing their doctoral thesis, of 14 students preparing their graduation thesis and of a few secondary school students in summer stage.

8.3 Goal oriented training

In the frame of the EU actions to train young engineers in Fusion research, Consorzio RFX is involved in the EFDA “Goal-oriented training” programmes.

During 2012 six trainees were trained at RFX: 2 on power supply technology and 4 on neutral beam injection physics and technology.

1. GOT on Power Supply Engineering

It is recalled that this training program is divided in two main areas:

- General engineering training and experience to provide an overall view of the features and issues concerning fusion power systems
- Specific training and experience in the selected technical areas

The General Training is mainly performed via integrated courses and shadowing activities jointly organized among the Partners (CCFE, CEA, ENEA, KIT and Consorzio RFX, who is the program coordinator); the Specific Training via the involvement of the Trainees in specific projects mainly at their own Institutions.

The details of the integrated courses performed during the third year (2012) can be found in the GOT-PSE website (https://www.igi.cnr.it/gotpse/), which has been developed by Consorzio RFX for the sharing of the GOT-PSE documentation and really proved to be very useful.

The specific training of the two Consorzio RFX Trainees is very well progressing; their involvement in the activities of the RFX, NBI and BA programs has further increased in the third year, with effective contributions.

2. GOT on Neutral Beam Engineering

The Goal Oriented Training program in Neutral Beam Engineering (GOT- NIPEE) is a collaborative program among the following three participant Associations: KIT, IPP and Consorzio RFX, who is the Program Coordinator.

In 2012 the specific training of the 4 Consorzio RFX Trainees has been regularly carried out by their participation to the RFX experiment activities and NBI design and by their participation to specific courses and visits to other laboratories and facilities.

8.4 Information to the public

In 2012, the activity of public information and outreach was focused mainly on the PRIMA Project. In February 2012, the event for the lauching of the PRIMA Project saw the gathering of fusion expertise. The ITER Director General, prof. Motojima, the

Director of F4E, Dott. Briscoe, the Director of the Energy Directorate at Research Directorate General of the European Commission, Dott. Liberali, joined the head table together with the President of Consorzio RFX, Prof. Gnesotto and the Vice President of CNR, Prof. Messa. The event highlighted the start of the construction of the Neutral Beam Test Facility. A strong audience and high-level representatives from the Italian local authorities, national research organizations, politicians, delegates from Domestic Agencies involved in the project listened to the presentations on the ITER project, on F4E contribution and on the PRIMA project. The aim of the initiative was not only to promote and launch the PRIMA project, but also to highlight that Italy, also through Consorzio RFX, is at the forefront of Europe's Fusion Programme. The event was very successful.

During 2012 the PI activity continued: speeches were given whenever requested and interviews or insight articles were published on newspapers. In September, Consorzio RFX participated to the CNR European Night of Research, which was visited by an impressive audience. On the occasion of this large event, Consorzio gave interviews which were broadcasted on national TV and radio channels.

As in the last years, Consorzio RFX participated in the organization of "Sperimentando", a large interactive exhibition on science phenomena and principles, annually organized in Padova and finalized to young students experimenting small devices and exhibits to explain a specific science topic chosen year by year. In 2012 the exhibition focused on "It's a matter of equilibrium".

Furthermore, lectures continued to be given, on the occasion of visits of secondary school students to the plant.

9. LIST OF PUBBLICATIONS

1° semester

ARTICLES PUBLISHED

Buratti, P, Baruzzo, M, , Challis, CD, Chapman, IT, Crisanti, F, Figini, L Gryaznevich, M Hender, TC Howell, DF Han, H, Imbeaux, F, Joffrin, E, Hobirk, J, Kwon, OJ, Litaudon, X, Mailloux, J, JET-EFDA Contributors
Kink instabilities in high-beta JET advanced scenarios
Nucl. Fusion **52**, *2, 023006 doi: 10.1088/0029-5515/52/2/023006 (2012)*

Marchiori, G, Baruzzo, M, Bolzonella T, Liu, YQ, Soppelsa, A, Villone, F
Dynamic simulator of RWM control for fusion devices: modelling and experimental validation on RFX-mod
Nucl. Fusion **52**, *2, 023020 doi: 10.1088/0029-5515/52/2/023020 (2012)*

Munaretto S, Dal BelloS, Innocente P, Agostini M, Auriemma F. Barison S, Canton A, Carraro L, De Masi G, Fiameni S, Scarin P, Terranova D
RFX-mod wall conditioning by lithium pellet injection
Nucl. Fusion **52**, *2, 023012 doi: 10.1088/0029-5515/52/2/023012 (2012)*

Zweben SJ, Terry JL, Agostini M, Hager R, Hughes JW, Myra JR, Pace DC, Alcator C-Mod Group
Search for zonal flows in the edge turbulence of Alcator C-Mod
Plasma Phys. Control. Fusion ***54****, 2, 025008 doi: 10.1088/0741-3335/54/2/025008 (2012)*

Ruzzon A, Elskens Y, Doveil F
A symplectic, symmetric algorithm for spatial evolution of particles in a time-dependent field
Commun Nonlinear Sci Numer Simulat ***17*** *(2012) 769–779*

Desideri D, Maschio A, Bolzan M, Natali M, Spolaore M
Characterization of nanostructured copper films for electromagnetic shield
Compel-The Intern. Journal For Computation And Mathematics In Electrical And Electronic Engineering ***31****, 4, 1122-1132 doi: 10.1108/03321641211227366 (2012)*

Desideri D, Maschio A, Micu DD, Miron OR, Spolaore M
Equivalent Model of a Magnetron Sputtering Device with Ferromagnetic Yoke
Przeglad Elektrotechniczny ***88,*** *7B, 134-137 (2012)*

D.F. Escande, F. Sattin
Calculation of transport coefficient profiles in modulation experiments as an inverse problem
Phys. Rev. Lett. ***108****, 125007 (2012)*

Frassinetti L, Beurskens MNA, Scannell R, Osborne TH, Flanagan J, Kempenaars M, Maslov M, Pasqualotto R, Walsh M, JET-EFDA Contributors
Spatial resolution of the JET Thomson scattering system
Rev.Sci. Instrum. ***83****, 1, 013506 doi: 10.1063/1.3673467 (2012)*

G. Chitarin, P. Agostinetti, N. Marconato, D. Marcuzzi, E. Sartori, G. Serianni, P. Sonato,
Concepts for the magnetic design of the MITICA neutral beam test facility ion accelerator
Rev. Sci. Instrum. ***83****, 2, 02B107 (2012).*

De Muri M, Dalla Palma M, Fasolo D, Pasqualotto R, Pomaro N, Rizzolo A, Serianni G, Tollin M
Design and specifications of the diagnostics for the instrumented calorimeter of Source for the production of Ions of Deuterium extracted from Radio frequency plasma
Rev.Sci. Instrum. ***83****, 2, Part 2, 02B724 doi: 10.1063/1.3678212(2012)*

Pasqualotto R, Serianni G, Sonato P, Agostini M, Brombin M, Croci G, Dalla Palma M, De Muri M, Gazza E, Gorini G, Pomaro N, Rizzolo A, Spolaore M, Zaniol B
Diagnostics of the ITER neutral beam test facility
Rev.Sci. Instrum. ***83****, 2, Part 2, 02B103 doi: 10.1063/1.3662017 (2012)*

Rebai M, Cavenago M, Croci G, Dalla Palma M, Gervasini G, Ghezzi F, Grosso G, Murtas F, Pasqualotto R, Cippo EP, Tardocchi M, Tollin M, Gorini G
A neutron diagnostic for high current deuterium beams
Rev.Sci. Instrum. ***83****, 2, Part 2, 02B721 doi: 10.1063/1.3673013 (2012)*

Serianni G, Dalla Palma M, De Muri M, Fasolo D, Pasqualotto R, Pomaro N, Rizzolo A, Tollin M
Thermal and electrostatic simulations of the diagnostic calorimeter for the Source for Production of Ion of Deuterium Extracted from RF plasma beam
*Rev .Sci. Instrum. **83**, 2, Part 2, 02B725 doi: 10.1063/1.3678330 (2012)*

P. Zaccaria, P. Agostinetti, D. Marcuzzi, M. Pavei, N. Pilan, A. Rizzolo, P. Sonato, F. Spada, L. Trevisan
Progress in the MITICA beam source design
*Rev. Sci. Instrum. **83**, 2, 02B108 (2012).*

P. Agostinetti, G. Chitarin, D. Marcuzzi, M. Pavei, A. Rizzolo, G. Serianni, P. Sonato, L. Trevisan, P. Veltri
Detail design of the Electron Dump for the SPIDER negative Ion Beam Source
*IEEE Trans. Pl. Sci. **40** (2012) 629-634*

N. Pilan, P. Agostinetti, L. Grando, S. Kiyama, A. Rizzolo, H. Sakakita, M. Tollin, M. Valisa
The Monte Carlo Simulation of a 1MW Neutral Beam Injector on RFX-mod
*IEEE Trans. Pl. Sci. **40** (2012) 1042-1051*

A. Rizzolo, P. Agostinetti, M. Breda, M. Maniero, D. Marcuzzi, M. Moressa, M. Valente
Thermo fluid dynamics tests on the single channel prototypes for the SPIDER grids
*Fusion Sci. and Tech. **62** (2012) 164-170.*

M. Cavenago, T. Kulevoy, S. Petrenko, G. Serianni, V. Antoni, M. Bigi, F. Fellin, M. Recchia, and P. Veltri
Development of a versatile multiaperture negative ion source
*Rev. Sci. Instrum. **83**, 02A707 (2012).*

P. Veltri, P. Agostinetti, M. Cavenago, G. Serianni
Study of space charge compensation Phenomena in Charged Particle Beams
*Rev. Sci. Instrum. **83**, 02A709 (2012).*

R. Lorenzini, A. Alfier, F. Auriemma, A. Fassina, P. Franz, P. Innocente, D. López-Bruna, E. Martines, B. Momo, G. Pereverzev, P. Piovesan, G. Spizzo, M. Spolaore, D. Terranova
On the energy transport in internal transport barriers of RFP plasmas
Nucl. Fusion **52**, *062004 (2012).*

P. Brun, P. Brun, M. Vono, P. Venier, E. Tarricone, V. Deligianni, E. Martines, M. Zuin, S. Spagnolo, R. Cavazzana, R. Cardin, I. Castagliuolo, A. La Gloria Valerio, A. Leonardi
Disinfection of ocular cells and tissues by atmospheric-pressure cold plasma
PLoS ONE **7**, *e33245 (2012).*

Marco Boldrin, Antonio De Lorenzi, Mauro Recchia, Vanni Toigo, Tullio Bonicelli , Muriel Simon
The Transmission Line for the SPIDER experiment
Fusion Eng. Des. ***86*** *(2011) 754–758*

Giudicotti L, Pasqualotto R
Characterization of fast microchannel plate photomultipliers for the ITER core LIDAR Thomson scattering system
J of Instrum. ***7****, C02037 doi: 10.1088/1748-0221/7/02/C02037 (2012)*

Onofri M, Vecchio A, De Masi G, Veltri P
Propagation of gravity waves in a convective layer
Astrophysical Journal, ***746****, 1, 58 doi: 10.1088/0004-637X/746/1/58 (2012)*

Liu SF, Zhang CL, Kong W, Guo SC, Dong JQ, Liu LM, Liu Q , Liu ZY
Gyrokinetic study of impurity mode in reversed-field pinch
EPL, ***97****, 5, 55004 doi: 10.1209/0295-5075/97/55004 (2012)*

Paccagnella R
Plasma flow structures as analytical solution of a magneto-hydro-dynamic model with pressure
Phys. of Plasmas ***19****, 3, 032506 doi: 10.1063/1.3694048 (2012)*

M. Brombin, M. Boldrin, M. Dalla Palma, R. Ghiraldelli, F. Molon, N. Pomaro, G. Serianni, and R. Pasqualotto

Optical Transmission of Thermal Measurements From High Voltage Devices in High Vacuum Conditions
IEEE T Plasma Sci. ***40****, 3, (2012)*

Barp M. Gaio E, Toigo V
Studies on the ITER NBI Residual Ion Dump Power Supply System
IEEE T Plasma Sci. ***40,*** *3 SI, 659-664 Part 1 doi: 10.1109/TPS.2011.2180930 (2012)*

Ferro A, Zanotto L, Toigo V
Control Strategy for the Acceleration Voltage of the ITER Neutral Beam Injector
IEEE T Plasma Sci. ***40,*** *3 SI, Part 1 564-569 doi: 10.1109/TPS.2011.2173355 (2012)*

Gaio E, Maistrello A, Coffetti A, Gargano T, Perna M, Novello L, Coletti A, Matsukawa M, Yamauchi K
Final Design of the Quench Protection Circuits for the JT-60SA Superconducting Magnets
IEEE T Plasma Sci. ***40****, 3 SI, Part 1, 557-563 doi: 10.1109/TPS.2011.2171008 (2012)*

Naylor GA, Scannell R, Beurskens M, Walsh MJ, Pastor I, Donne AJH, Snijders B, Biel W, Meszaros B, Giudicotti L, Pasqualotto R, Marot L
The ITER Thomson scattering core LIDAR diagnostic
J Instrum. ***7****, C03043, doi: 10.1088/1748-0221/7/03/C03043 (2012)*

Croci G, Rebai M, Claps G, Cavenago M, Dalla Palma M, Gervasini G, Grosso G, Murtas F, Pasqualotto R, Cippo EP, Tardocchi M, Tollin M, Gorini G
nGEM neutron diagnostic concept for high power deuterium beams
J Instrum. ***7****, C03010, doi: 10.1088/1748-0221/7/03/C03010 (2012)*

Pasqualotto R
Design of laser-aided diagnostics for the negative hydrogen ion source SPIDER
J Instrum. ***7****, C04016 doi: 10.1088/1748-0221/7/04/C04016 (2012)*

Gelfusa M, Murari A, Gaudio P, Boboc A, Mazon D, Avino F, Lupelli ,I Orsitto FP, Tudisco O, JET-EFDA Contributors
New Approximations and Calibration Methods to Provide Routine Real-Time Polarimetry on JET

IEEE T Plasma Sci. ***40****, 4, 1149-1161 doi: 10.1109/TPS.2012.2186641 (2012)*

Zilli, E, Brombin M, Boboc A, Murari A, JET-EFDA Contibutors
On the Causes of Anomaly in the Polarimetric Measurements at JET
IEEE T Plasma Sci. ***40****, 4, 1142-1148 doi: 10.1109/TPS.2012.2186811 (2012)*

Murari A, Mazon D, Martin N , Vagliasindi G, Gelfusa M, JET-EFDA Contributors
Exploratory Data Analysis Techniques to Determine the Dimensionality of Complex Nonlinear Phenomena: The L-to-H Transition at JET as a Case Study
IEEE T Plasma Sc. ***40****, 5, Part 2, 1386-1394 doi: 10.1109/TPS.2012.2187682 (2012)*

Zaniol B, Pasqualotto R, Barbisan M
Design of a beam emission spectroscopy diagnostic for negative ions radio frequency source SPIDER
Rev.Sci. Instrum. **83**, 4, 043117, *doi*: 10.1063/1.4705739 (2012)

Spizzo G, Agostini M, Scarin , Vianello N, White RB, Cappello S, Puiatti ME, Valisa M, RFX-Mod Team
Edge topology and flows in the reversed-field pinch
Nucl. Fusion ***52****, 5, 054015 doi: 10.1088/0029-5515/52/5/054015 (2012)*

Murari A, Lupelli I, Gaudio P, Gelfusa M, Vega J
A statistical methodology to derive the scaling law for the H-mode power threshold using a large multi-machine database
Nucl. Fusion ***52****, 6, 063016 doi: 10.1088/0029-5515/52/6/063016 (2012)*

Nocente M, Tardocchi M, Kiptily VG, Blanchard P, Chugunov I, Conroy S, Edlington T, Fernandes AM, Ericsson G, Johnson MG, Gin D, Grosso G, Hellesen C, Kneupner K, Lerche E, Murari A, Neto A, Pereira RC, Cippo EP, Sharapov S, Shevelev A, Sousa J, Syme DB, Van Eester D, Gorini G, JET-EFDA Contributors
High-resolution gamma ray spectroscopy measurements of the fast ion energy distribution in JET He-4 plasmas
Nucl. Fusion **52**, *6*, 063009 *doi*: 10.1088/0029-5515/52/6/063009 (2012)

Wang ZR, Guo SC, Liu YQ, Chu MS
Kinetic damping of resistive wall mode in reversed field pinch

Nucl. Fusion ***52****, 6, 063001 doi: 10.1088/0029-5515/52/6/063001 (2012)*

Agostini M, Scaggion A, Scarin P, Spizzo G, Vianello N
Interplay between edge magnetic topology, pressure profile and blobs in the edge of RFX-mod
Plasma Phys. Control. Fusion ***54****, 6, 065003 doi: 10.1088/0741-3335/54/6/065003 (2012)*

Gonzalez S, Vega J, Murari A, Pereira A, Dormido-Canto S, Ramirez JM, JET-EFDA Contributors **Automatic location of L/H transition times for physical studies with a large statistical basis** *Plasma Phys. Control. Fusion* ***54****, 6, 065009 doi: 10.1088/0741-3335/54/6/065009 (2012)*

Naulin V, Xu G, Vianello N, Madsen J, Schrittwieser R, Ionita C, Maszl C, Mehlmann F, Yan N, Nielsen AH, Rasmussen JJ
Profiles and Fluctuations in Edge and SOL Turbulence
Contrib. Plasma Phys. ***52****, 5-6, SI, 391-400 doi: 10.1002/ctpp.201210022 (2012)*

2° semester

ARTICLES PUBLISHED

Carati, M. Zuin, A. Maiocchi, M. Marino, E. Martines, L. Galgani,
Transition from order to chaos, and density limit, in magnetized plasmas
Chaos **22***. 033124 (2012).*

P. Veltri, P. Agostinetti, G. Serianni, V. Antoni, M. Cavenago “Effects of Negative Ion Source **Characteristics on Beam Optics: The Case of SPIDER**
IEEE Trans. Pl. Sci. ***40*** *(2012) 2279-2284*

L. Grisham, P. Agostinetti, P. Blatchford, D. Boilson, J. Chareyre, G. Chitarin, H. P. L. de Esch, P. Franzen, U. Fantz, M. Gagliardi, R. S. Hemsworth, M. Kashiwagi, A. Krylov, M. Kuriyama, D. Marcuzzi, M. Roccella, L. Rios, P. Sonato, V. Pilard, M. Tanaka, H. Tobari and P. Zaccaria
Recent Improvements to the ITER Neutral Beam System Design
Fusion Eng. Des. ***87*** *(2012) 1805-1815. novembre*

Wang, ZR, Guo SC, Lu YQ
Drift kinetic effects on the resistive wail mode stability-Comparison between reversed field pinches and tokamaks
Phys. of Plasmas ***19****, 7, 072518 doi: 10.1063/1.4737200 luglio (2012)*

Rizzolo A, Agostinetti P, Breda M, Maniero M, Marcuzzi D, Moressa M, Valente M
Thermo fluid dynamics tests on the single channel prototypes for the SPIDER grids
Fusion Sci. and Tech. ***62****, 1, 164-170, JUL-AUG (2012)*

Dalla Palma, M (Dalla Palma, Mauro)[1]; Zaccaria, P (Zaccaria, Pierluigi)
Procedures for multiaxial creep-fatigue verifications of nuclear components
Fusion Sci. and Tech. ***62****, 1, 122-128, JUL-AUG (2012)*

M. B. McGarry, P. Franz, D. J. Den Hartog, J. A. Goetz, M. A. Thomas, M. Reyfman, and S. T. A. Kumar
High-performance double-filter soft x-ray diagnostic for measurement of electron temperature structure and dynamics
Rev. Sci. Instrum. ***83****, 10E129 (2012) doi.org/10.1063/1.4740274 August*

Y. Sun, Y. Liang, KC.Shaing, KC, YQ Liu, HR.Koslowski, S. Jachmich, B. Alper, A. Alfier, O. Asunta, P. Buratti, G. Corrigan, E. Delabie, C. Giroud, MP. Gryaznevich, D. Harting, T. Hender, E. Nardon, V. Naulin, Parail, V (Parail, V.)[5]; Tala, T (Tala, T.)[12]; Wiegmann, C (Wiegmann, C.)[1]; Wiesen, S (Wiesen, S.)[1]; Zhang, T (Zhang, T.)[1] Group Author(s): JET-EFDA Contributors
Non-resonant magnetic braking on JET and TEXTOR
Nucl. Fusion ***52****, 8, 083007 doi: 10.1088/0029-5515/52/8/083007 AUG (2012)*

Bonheure, G (Bonheure, Georges)[1]; Hult, M (Hult, M.)[3]; de Orduna, RG (de Orduna, R. Gonzalez)[3]; Arnold, D (Arnold, D.)[4]; Dombrowski, H (Dombrowski, H.)[4]; Laubenstein, M (Laubenstein, M.)[5]; Wieslander, E (Wieslander, E.)[3]; Vidmar, T (Vidmar, T.)[6]; Vermaercke, P (Vermaercke, P.)[6]; Von Thun, CP (Von Thun, Christian Perez)[7]; Reich, M (Reich, M.)[7]; Jachmich, S (Jachmich, S.)[1]; Murari, A (Murari, A.)[8]; Popovichev, S (Popovichev, S.)[9]; Mlynar, J (Mlynar, J.)[10]; Salmi, A (Salmi, A.)[11]; Asunta, O (Asunta, O.)[11]; Garcia-Munoz, M (Garcia-Munoz, M.)[7]; Pinches, S (Pinches, S.)[9]; Koslowski, R (Koslowski, R.)[12]; Nielsen, SK (Nielsen, S. Kragh)[13] Group Author(s): JET-EFDA Contributors

Experimental investigation of the confinement of d(He-3,p)alpha and d(d,p)t fusion reaction products in JET
*Nucl. Fusion **52**, 8, 083004 doi: 10.1088/0029-5515/52/8/083004 AUG (2012)*

Bagatin M., Coniglio A., D'Arienzo M., De Lorenzi A., Gerardin S., Paccagnella A., Pasqualotto R., Peruzzo S., Sandri S.
Radiation environment in the ITER neutral beam injector prototype
*IEEE Transactions on Nuclear Science **59**, 4, 1099-1104, http://dx.doi.org/10.1109/TNS.2012.2187461 (2012)*

P. Veltri, P. Agostinetti, G. Serianni, V. Antoni, and M. Cavenago
Effects of Negative Ion Source Characteristics on Beam Optics: the case of SPIDER
*IEEE T Plasma Sci, **40**, 9, SEPTEMBER(2012)*

P. Zanca, L. Marrelli, R. Paccagnella, A. Soppelsa, M. Baruzzo, T. Bolzonella, G. Marchiori, P. Martin, P. Piovesan
Feedback control model of the m=2, n=1 resistive wall mode in a circular plasma
*Plasma Phys. Control. Fusion **54**, 9, 094004 doi: 10.1088/0741-3335/54/9/094004 SEP (2012)*

M. Odstrcil, J. Mlynar, TB. Odstrcil, Alper, A. Murari
Modern numerical methods for plasma tomography optimisation
*Nuclear Instruments & Methods In Physics Research Section A-Accelerators Spectrometers Detectors And Associated Equipment **686**, 156-161 doi: 10.1016/j.nima.2012.05.063 SEP (2012)*

Craciunescu, T Murari, A Tiseanu, I Vega, J JET-EFDA Contributors
Phase congruency image classification for marfe detection on JET with a carbon wall
*Fusion Sci. and Tech. **62,** 2, 339-346 OCT (2012)*

Verdoolaege, G Karagounis, G Murari, A Vega, J Van Oost, G JET-EFDA Contributors
Modeling fusion data in probabilistic metric spaces: applications to the identification of confinement regimes and plasma disruptions
*Fusion Sci. and Tech. **62**, 2, 356-365 OCT (2012)*

FS. Zaitsev, S. Matejcik, A. Murari, Suchkov EP, JET-EFDA Contributors
A New Method To Identify The Equilibria Compatible With The Measurements Using The Technique Of The epsilon-NETS
Fusion Sci. and Tech. ***62****, 2,* 366-373 *OCT (2012)*

Murari, A Peluso, E Gaudio, P Gelfusa, M Maviglia, F Hawkes, N JET-EFDA Contributors **A statistical investigation of the effects of edge localized modes on the equilibrium reconstruction in JET**
Plasma Phys. Control. Fusion ***54,*** *10, 105005 doi: 10.1088/0741-3335/54/10/105005 OCT (2012)*

ARTICLES IN PROGRESS

P. Zanca, G. Marchiori, L: Marrelli, L. Piron
Advanced feedback control of MHD instabilities: comparison of compensation techniques for radial sensors
accepted for publication on Plasma Phys. Control. Fusion (2012)

E. Sartori and P. Veltri
AVOCADO a numerical code to calculate gas pressure distribution
accepted for publication on Vacuum, October 2012

L.R. Grisham, P. Agostinetti, G. Barrera, P. Blatchford, D. Boilson, J. Chareyre, G. Chitarin, H.P.L. de Esch, A. De Lorenzi, P. Franzen, U. Fantz, M. Gagliardi, R.S. Hemsworth, M. Kashiwagi, D. King, A. Krylov, M. Kuriyama, N. Marconato, D. Marcuzzi, M. Roccella, L. Rios, A. Panasenkov, N. Pilan, M. Pavei, A. Rizzolo, E. Sartori , G. Serianni, P. Sonato, V. Pilar e, M. Tanaka, H. Tobari, **P. Veltri**, P. Zaccaria
Recent improvements to the ITER neutral beam system design
accepted for publication on Fusion Eng. Des., October 2012.

P. Agostinetti, G. Chitarin, H.P.L de Esch, D. Marcuzzi, N. Marconato E. Sartori, G. Serianni, P. Sonato, P. Veltri and P. Zaccaria
Optimization of the electrostatic and magnetic field configuration in the MITICA accelerator

Submitted to Fusion Engineering and Design

P.Veltri, P. Agostinetti, M. Dalla Palma, E. Sartoria and G.Serianni
Evaluation of power loads on MITICA injector components
27th Symposium on Fusion Technology, Liège, Belgium, 2012,
Submitted to Fusion Eng. and Des.

Marco Boldrin, Antonio De Lorenzi, Hans Decamps, Luca Grando, Muriel Simon, Vanni Toigo
Design status and procurement activities of the High Voltage Deck1 and Bushing for the ITER Neutral 27th Symposium on Fusion Technology, Liège, Belgium, 2012,
Submitted to Fusion Eng. and Des.

Pesce, N. Pomaro, A. Zamengo, M. Bigi and V. Toigo
Modeling and analysis of breakdown EMI protection for MITICA insulation and embedded diagnostics
27th Symposium on Fusion Technology, Liège, Belgium, 2012,
Submitted to Fusion Eng. and Des.

Vanni Toigo, Loris Zanotto, Marco Bigi, Hans Decamps, Alberto Ferro, Elena Gaio, Daniel Gutiérrez, Kazuki Tsuchida and Kazuhiro Watanabe
Progress of the ITER NBI acceleration grid power supply reference design
27th Symposium on Fusion Technology, Liège, Belgium, 2012,
Submitted to Fusion Eng. and Des.

G. Mazzucco, D. Muraro, V. Salomoni, C. Majorana, D. Marcuzzi, W. Rigato, P. Sonato, P. Zaccaria, V. Toigo, T. Inoue, J. Takemoto, H. Tobari, K. Tsuchida, H.Yamanaka, K. Watanabe
Structural analyses and integrated design of the MITICA Injector assembly
27th Symposium on Fusion Technology, Liège, Belgium, 2012,
Submitted to Fusion Eng. and Des.

G. Chitarin, P. Agostinetti, D. Marcuzzi, N. Marconato, G. Serianni, P. Sonato, P. Veltri
Optimization of the electrostatic and magnetic field configuration in the MITICA accelerator
27th Symposium on Fusion Technology, Liège, Belgium, 2012,

Submitted to Fusion Eng. and Des.

S. Peruzzo, P. Bettini, N. Marconato, A. Soppelsa, Albanese, M. Caputano, M. Mattei, G. Rubinacci, F. Villone
Integrated procedure for halo current reconstruction in ITER
Transactions on Plasma Science accepted for publication (2012)

F. Sattin, D.F. Escande, Y. Camenen, A.T. Salmi, T. Tala and JET EFDA Contributors
Estimate of convection-diffusion coefficients from modulated perturbative experiments as an inverse problem
Plasma Phys. Control. Fusion (apparirà nel numero speciale di dicembre 2012)

CONGRESS PROCEEDINGS (1° semester)

A. Murari, A. Buscarino, L. Fortuna, M. Frasca, Iachello, M., G. Mazzitelli 16TH IEEE
Identifying JET Instabilities with Neural Networks
Mediterranean Electrotechnical Conference (MELECON) Book Conf. Proceediings 932-935, 2012

NATIONAL AND INTERNATIONAL CONGRESS PRESENTATIONS (1 semester)

C. Finotti, E. Gaio, I. Benfatto, A.D. Mankani and J. Tao
Analytical model for stability analysis in high power ac/dc converters applied to the ITER case
15th IEEE International Conference on Harmonics and Quality of Power, 17-20 June 2012 IEEE Proc. to be published

CANTON Alessandra, S.Dal Bello, M.Agostini, L.Carraro, R.Cavazzana, S.Fiameni, L.Grando, B.Rais, M.Spolaore, M.Zuin
Studies of Spatial Uniformity of Glow Discharge Cleaning Plasmas on the RFX-mod Device
20th International Conference on Plasma Surface Interaction 2012, Eurogress, Aachen, Germany, 21– 25/05/2012

Edge simulation of FTU Tokamak with B2-Eirene
S. Munaretto[1], M.L. Apicella[2], P. Börner[3], P. Innocente[1], G. Mazzitelli[2], S. Wiesen[3] and FTU Team
20th International Conference on Plasma Surface Interaction 2012, Eurogress, Aachen, Germany, 21. – 25.05.2012

P. Scarin, M. Agostini, L. Carraro, A.Scaggion, G. Spizzo, M. Spolaore, N. Vianello
Boundary Plasma Physics in RFX-mod: Radial Electric Field and Transport Topology
20th International Conference on Plasma Surface Interaction 2012, Eurogress, Aachen, Germany, 21– 25/05/2012

L. Giudicotti, R. Pasqualotto
Dual-laser calibration of Thomson scattering systems in RFX-mod and ITER
19th Topical Conference High-Temperature Plasma Diagnostics, Monterey, CA, May 6-10, 2012
To be published in a special edition of the Review of Scientific Instruments (RSI)

R. Pasqualotto, M.Agostini, M.Brombin, G.Serianni,
Design of a visible tomography diagnostic for negative ion RF source SPIDER
19th Topical Conference High-Temperature Plasma Diagnostics, Monterey, CA, May 6-10, 2012
To be published in a special edition of the Review of Scientific Instruments (RSI)

A. Luchetta, G. Manduchi, C. Taliercio, A. Soppelsa, F. Paolucci, F. Sartori, P. Barbato, R. Capobianco, M. Breda, F. Molon, M. Moressa, S. Polato, P. Simionato, E. Zampiva
Prototyping Control and Data Acquisition for the ITER Neutral Beam Test Facility
18th IEEE/RTSS Real Time Conference, Berkeley CA June 11-15 2012 to be publisdhed on EEE Transactions on Nuclear Science (TNS)

MARTINES Emilio and the RFX-mod team
Spontaneously occurring helical states: a new paradigm for ohmically heated fusion plasmas

invited 5th International Workshop and Summer School on Plasma Physics (Kiten (Bulgaria) 25-30 June 2012

L. Zanotto and A. Maistrello
Impact of facilities for thermonuclear fusion research on the Italian Extra High Voltage grid
ICHQP 2012: 15th IEEE International Conference on Harmonics and Quality of Power

BOOKS

Ivan Cibrario Bertolotti, Gabriele Manduchi
Real-Time embedded systems
CRC Press – Taylor & Francis Group – Boca Raton FL, April 2012

CONGRESS PROCEEDINGS (2° Semester)

N. Vianello and the RFX-mod team, "The role of 3D fields on edge turbulence and SOL", invited at the Workshop on Electric Fields, Turbulence and Self-Organisation
in Magnetized Plasmas EFTSOMP 2012, 9-10 July 2012, Stockholm, Sweden

L. Zanotto, A. Maistrello, L. Novello and V. Toigo
Impact of Consorzio RFX facilities for thermo Nuclear Fusion research on the Italian Extra High Voltage network
Proceedings of ICHQP 2012

Matteo Agostini, L Carraro, R Cavazzana, G De Masi, A Scaggion, P Scarin, Monica Spolaore, Nicola Vianello, and B Zaniol.
Interaction between turbulence and electron profiles in the RFX-mod helical plasma edge.
39th EPS Conference on Plasma Physics, Stocholm, Sweden 2012 p. P1.037.

S Spagnolo, M Zuin, I Predebon, F Sattin, F Auriemma, R Cavazzana, A Fassina, R Paccagnella, E Martines, Monica Spolaore, M Veranda, and Nicola Vianello

Observations of rhoi-scale wavelength instabilities in the microtearing frequency range in RFX-mod plasma.
39th EPS Conference on Plasma Physics, 2012 p. P1.047.

G De Masi, Matteo Agostini, F Auriemma, R Cavazzana, E Martines, B Momo, P Scarin, Monica Spolaore, Gianluca Spizzo, Nicola Vianello, and M Zuin.
Edge flow and radiation in Helium discharges in RFX.
39th EPS Conference on Plasma Physics, 2012 p. P5.003.

F Mehlmann, Roman W Schrittwieser, Volker Naulin, J J Rasmussen, H W Muller, C Ionita, A Nielsen, Nicola Vianello, and V Rohde.
Radial transport of poloidal momentum in ASDEX Upgrade in L-mode and H-mode.
39th EPS Conference on Plasma Physics, Stockholm, Sweden 2012 p. P2.090.

F. Sattin, D.F. Escande, Y. Camenen, A.T. Salmi, T. Tala and JET EFDA Contributors
Estimate of convection-diffusion coefficients from modulated perturbative experiments as an inverse problem
39th EPS Conference on Plasma Physics, Stockholm, Sweden 2012 invited talk I4.416

,S. Hanke, Chr. Day, M. Dremel, F. Fellin, X. Luo, M. Scannapiego, , P. Wikus, P. Zaccaria, "Development of a large NBI cryopump", TOFE 2012, 20th Topical Meeting on the Technology of Fusion Energy, Nashville TN (United States), 27-31 August 2012

G. Chitarin, N. Marconato, P. Agostinetti, G. Serianni, P. Sonato
Flexible magnetic design of the MITICA plasma source and accelerator
3rd International Symposium on Negative Ions, Beams and Sources, Jyväskylä, Finland, 2012.

P. Sonato, V. Antoni, M. Bigi, G. Chitarin, A. Luchetta, D. Marcuzzi, R. Pasqualotto, N. Pomaro, G. Serianni, V. Toigo, P. Zaccaria on behalf of the international team working on the design and implementation of the ITER Neutral Beam Test Facility
Status of PRIMA, The Test Facility For ITER Neutral Beam Injectors
3rd International Symposium on Negative Ions, Beams and Sources, Jyväskylä, Finland, 2012.

P. Agostinetti, G. Chitarin, P. Franzen, G. Serianni, P. Veltri
Benchmark of the SLACCAD code against data from the MANITU radio frequency ion source at IPP
3rd International Symposium on Negative Ions, Beams and Sources, Jyväskylä, Finland, 2012

M. Cavenago, G. Serianni, T. Kulevoy, S. Petrenko, P. Agostinetti, V. Antoni, M. Bigi, D. Conventi, F. Fellin, A. Minarello, M. De Muri, R. Pasqualotto, M. Recchia, M. Rigato, M. Sattin, M. Barbisan, F. Rossetto, M. Valente and P. Veltri
Construction of a Versatile Negative Ion Source and Related Developments
Aip conference proceeding of 3rd International Symposium on Negative Ions, Beams and Sources, 3-7 September 2012, Jyväskylä, Finland.

H.P.L. de Esch, M. Kashiwagi, T. Inoue, G. Serianni, P. Agostinetti, G. Chitarin, N. Marconato, E. Sartori, P. Sonato, P. Veltri and R.S. Hemsworth
Status Physics Design of the HNB Accelerator for ITER
Aip conference proceeding of 3rd International Symposium on Negative Ions, Beams and Sources, 3-7 September 2012, Jyväskylä, Finland.

P. Veltri, M. Cavenago and G. Serianni,
Spatial characterization of the space charge compensation of negative ion beams
Aip conference proceeding of 3rd International Symposium on Negative Ions, Beams and Sources, 3-7 September 2012, Jyväskylä, Finland

F. Sattin, D.F. Escande, Y. Camenen, A.T. Salmi, T. Tala and JET EFDA Contributors
Estimate of convection-diffusion coefficients from modulated perturbative experiments
17th Joint EU-US TTF and 4th EFDA TTG Meeting (Padova 2012), poster P2.8

M. Spolaore
Electromagnetic turbulent structures features in the edge region of toroidal plasma configurations
17th Joint EU-US TTF and 4th EFDA TTG Meeting (Padova 2012), oral O1.1

M. Agostini

Impact of the helical magnetic topology on the edge of RFX-mod
17th Joint EU-US TTF and 4th EFDA TTG Meeting (Padova 2012), oral O1.7

S. Spagnolo
Observation of resistive interchange modes in a reversed field pinch plasma
17th Joint EU-US TTF and 4th EFDA TTG Meeting (Padova 2012), poster P1.14

L. Piron
Effects of 3D magnetic fields on plasma rotation in RFX-mod tokamak plasmas: experimental results and modeling
17th Joint EU-US TTF and 4th EFDA TTG Meeting (Padova 2012), oral O2.8

M. Zuin
Experimental investigation of microtearing modes in reversed field pinch plasmas
17th Joint EU-US TTF and 4th EFDA TTG Meeting (Padova 2012), poster P3.16

Fellin F., Passardi G., Valente M., Zaccaria P.

The MITICA facility: a possible optimization of the cryogenic plant cooling capacity

12ᵗh CRYOGENICS 2012, IIR Conference, 11-14 September 2012 Dresden (D) – Proceedings, Section: Cryogenics in particle physics & fusion, Paper

Valente M., Fellin F., Haas H., Hanke S., Scannapiego M., Zaccaria P.,

Design Proposal For MITICA Cryogenic Plant

12ᵗh CRYOGENICS 2012, IIR Conference, 11-14 September 2012 Dresden (D) – Proceedings, Section: Cryogenics in particle physics & fusion, Paper ID: 020, Page: 34

D.F. Escande, F. Sattin, Y. Camenen, A.T. Salmi, T. Tala and JET EFDA Contributors
Calculation of transport profiles in modulation experiments with source without transport codes
24th IAEA Fusion Conference (San Diego USA, October 8-13, 2012), poster TH/P2-18

Nicola Vianello, Matteo Agostini, L Carraro, R Cavazzana, G De Masi, E Martines, B Momo, P Scarin, S Spagnolo, Gianluca Spizzo, Monica Spolaore, and M Zuin.
3D Effects on RFX-mod helical boundary region
24th IAEA Fusion Conference (San Diego USA, USA, October 8-13, 2012), pp. EX-P8-02.

A. Masiello, G. Agarici, T. Bonicelli, F. Fantini, M. Gagliardi, F. Paolucci, M. Simon, P. Wikus, P.Batchford, D. Boilson, M. Dalla Palma, C. Day, M. Dremel, H. Decamp, P. Franzen, J. Graceffa, B. Heinemann, S. Hanke, R.Hemsworth, M. Kuriyama, A. Luchetta, D. Marcuzzi, R. Pearce, W Rigato, B. Schunke, L. Svensson, V. Toigo, P. Zaccaria, P. Sonato
EU development of the ITER Neutral beam injector and test facility
24th IAEA Fusion Conference (San Diego USA, October 8-13, 2012)

G. Ambrosino, S.Arshad, G. Vayakis, R. Albanese, L. Appel, M. Ariola, P. Bettini, M.Brombin, C. Cianfarani, V. Coccorese, F. Crisanti, R.S. Delogu, V. Fusco, T.C. Hender, M. Mattei, P. Micozzi, S.Peruzzo, A. Pironti, G. Ramogida, G. Rubinacci, O. Tudisco, F. Villone, G. Vlad, L. Zabeo
System-Level Optimization of ITER Magnetic Diagnostics: Preliminary Results
24th IAEA Fusion Conference (San Diego USA, October 8-13, 2012)

P. Sonato, D. Boilson, T. Bonicelli, A.K. Chakraborty, C. Day, P. Franzen, G. Gorini, T. Inoue, J. Milnes, T. Minea, H.P.L. De Esch, P. Agostinettia M. Agostini, V. Antoni, M. Barbisan, P. Bettini, M. Bigi, M. Boldrin, M. Brombin, M. Cavenago, G. Chitarin, G. Croci, M. Dalla Palma, S. Dal Bello, M. De Muri, A. De Lorenzi, F. Fellin, A. Ferro, A. Fiorentin, L. Grando, S. Hanke, M. Kashiwagi, A. Luchetta, G. Manduchi, N. Marconato, D. Marcuzzi, R. Pasqualotto, M. Pavei, S. Peruzzo, A. Pesce, N. Pilan, N. Pomaro, M. Recchia, W. Rigato, A. Rizzolo, E. Sartori, G. Serianni, A. Soppelsa, A. Sottocornola, M. Spolaore, C. Taliercio, M. Taniguchi, H. Tobari, V. Toigo, M. Valente, P. Veltri, K. Watanabe, P.Zaccaria, B. Zaniol, A. Zamengo, L. Zanotto
Design of the MITICA neutral beam injector: from physics analysis to engineering design
24th IAEA Fusion Conference (San Diego USA, October 8-13, 2012)

Peruzzo S., Arshad S., Brombin M., Chitarin G., Gonzales W., Grando L., Portales M., Rizzolo A., Vayakis G., Vermeeren L.
R&D on ITER in-vessel magnetic sensors
presented at 27th Symposium on Fusion Technology, Liège (Belgium), 2012, submitted to Fusion Engineering and Design

V. Toigo, U.K. Baruah, M. Bigi, M. Boldrin, T. Bonicelli, H. Decamps, T. Inoue, A. De Lorenzi, N. Pomaro, M. Simon, N.P. Singh, K. Watanabe, H. Yamanaka, L. Zanotto, M. Barp, R.J. Dave, H. Dhola, A. Ferro, C. Finotti, J. Framarin, E. Gaio, S.A. Gajjar, L. Grando, V. Gupta, D. Gutierrez, D. Lathi, A. Maistrello, L. Novello, D.C. Parmar, A.M. Patel, A. Pesce, B.M. Raval, M. Recchia, A.A. Roy, J. Takemoto, M. Tanaka, A.M. Thakar, K. Tsuchida, A. Zamengo
Design Status of Power Supply Systems for SPIDER and MITICA NBI Experiments
Presented at SOFT 2012

Junior Jader Framarin, Mauro Recchia, Lucio Baseggio, Marco Bigi, Vannino Cervaro, Daniele Zella, and Vanni Toigo
Design, assembly and commissioning of a 15kV 1MHz resonant circuit for radiofrequency insulation testing
Presented at SOFT 2012

Bettini P., Marconato N., Furno Palumbo M., Peruzzo S., Specogna R., Albanese R., Rubinacci G., Ventre S., Villone F.,
Numerical modeling of 3D halo current path in ITER structures
presented at 27th Symposium on Fusion Technology, Liège (Belgium), 2012, submitted to Fusion Engineering and Design

Ph. Moreau, A. Le-Luyer, P. Malard, P. Pastor, F. Saint-Laurent, P. Spuig, J. Lister, M. Toussaint, P. Marmillod, D. Testa, S. Peruzzo, J. Knaster, G. Vayakis, S. Hughes, K.M. Patel
Prototyping and testing of the Continuous External Rogowski ITER magnetic sensor
presented at 27th Symposium on Fusion Technology, Liège (Belgium), 2012, submitted to Fusion Engineering and Design

P. Franz, M. Gobbin, L. Marrelli, A. Ruzzon, A. Fassina
Thermal Dynamics of QSH Regimes in RFX-Mod

Bullettin of the American Physical Society, 54th Annual Meeting of the APS Division of Plasma Physics (APS2012), Providence, RI

Gianluca Spizzo, R B White, Matteo Agostini, P Scarin, and Nicola Vianello.
Ambipolar edge electric field with energy dependence.
*Bullettin of the American Physical Society, 54th Annual meeting of the **APS** Division of Plasma Physics, Providence, Rhode Island 2012 vol. 57 (12) p. JP8.00169.*

Monica Spolaore, Nicola Vianello, Matteo Agostini, R Cavazzana, G De Masi, E Martines, B Momo, A Scaggion, P Scarin, S Spagnolo, Gianluca Spizzo, M Zuin, I Furno, F Avino, A Fasoli, C Theiler, D Carralero, A Alonso, and C Hidalgo.
Inter-machine scalings of plasma filament electromagnetic features.
Bullettin of the American Physical Society, 54th Annual meeting of the APS Division of Plasma Physics, Providence, Rhode Island 2012 vol. 57 pp. 1-1.

M Zuin, S Spagnolo, I Predebon, F Sattin, F Auriemma, R Cavazzana, A Fassina, E Martines, R Paccagnella, Monica Spolaore, and Nicola Vianello.
Experimental Observation of Microtearing Modes in the RFX-mod Reversed Field Pinch Plasma.
Bullettin of the American Physical Society, 54th Annual meeting of the APS Division of Plasma Physics, Providece, Rhode Island 2012 vol. 57 (12) pp. 1-1.

S. C. Guo, Z. R. Wang, X. Y. Xu, Y. Q. Liu
MHD instabilities in non-circular Reversed field pinch plasmas
Bullettin of the American Physical Society, 54th Annual meeting of the APS Division of Plasma Physics, Providece, Rhode Island 2012 Section JP8-170

S. F. Liu, S. C. Guo, J. Q. Dong
Trapped electron effects on ITG modes and TEM in the reversed-field pinch"
Bullettin of the American Physical Society, 54th Annual meeting of the APS Division of Plasma Physics, Providece, Rhode Island 2012 Section JP8-171

INTERNAL TECHNICAL NOTES

1) A. Soppelsa "Implementation of a family of implicit 2D Fourier operators for sub-grids of sensors", AI-NT-028, 07/03/2012;
2) P. Zanca "RFX locking code: comparison between thin-shell and thick-shell formulations", FC-NT-84, 14/02/2012;
3) L. Piron, P. Zanca "Mini-report of possible modifications for the upgraded RFX-MOD experiment", FD-NT-81, 24/01/12;

4) L. Piron, P. Zanca "Impact of the upgraded mode controller on tearing mode dynamics", FD-NT-82, 02/03/12;
5) A. Fassina, P. Franz, M. Gobbin, L. Marrelli, A. Ruzzon "Temperature profile dynamics in QSH regimes with multichords Soft X Rays diagnostic", FD-NT-83, 06/03/12;
6) P. Barbato, G. Pesavento, R. Gobbo, F. Baldo, V. Cervaro, L. Lotto, M. Fincato, L. Franchin,A. Pesce, N. Pilan "HVPTF – THE 300kV TEST FACILITY: FINAL REPORT", RFX-IE-TN-026rev3, 24/05/2012;
7) S. Peruzzo, M. Brombin, "Review of sensor specifications and environmental constraints for ITER in-vessel magnetic discrete sensors", RFX-IE-TN-033, 01/02/2012;
8) P.Bettini, R.Delogu, S.Peruzzo "Analysis of Chit 1.22 raised at the CDR of ITER Magnetic Diagnostic Part C: "Resolution requirements for the halo current measurements", RFX-IE-TN-035rev1, 26/03/2012;
9) N. Pilan, G. Chitarin "Proposal of experimental campaign at the HVPTF: magnetic field effect on the voltage holding", RFX-IE-TN-036rev3, 30/03/2012;
10) M.Brombin, M.Fincato W.Gonzalez, L.Grando, S.Peruzzo, A.Rizzolo, A.Tiso "Conceptual Design Report of ITER in-vessel magnetic discrete sensors, RFX-IE-TN-037, 28/03/2012;
11) M. Brombin, S. Peruzzo "Technical specification for magnetic sensor prototypes based on LTCC technology", RFX-IE-TN-038, 09/07/2012;
12) M. Brombin, "Irradiation test specifications for in-vessel magnetic discrete sensors", RFX-IE-TN-039, 09/09/2012;
13) V. Antoni, A. De Lorenzi, N. Pilan, E. Spada "High Voltage holding in a MV accelerator for DEMO Final Report", RFX-IE-TN-040, 22/02/2012;
14) N. Pilan, L. Lotto, M. Fincato, R. Rizzieri ,G. Chitarin, G. Pesavento, R. Gobbo, V. Cervaro, L. Franchin, P. Barbato, D. Friso" High Voltage Test facility campaign report 2012", RFX-IE-TN-041, 18/12/2012;
15) W.Gonzalez, F.Degli Agostini, M.Fincato, F.Rossetto "Design proposal of high vacuum system for out-gassing measurements", IP-NT-169, 28/05/2012;
16) W. Gonzalez "Proposal for out-gassing tests of magnetic sensor prototypes", IP-NT-170, 07/09/2012;
17) P. Barbato, M. Moressa "Monitoraggio della rete PLC tramite Wire Shark", SC-NT-114, 17/02/2012;
18) R. Ghiraldelli , L. Migliorato "proposta tecnica per l'aggiornamento del software di progettazione elettronica", SC-NT-115, 29/02/2012;
19) P. Barbato "Aggiornamento del sistema di Sicurezza per la navigazione Internet", SC-NT-116, 07/05/2012;
20) M. Carraro "SOPHOS Nuovo sistema centralizzato antivirus", SC-NT-117, 06/06/2012;
21) P. Barbato "aggiornamento infrastruttura wifi: nuove reti RFXNET e RFXNET_guest", SC-NT-118, 31/07/2012;
22) M. Carraro "SPIDER Control Room Proposte a confronto Thin client e Fat client", SC-NT-119, 27/06/2012;
23) S. Polato, E. Scek Osman, D. Ravarotto "Proposta architetturale per la messa in produzione del sistema di esecuzione remotizzata delle checklist del gruppo SXD", SC-NT-121, 18/07/2012;

24) S. Polato "Guida al recovery di RO1 (server di interfaccia ai Camac Serial Highway Driver)", SC-NT-123, 09/07/2012;
25) M. Carraro "Nuovo Protocollo del Consorzio RFX Note Installazione", SC-NT-124, 29/07/2012;
26) M. Carraro "EXPLORA Sistema di Visualizzazione WEB del Cartellino", SC-NT-125, 31/07/2012;
27) P. Barbato, M. Moressa, S. Polato "Confronto tra le tecnologie di aggregazione di banda", SC-NT-126, 18/10/2012;
28) P. Barbato "aggiornamento del sistema di sincronizzazione temporale basata sul network time protocol", SC-NT-127, 14/11/2012;
29) A. Ferro "Calibration assessment of voltage and current measurements of RFX ac/dc conversion system", SE-NT-140, 10/01/2012;
30) J.J. Framarin, C. Finotti "Aggiornamento e conversione in linguaggio Fortran della pre-esistente routine in C++ per il calcolo del consumo energetico mensile degli impulsi di RFX", SE-NT-141, 09/10/2012;
31) Servizio Prevenzione e Protezione, Servizi Amministrativi "procedura di individuazione e valutazione dei rischi interferenziali ai sensi dell'art. 26 del d.lgs. 81/08", UM-NT-135rev2, 16/07/2012;
32) M. Battistella "MISURE DI PREVENZIONE INCENDI E DI EMERGENZA DEL CONSORZIO RFX ai sensi dell'art. 26 del DLgs 81/08". UM-NT-145rev6, 08/06/2012;
33) M. Battistella "verifica annuale del piano di emergenza del consorzio rf del 18 ottobre 2012", SPP-NT-001, 12/11/2012;
34) G. Lazzaro "Relazione sull' attività di manutenzione delle connessioni di potenza dei sezionatori PMSI svolta nel periodo dicembre 2011-gennaio 2012", SXA-NT-103, 23/01/2012;
35) G. Lazzaro "capitolato lavori per la messa in sicurezza dell'equipaggiamento elettrico dell' iniettore diagnostico di neutri dell'esperimento RFX", SXA-NT-104, 26/03/2012;
36) G. Lazzaro "Relazione sulle misure elettriche svolte sulla rete di Continuità Assoluta che alimenta il CED dell'Istituto di Ingegneria Biomedica dell'Area del CNR di Padova", SXA-NT-105, 06/11/2012;
37) P. Simionato "Caesium Oven IMPLEMENTAZIONE con CODAC" SXC-NT-040, 26/01/2012;
38) F. Molon "Acquisizione continua in MDSPlus e visualizzazione in jScope delle temperature di due termocoppie della diagnostica DLI3: Liquid Lithium Limiter", SXC-NT-041, 16/05/2012;
39) M. Breda, R. Capobianco, P. Simionato "SPIDER CODAS Human Machine Interface Prototype Implementation", SXC-NT-042, 29/06/2012;
40) F. Molon, M. Moressa "Migrazione e ottimizzazione del database per il salvataggio degli allarmi d'impianto dell'esperimento RFX (da MSSQL 2000 a MySQL 2012)", SXC-NT-043, 04/07/2012;
41) R. Capobianco "Valutazione di CODAC Core System versione 3.1 e confronto con la versione 2.1", SXC-NT-044, 31/07/2012;
42) R. Ghiraldelli "Progettazione e realizzazione della scheda elettronica per alimentare i moduli di condizionamento in un prototipo del sistema di misure termiche di SPIDER", OEN-NT-17, 21/03/2012;

43) R. Ghiraldelli “Progettazione e realizzazione della scheda elettronica per controllare l’iniettore di pellet di litio multiplo”, OEN-NT-18, 29/05/2012;
44) A. Maistrello “Descrizione dell’interfaccia per il controllo del prototipo di Quench Protection Circuit per JT-60SA”, BA-NT-34, 07/03/2012;
45) F. Baldo, R. Capobianco “Descrizione del sistema di controllo e protezione dell’interruttore ibrido da 10kA”, BA-NT-37, 27/11/2012;
46) G. Lazzaro “revisione del progetto esecutivo degli edifici del complesso denominato PRIMA database forometrie rev.3”, RFX-PRIMA-TN-031rev3, 24/09/2012;
47) F. Fellin “Auxiliary plants: Proposed layout for MV/LV transformers and for control cubicles in PRIMA Buildings”, RFX-PRIMA-TN-041, 19/01/2012;
48) F. Fellin “Report on activities carried out for the PRIMA Cooling Plant under F4E Grant 306”, RFX-PRIMA-TN-044rev3, 02/02/2012;
49) F. Fellin “Cooling Plant: SPIDER and MITICA Preliminary technical evaluation of Bidders General part Reserved document – This document cannot be distributed without author and F4E authorizations”, RFX-PRIMA-TN-048, 30/03/2012;
50) F. Fellin “Cooling Plant: SPIDER and MITICA Preliminary technical evaluation of Bidders Electrical Plant Reserved document – This document cannot be distributed without author and F4E authorizations”, RFX-PRIMA-TN-049, 30/03/2012;
51) F. Fellin “Cooling Plant: SPIDER and MITICA Preliminary technical evaluation of Bidders Control Plant Reserved document – This document cannot be distributed without author and F4E authorizations”, RFX-PRIMA-TN-050, 30/03/2012;
52) G. Lazzaro “Minuta dei rilievi a seguito revisione della perizia di variante relativamente al punto 9 Forometrie”, RFX-PRIMA-TN-051, 12/11/2012;
53) N. Pilan, G. Chitarin “Proposal of experimental campaign at the HVPTF: magnetic field effect on the voltage holding”, RFX-MITICA-TN-036rev3, 30/03/2012;
54) P. Agostinetti, F. Fellin, A. Rizzolo “Evaluations on the conditioning system of the plasma grid and bias plate in MITICA” RFX-MITICA-TN-043rev2, 24/05/2012;
55) L. Zanotto “Final report summarising all the AGPS-CS & GRPS activities”, RFX-MITICA-TN-107rev2, 28/02/2012;
56) M. Bigi “Final report summarising all the supporting activities with JADA procurement interface”, RFX-MITICA-TN-117rev2, 31/05/2012;
57) M. Boldrin “Final report summarising all the MITICA HVD1 & BUSHING activities” RFX-MITICA-TN-137rev2, 22/02/2012;
58) D. Marcuzzi “MITICA Beam Source Development Requirement Document (DRD) (PBS 53-MI-S1 and 53-MI-A1)”, RFX-MITICA-TN-142rev2, 07/07/2012;
59) M. Valente “Cost comparison between three different possible sizes for Helium refrigerator in MITICA Cryogenic Plant”, RFX-MITICA-TN-143, 17/01/2012;
60) V. Toigo, L., Zanotto “AGPS-CS Dummy Load: Cost assessment”, RFX-MITICA-TN-144, 02/01/2012;
61) E. Sartori “Gas Density Distribution In MITICA Beam Line”, RFX-MITICA-TN-147, 24/04/2012;
62) M. Boldrin, A. Pesce “MITICA NBI power supplies integrated tests: evaluation of arc energy cumulated during breakdown simulation tests MITICA High Voltage Hall constraints”, RFX-MITICA-TN-149, 25/05/2012;
63) P. Agostinetti, G. Chitarin, N. Marconato, D. Marcuzzi, N. Pilan, E. Sartori, G. Serianni, P. Sonato, F. Spada, P. Veltri, P.Zaccaria “Report on Meeting on the MITICA accelerator held on 25 June 2012”, RFX-MITICA-TN-152, 30/07/2012;

64) P. Agostinetti, G. Chitarin, N.Marconato “Optimization of magnetic field for MITICA”, RFX-MITICA-TN-153, 30/11/2012;
65) A. Ferro “studies on compliance of the agps-cs alternative scheme with agps requirements”, RFX-MITICA-TN-158, 24/10/2012;
66) A. Luchetta, N. Pomaro “SPIDER CODAS/Interlock Interface Sheet with Ion Source and Extraction Power Supply”, RFX-SPIDER-TN-113rev4, 08/11/2012;
67) M. Dalla Palma, R. Pasqualotto, M. Tollin “Review of the ITER India design for the integration of the Beam Dump in the SPIDER experiment”, RFX-SPIDER-TN-114rev2, 05/04/2012;
68) G. Manduchi, R. Capobianco, F. Molon “SPIDER Control and Data Acquisition Prototype”, RFX-SPIDER-TN-159rev4, 01/10/2012;
69) A. Zamengo, A. Pesce “SPIDER PS integrated modelling final report”, RFX-SPIDER-TN-180rev2, 31/05/2012;
70) M. Bigi “Final report summarising all the supporting activities with INDA procurement interface”, RFX-SPIDER-TN-186rev2, 31/05/2012;
71) M. Spolaore “Electrostatic sensors for SPIDER: R&D activities and prototypes”, RFX-SPIDER-TN-188, 12/01/2012;
72) G. Manduchi “Results of Tests on SPIDER Control and Data Acquisition Prototype”, RFX-SPIDER-TN-191rev3, 10/10/2012;
73) P. Agostinetti, G. Chitarin, N. Marconato, D. Marcuzzi, L. Romanato “Magnetic field measurements on the Multi-Channel Prototypes of the SPIDER/MITICA grids”. RFX-SPIDER-TN-204, 08/05/2012;
74) A. Luchetta, R. Capobianco, E. Zampiva “Acceleration Grid Power Supply Interface Sheet with SPIDER CODAS, Interlock and Safety Systems”, RFX-SPIDER-TN-205rev3, 05/09/2012;
75) C. Taliercio “Reply to F4E comments on deliverables of Grant F4E-2011-GRT-306 concerning Subtask B3 – SPIDER CODAS”, RFX-SPIDER-TN-206, 07/06/2012;
76) P. Zaccaria, M. Dalla Palma, M. Tollin “Review of the ITER India CAD and drawings for procurement of SPIDER Beam Dump”, RFX-SPIDER-TN-214, 20/09/2012;
77) C. Taliercio, P.Simionato, R.Capobianco “SPIDER ISEPS miniCODAS”, RFX-SPIDER-TN-217, 09/11/2012;
78) N. Fonnesu “An image filtering technique for SPIDER visible tomography”, RFX-SPIDER-TN-218, 30/10/2012;
79) M. Bigi “Technical content for ISEPS Deviation Request”, RFX-SPIDER-TN-222rev2, 19/12/12;
80) D. Marcuzzi, M.Bigi, M.Boldrin, R.Pasqualotto, W.Rigato, M.Spolaore “REPLY to THALES ENQUIRY (29/11/2012)”, RFX-SPIDER-TN-227, 07/12/2012;
81) F. Fellin “Structural characteristics of NIO1 hall”, RFX-NIO-TN-001, 08/11/2012;
82) P. Veltri, L. Baseggio, M. Boldrin, G. Serianni “Relazione sui Test di Tenuta di Tensione degli isolatori ceramici di NIO”, RFX-NIO-TN-002, 14/05/2012;
83) R. Paccagnella “Second progress report of the GRT-334 named:“”Model validation of M3D MHD code and construction of ITER model for simulation of asymmetric VDEs and associated electro-magnetic load”, RFX-VDE-TN-02, 15/03/2012;
84) R. Paccagnella, M. Baruzzo, P. Bettini, R. Delogu, M. Furno Palumbo Final Report of the GRT-334 named:“”Model validation of M3D MHD code and construction of

ITER model for simulation of asymmetric VDEs and associated electro-magnetic load “, RFX-VDE-TN-03, 15/10/2012;

TECHNICAL SPECIFICATION

1) M. Boldrin “Technical Specification for the HVD1 and HV bushing”, RFX-MITICA-TS-007, 20/04/2012;
2) A. Rizzolo, D. Marcuzzi “TECHNICAL SPECIFICATION FOR ELECTRON BEAM HETEROGENEOUS JOINT SAMPLES”, RFX-MITICA-TS-008rev2, 02/10/2012;
3) N. Pomaro, M. Dalla Palma “chnical Specification of the Thermal Sensor Prototypes for MITICA Beam Line Components”, RFX-MITICA-TS-009, 05/04/2012;
4) M. Bigi, M. Recchia “Call for Tender technical specifications of NIO1 isolation transformer”, RFX-NIO-TS-02, 09/05/2012;
5) M. Bigi, M. Recchia “Call for Tender technical specifications of NIO1 isolation transformer – Version for distribution to Tenderers”, RFX-NIO-TS-03, 09/05/2012;